NPS-61SW0031A

United States
Naval Postgraduate School

COMPILATION OF RESEARCH SUMMARIES

THIRTEENTH AFOSR CONTRACTORS' MEETING ON
PHYSICAL ENERGETICS

by

F. Schwirzke and A. W. Cooper

15 April 1970

NAVAL POSTGRADUATE SCHOOL
Monterey, California

Rear Admiral R. W. McNitt, USN
Superintendent

R. F. Rinehart
Academic Dean

ABSTRACT:

This report contains the material presented in the form of panel discussions at the Thirteenth Annual Air Force Office of Scientific Research Contractors' Conference on Physical Energetics held at the Naval Postgraduate School, Monterey, California, from the 5th to the 7th of May 1970.

It was the purpose of this conference to facilitate the exchange of latest information on research in non-chemical energy sources, release mechanisms and conversion processes. The conference was attended by the AFOSR contractors and grantees performing research in these areas together with representatives of the Army, Navy, Air Force, DOD, NASA and AEC.

COMPILATION OF RESEARCH SUMMARIES

THIRTEENTH AFOSR CONTRACTORS' MEETING

ON

PHYSICAL ENERGETICS

5-7 May 1970
Naval Postgraduate School
Monterey, California

THIRTEENTH AFOSR CONTRACTORS' MEETING ON PHYSICAL ENERGETICS

5-7 May 1970

AGENDA

Tuesday
5 May 1970

0800	Registration		
0830	Opening Remarks	NPS and AFOSR Representatives	
0900	Injection and Plasma Generation	Panel 1 (Part 1)	Page 5
1030	COFFEE		
1045	Injection and Plasma Generation	Panel 1 (Part 2)	
1230	LUNCH		
1330	Turbulence and Waves	Panel 2 (Part 1)	Page 54
1500	COFFEE		
1515	Turbulence and Waves	Panel 2 (Part 2)	
1700	ADJOURN		

Wednesday
6 May 1970

0830	Confinement and Instabilities	Panel 3 (Part 1)	Page 72
1015	COFFEE		
1030	Confinement and Instabilities	Panel 3 (Part 2)	
1230	LUNCH		
1330	Calculations and Instrumentation	Panel 4 (Part 1)	Page 121
1500	COFFEE		
1515	Calculations and Instrumentation	Panel 4 (Part 2)	
1700	ADJOURN		
1845	RECEPTION COCKTAILS		
1930	BANQUET Professor E. C. Haderlie, Guest Speaker		

Thursday
7 May 1970

0830	Low Temperature Plasmas	Panel 5 (Part 1)	Page 145
1015	COFFEE		
1030	Low Temperature Plasmas	Panel 5 (Part 2)	
1230	LUNCH		
1330	Round Table Discussion of Future Plasma Applications	Panel 6 (Part 1)	

Thursday (Cont'd)
7 May 1970

1500	COFFEE	
1515	Round Table Discussion of	Panel 6 (Part 2)
1700	Closing Remarks	NPS and AFOSR Representatives
1715	ADJOURN	

THIRTEENTH AFOSR CONTRACTORS' MEETING ON PHYSICAL ENERGETICS

5-7 May 1970

PANEL 1. INJECTION AND PLASMA GENERATION

Name	Topic
Dr. Willard H. Bennett North Carolina State University Department of Physics Raleigh, North Carolina 27607	Production of Extremely Dense Hot Plasmas
Professor S. Gruber Department of Engineering Case Western Reserve University Cleveland, Ohio 44106	Controlled Beam-Plasma Interaction in Non-Uniform Magnetized Plasmas
Dr. A. Haught United Aircraft Research Labs United Aircraft Corporation East Hartford, Connecticut 06108	Laser Irradiated Single Particle Plasmas
Professor C. D. Hendricks Department of Electrical Engineering Columbia University New York, N Y. 10027	Electron Sheath Extraction of Ions from a Plasma Thermonuclear Reactions Initiated in Particle-Particle Collisions
Dr. M. Lubin Dept. of Mechanics & Aerospace Science University of Rochester Rochester, N. Y. 14627	Interaction of Laser Produced Plasmas with a Magnetic Field
Professor F. Schwirzke Department of Physics Naval Postgraduate School Monterey, California 93940	Laser Created Plasma and Collisionless Shock Wave Phenomena
Dr. John G. Siambis Department of Electrical Engineering Carnegie-Mellon University Pittsburgh, Pennsylvania 15213	Streaming Plasma Interaction with Longitudinal Magnetic Fields

PRODUCTION OF EXTREMELY DENSE HOT PLASMAS

Willard H. Bennett, North Carolina State University, Raleigh, N. C.

The immediate objective in this program is to develop methods for concentrating the beams from very high current high voltage pulsed electron beam machines into streams with very small diameters, by using the self-magnetic field of a linear pinched discharge. Machines delivering 30 nanosecond pulses of 100,000 amperes at 5,000,000 volts have been used in this work. The method which has been used is to produce a linear pinched discharge in argon at 0.2 Torr and while the pinched discharge is still of the order of one centimeter in diameter, to project the pulse of high energy electrons through a 0.002-inch metal sheet into the end of the linear pinched plasma column so that the self-magnetic field of the linear pinch serves to draw the relativistic electron beam towards the axis.

Experimental confirmation has been attained for several unusual characteristics predicted theoretically for these relativistic beams as they interact with a pinched discharge and which are not familiar with ordinary discharges. The injection of the pulsed beams into the pinched column induces reverse current densities initially which are everywhere equal and opposite to the injected relativistic current densities. It has also been predicted that the production of induced reversed current makes the residual electrons in the beam channel move backwards so that they are unpinched, that is, they are magnetically driven out of the beam channel, whereupon the injected relativistic electron beam is able to pinch itself far more intensely so that the radius of the relativistic beam is reduced to a very much smaller value than it had at injection. It is anticipated that by properly adjusting the parameters and by developing methods for delivering the relativistic electron beam through the thin metal foil within a half-angle of divergence of less than one degree, a resulting radius of beam less than one-tenth millimeter should be attained.

The production of the electron beam within the small angle of divergence is to be called "narrow injection." Methods for producing narrow injection in the existing high energy pulsed electron beam machines is the principal objective of this program at this time and it is anticipated

that to attain this it will be necessary to develop some rather sophisticated methods for making the pinched discharge interact appropriately with the discharge system in the high voltage tube of the high energy machines. These methods are under development.

An ancillary objective of this program to run concurrently with the above is to study the processes in targets which will be produced when electron beams with power densities of the order of 1,000,000,000,000,000 watts per square centimeter strike various kinds of solid state targets.

In the early phases of this work we have already found that our basic cathode which is slightly concave and approximately two inches in diameter can be made to deliver 100,000 amperes at the full 5,000,000 volts across a two-inch gap with no damage whatsoever to either the cathode or the anode. This demonstrates that the concept of a plasma cathode for these purposes is sound and that the physical processes in these discharges can be investigated effectively. These are being studied both experimentally and theoretically preparatory to proceeding with the investigation of the interaction of the pinched discharge with the discharge system in the high voltage tube.

Although the scope of the immediate program is limited to the production of extremely high power densities in beams, there are some very important areas of application which will become accessible as soon as the objective of the program is attained. A few of these can be mentioned as follows: (1) the production of thermonuclear power by nuclear fusion at plasma densities more than 10,000 times as great as any ever attained before on earth; (2) the production of transuranic elements in quantities greater than micrograms rather than atom-by-atom as presently done in the biggest of accelerators and hence to produce such elements at very much higher atomic numbers than presently attainable; (3) production and study during very short intervals of very small bits of plasmas similar to those in the interior of stars and in nuclear explosions; and (4) the coherent acceleration of small clumps of ions of the order of 100,000,000,000 ions to energies greater than 10,000,000,000 electron volts per nucleon (if the ions are, for example uranium, energies greater than 1,000,000,000,000 electron-volts per ion) and projecting these accelerated ion clumps of

selected composition into solid state targets of selected composition, to produce nuclear processes which never occurred before in the history of the universe except possibly at the moment of the "big bang" if indeed such was the origin of the universe.

CONTROLLED BEAM-PLASMA INTERACTION IN NON-UNIFORM MAGNETIZED PLASMAS

by

S. Gruber
Division of Electrical Sciences and Applied Physics
Case Western Reserve University

Oscillations in beam-plasma systems are usually generated from uncontrolled fluctuations in space charge. The observed spectra of such oscillations are dominated by the frequencies exhibiting maximum growth rates and are generally broad band as the result of multimode excitation from these fluctuations. Recently efforts were made to control beam-plasma instabilities by modulation of the electron beam[1,2] and preparation of its distribution function.[3,4] These techniques have been sufficiently successful to give impetus to more experimental efforts using beam-plasma interactions in a controlled manner. We have undertaken an experimental program to study controlled beam-plasma interactions in an inhomogeneous medium with these aims:

(1) "Plugging" Mirror Machines

(2) Acceleration of Plasmas

A large and successful effort is being directed toward the rf acceleration of plasma at the Centre d'Etudes Nucleaires de Saclay in France.[5] Their efforts are concentrated on experiments where rf fields are imparted to a plasma (which may be also produced by these same fields) in a gradient of magnetic field so that the electron cyclotron frequency matches the wave frequency in the gradient. This results in the acceleration of plasma into the low field region. The rf energy is either applied in a resonant structure or in a travelling wave structure. The experimental program to follow is designed to investigate the effect of localized beam-plasma interactions in a gradient of static magnetic field upon the acceleration and heating of plasma.

Experiment

The electron beam is density modulated by an rf source at the frequency where the wave interaction is to be studied. This is accomplished by the experimental set up shown in Fig. 1. The beam cathode (on the left) is

mounted flush with the interior wall of a re-entrant cavity. The grid is mounted flush with the other inside wall and is at the same time insulated from the wall to allow for a grid bias. The grid is approximately 0.3 mm from the cathode. This small spacing is necessary in order that transit time effects will be negligible up to 500 MHz. The anode is about 7.5 mm in front of the grid. The cavity is insulated from ground and is run at a negative potential with respect to the grounded anode.

The emerging modulated beam is injected through a region of corkscrew magnetic field,[6] which is immersed in a region of axially directed uniform magnetic field. The corkscrew effects a non-adiabatic conversion of part of the axial velocity of the beam electrons into rotational motion. The beam enters into the mirror region where it is to interact with the plasma present. A second and very much weaker beam is injected from the other side of the mirror. It is axially directed and unmodulated and is used as a method of probing the fields within the confining region. A collector for the probing beam is located to the left of the mirror.

The electron density as well as the magnetic field varies along the axis of the machine. If the energy of the beam electrons on emerging from the corkscrew field is properly chosen the beam could be nearly reflected from the mirror maximum. This would have the effect of enhancing the growth rate of the instability. In Fig. 2 we show a sketch of the plasma density, n_p, axial magnetic field strength, B_z and beam density, n_b, as a function of the distance from the electron gun toward the mirror maximum.

References

1. Ya. B. Fainberg, Invited Paper, International Symposium on Beam-Plasma Interactions, Prague, Sept. 4-6, 1967. Czechoslovak J. Phys., April 1968.

2. A. K. Berezin, G. P. Berezina et al, Atom. Energiya 18, 407 (1965).

3. S. Gruber, International Symposium on Beam-Plasma Interactions, Prague.

4. M. Seidl and P. Sunka, Eighth International Conference on Phenomena in Ionized Gases, Vienna, Springer-Verlag, Vienna (1967).

5. T. Consoli et al, C. R. Acad. Sci., Paris 258, 4454 (1964).

6. R. C. Wingerson et al, Phys. Fluids 7, 1475 (1964).

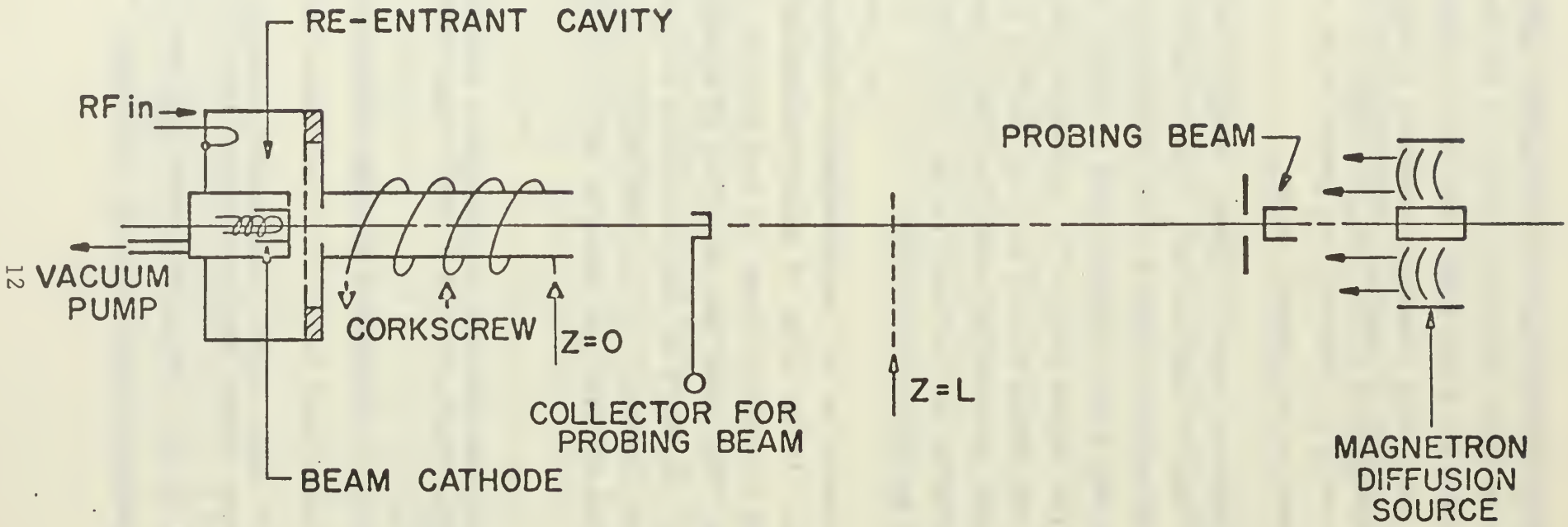
RE-ENTRANT CAVITY
RF in
PROBING BEAM
VACUUM PUMP
CORKSCREW
Z=0
Z=L
COLLECTOR FOR PROBING BEAM
BEAM CATHODE
MAGNETRON DIFFUSION SOURCE

Fig. 1

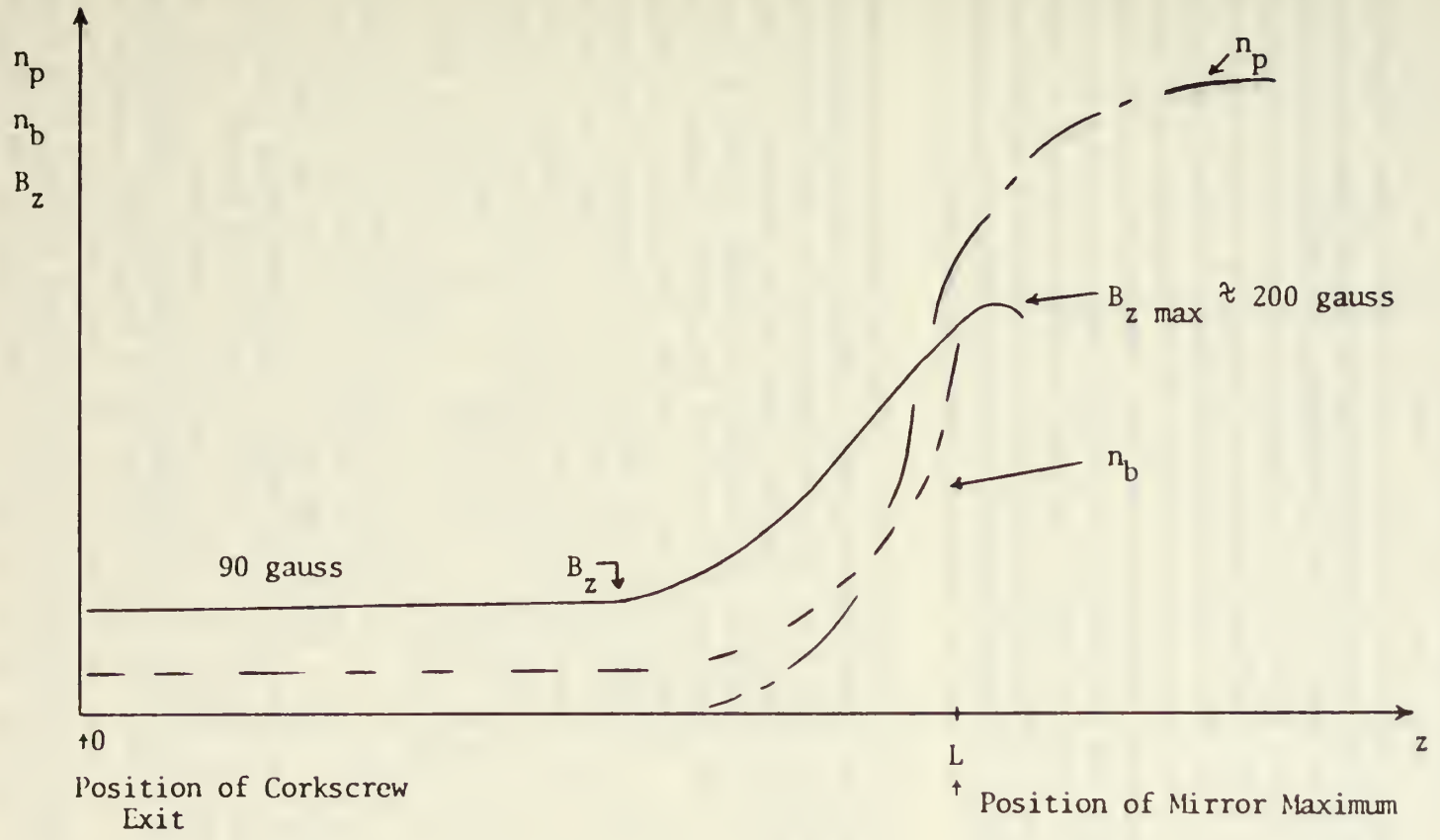
n_p
n_b
B_z
n_p
$B_{z\ max} \approx 200$ gauss
n_b
90 gauss
B_z
0
L
z
Position of Corkscrew Exit
Position of Mirror Maximum

Fig. 2

LASER IRRADIATED SINGLE PARTICLE PLASMAS

A. F. Haught, D. H. Polk, W. J. Fader, and J. C. Woo

United Aircraft Research Laboratories
East Hartford, Connecticut

The production in vacuum of isolated, high density, high temperature plasmas and the investigation of the confinement of these plasmas in simple mirror and minimum-B magnetic fields are being studied under AFOSR support and in parallel programs supported by Corporate and USAEC funds. This technique has been demonstrated to be an effective means of producing a spherically-expanding, uncontaminated plasma at high density and temperature.[1] Using the low frequencies available with a recently developed, variable-frequency (10-400 Hz) suspension voltage source, particles up to 40 μ radius can be conveniently suspended to yield plasmas containing up to 10^{17} atoms and, with the existing ruby laser pulse (7 joule, 15 nsec), having an average energy of ~ 200 eV. Mass spectrometer measurements show that the plasma contains an indetectable fraction (≤ 2 percent) of impurities and, at plasma energies in excess of 100 eV, consists of H^+ and predominantly triply ionized lithium ions.

These plasmas can be produced within established magnetic containment fields, and calculations examining the plasma formation and expansion in the presence of a magnetic field show that the plasma heating and initial expansion are not significantly affected for plasmas formed within magnetic fields up to tens of kilogauss field strength. As a result the plasma energy is the same as that obtained for a free expansion plasma, and the plasma expansion is initially spherically symmetric. However, after the heating phase of the plasma development, interaction of the plasma with the magnetic field results in stopping of the cross-field plasma motion and thermalization of the expansion kinetic energy to produce a high temperature trapped plasma. Experimental studies confirm the results of these magnetohydrodynamic calculations and, in addition, provide information on the subsequent containment of the trapped plasma by simple mirror and minimum-B magnetic fields.[3,4] Charge collection measurements show that the cross-field plasma expansion is suppressed by a magnetic containment field and that more than 99 percent of the plasma leaves the trapping region along magnetic field lines, i.e., within the magnetic field mirror loss cones. Comb probe measurements permit determination of the transverse dimensions of the contained plasma and show that, throughout the plasma decay from the magnetic field, the plasma radius does not increase appreciably beyond that calculated for the initial trapping under the conditions of the experiment. This result implies that, on the time scale of the present experiments, instabilities do not act to produce significant cross-field movement of the plasma. Expansion velocity measurements along the direction of the loss cone show the increase in axial velocity expected for an expansion which has been altered from a spherical to a one-dimensional (axial) form. This result implies both that the transverse

expansion has been stopped and that the trapped plasma is thermalized upon capture by the magnetic field. Further evidence for plasma thermalization, predicted theoretically as consequence of shock collisional interactions in the magnetic field trapping process, is given by H_β line radiation studies showing reduced recombination and by time resolved retarding potential probe measurements of the ion energy distribution late in the plasma density decay. Retarding potential probe measurements show a contained ion temperature, equal to ~ 50 percent of the laser plasma average energy over the 50-200 eV plasma energy range examined. Microwave measurements of the plasma density decay show that, in sufficiently large minimum-B magnetic containment fields, the plasma decay time is equal to that predicted for Coulomb collisional scattering of a hydrogen plasma into the magnetic field mirror loss cones. Further support for a Coulomb scattering loss mechanism of the plasma density decay is provided by the $T^{3/2}$ dependence of the plasma decay time over the factor of four temperature range examined. Plasma decay times shorter than predicted by Coulomb scattering are observed in simple mirror fields and with lower strength minimum-B fields; in each case these are correlated experimentally with a large random cross-field plasma loss suggestive of a flute instability which is apparently suppressed for sufficiently large minimum-B field gradient.

In the present research period, time dependent mass spectrometer studies of the decaying plasma have been carried out and show rapid escape of the highly ionized lithium ions in the plasma followed by a more gradual decay of the hydrogen in agreement with a Coulomb scattering loss mechanism. These measurements also establish that the contained plasma late in its decay is composed primarily of hydrogen, a result used in comparison of the measured plasma decay time with that predicted on the basis of Coulomb scattering. Flux coil measurements have been performed which show that the spherical plasma expansion is stopped and the plasma trapped at $\beta \sim 1$, as predicted by a simple one-dimensional model of the plasma magnetic field interaction. Initial plasma capture at $\beta \sim 1$ appears inconsistent with subsequent Coulomb decay of a mirror confined plasma and has led to a study of the limitations on laser plasma capture in open-ended confinement field geometries. From the results of this study, the plasma capture and containment are separate processes, and their different dependence on temperature leads to a maximum plasma temperature for optimum long-term containment.[5] At low temperatures, the field diffuses rapidly into the plasma, but the lifetime is limited by the large Coulomb scattering loss. Increasing the plasma temperature to obtain a longer Coulomb scattering time also increases the characteristic time for the magnetic field to diffuse into the plasma. From the dependence of these two times on plasma temperature, theoretical calculations show that there is an optimum temperature of 1 keV which results in the greatest amount of plasma captured for the longest time.

However, both the temperature and the subsequent Coulomb decay time of a 1 keV plasma are too small for significant fusion output, and laser heating cannot be used to directly produce a magnetically confined fusion plasma. This

result, however, does not restrict the utilization of a laser produced plasma as a seed plasma from which a thermonuclear plasma is then generated within the magnetic confining field. In this approach, the laser produced plasma is used as a target for charge exchange with more energetic neutrals which are then trapped by the confining magnetic field. The high captured plasma density attainable with a laser produced plasma makes this a particularly attractive scheme, and the use of a neutral injection beam permits replacement of particles which have been lost by decay from the plasma. Calculations of the charge exchange heating and beam ionization have been carried out and show that a 100 mA, 20 keV neutral injection beam incident upon a 1 keV laser produced plasma of 10^{16} particles can result in the production of a 20 keV plasma at a density of 2×10^{13} cm^{-3}, a plasma of definite thermonuclear interest. A most attractive feature of this approach is that lasers to produce a 1 keV target plasma and neutral injection systems to provide the required 100 mA beam current lie within the present state-of-the-art.

On the basis of these results, a neutral beam injection-laser produced target plasma program has been undertaken. An existing 100 GW peak power, 0.1 nsec pulse duration laser will be used to produce the initial target plasma. Ion beam sources, which were developed under AFOSR support in another program (Contract AF33(657)-12385), have been obtained and will be adapted to provide neutral atom beam for injection into the target plasma. The AFOSR supported studies will be concerned with the neutral beam injection plasma heating which represents a logical continuation of the current program and is a prerequisite to the attainment of a steady state laser produced thermonuclear plasma. Studies of the confinement and stability of the plasma will be carried out in a program supported in part by the U.S. Atomic Energy Commission.

---

[1] Haught, A. F. and D. H. Polk, Phys. Fluids 9, 2047 (1966).

[2] Haught, A. F. and D. H. Polk, "Formation and Heating of Laser Irradiated Solid Particle Plasmas," Paper to be published in Phys. Fluids.

[3] Haught, A. F., D. H. Polk, and W. J. Fader, In Plasma Physics and Controlled Fusion Research, Conf. Proc., Novosibirsk, August 1968 (IAEA, Vienna, 1969) Vol. I, p. 925.

[4] Haught, A. F., D. H. Polk, and W. J. Fader, "Magnetic Field Confinement of Laser Irradiated Solid Particle Plasmas," Paper to be published in Phys. Fluids.

[5] Woo, J. C., Bull. Amer. Phys. Soc., Series II, Vol. 14, No. 11, 1022, Nov. 1969.

ELECTRON SHEATH EXTRACTION OF IONS FROM A PLASMA

C. D. Hendricks, A. W. Dipert and S. Grodzinsky
Charged Particle Research Laboratory
Department of Electrical Engineering
University of Illinois

Introduction

It has been proposed to create a source of ions by passing a sheet beam of electrons over a plasma. The sheet beam will act essentially as a negative electrode and will thus extract positively charged ions from the plasma while repelling the electrons from the plasma. The resulting beam of ions may then be focussed and used as an ion source to be used in fields such as electric propulsion and controlled thermonuclear research.

There are several requirements that an ion source should satisfy to be useful in electric propulsion. In order to obtain the highest thrust possible, it is necessary that the ion beam be of a high current density. Also the ion beam should have ideally only one species of ion in order that the efficiency in the use of the propellant be made as large as possible. To have a uniform thrust, it is obvious that the beam must also have a uniform density. Ion sources made for other uses will, of course, have other requirements dictated by their particular uses and needs.

Several different kinds of ion sources have been developed. Among them are the contact cesium-tungsten source, the duo-plasmatron, and the magnetron source. In addition, W. D. Owen(1) spoke of extracting ions from a plasma by using an electrode at a negative potential. The contact cesium-tungsten source was utilized by R. X. Meyer (2,3,4) who used a sheath of electrons to extract the ions. Magnetron sources have also been examined by several authors. Redhead (5) used this device for various pressure measurements while Jepsen and Helmer (6) studied various characteristics of both the normal and inverted magnetrons. Masek (7), in his investigations of the inverted magnetron as a bombardment ion engine, discovered that the radial ion density in this configuration was much more uniform than in the normal magnetron configuration (by a factor of 5). This would, of course, lead to a more uniform ion beam upon extraction from this source. Cobic and Matic (8) examined several characteristics of gas ionization in a magnetron and noted the effect of the magnetic field upon ionization. In addition, Cobic *et al*. (9) used a magnetron to produce a new kind of ion source for high-melting point materials. Gabovich (10) described several different gas discharge sources, including the duoplasmatron and plasmatron, and also studied such basic problems as the ionization of plasmas and the extraction of ions from plasmas.

Space charge limitations as expressed by the Langmuir-Childs law are the most severe limitations in most ion sources. The law states that:

$$J = \frac{4\epsilon}{9}\sqrt{\frac{2q}{m}}\left(\frac{V^{3/2}}{d^2}\right)k \qquad (1)$$

where J is the current density, V is the applied voltage, d is the anode cathode separation and k is the quality factor. There are several ways the

the current density in this relation may be increased. The separation d, if decreased with the voltage V held constant, will obviously increase J. A major problem which exists when a solid electrode is used for extraction is that if the separation distance, d, is made too small, disruptive voltage breakdown may occur. This is one of the major reasons that a sheet electron beam is to be used for extraction instead of a solid electrode. In the case of a sheet beam, this quasi-electrode (the sheet beam) may be placed closer to the source without voltage breakdown since extracted ions are free to pass completely through this extraction beam. Another advantage of using a sheet of electrons as the extraction electrode is that there is no longer any erosion which might occur due to the sputtering of some of the ions onto a solid electrode. (Again, the ions pass freely through the sheet electron beam.) Charge neutralization represents another way of increasing the current density. If particles of sign opposite to those being extracted (for instance, electrons) are injected in the extraction region, neutralization of the resulting space charge is affected which, in terms of the Langmuir-Child law, effectively increases k, the quality factor. This unwanted charge may be separated from the desired ionic charge later by means of magnetic fields (taking advantage of the great disparity between electron and ion cyclotron radii) as is done in isotope separators. Still another way of increasing the current density, J, is suggested by Danilov (11, 12). In his papers, Danilov states that by properly shaping the magnetic fields in the extracting region, it is theoretically possible to again increase k. This is a slightly different kind of space charge neutralization than that mentioned above in that in this case, neutralization results from magnetically induced Hall currents which will flow in the extraction region. These are three ways which will be investigated in the present research in order to try to maximize the output of the ion source.

The source of ions which will be utilized in the proposed research is the magnetron source. As was mentioned earlier, Masek (7) found that the inverted magnetron yielded a more uniform ion density than the normal configuration. A great advantage in using this kind of a source as opposed to a contact cesium-tungsten device is that corrosion is greatly reduced in using the magnetron. In his contact source, Meyer (2,3,4) reported that corrosion of the ionizer was indeed a major problem. This problem will be greatly reduced by use of the magnetron as the possible source of the plasma from which ions will be extracted.

A First Theoretical Model

As is obvious, the complete field solution of sheet beam of electrons passing over a plasma, formed in an inverted magnetron, is extremely difficult to obtain. Therefore, the first attempt at understanding the physics involved in this problem is contained in a hydrodynamic model for the plasma. The plasma is, therefore, approximated to be a highly conducting inviscid incompressible irrotational fluid with no free charge, which satisfies the Navier-Stokes and conservation of mass equations. Also the sheet beam is approximated by an electrode of potential, $-V_o$, with respect to the plasma. This seems to be a reasonable assumption since the potential of the electron sheath would be approximately that of the tungsten cathode which is part of the electron gun. In addition, since the operating pressure is approximately 10^{-4} torr, the mean free path of these electrons is large and, therefore, they do not interact much with each other. The model of this system is shown in Figure 1.

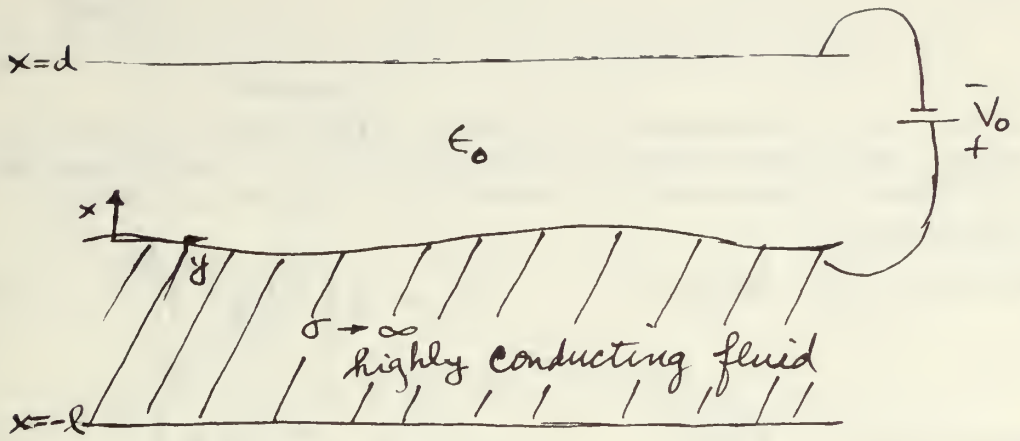

Figure 1.

The dispersion relation for this system is found by the use of a perturbation technique as described by Chandrasekhar (13) and Melcher (14). Small perturbations of the form

$$\xi = Re\left\{\hat{\xi}\, e^{j(\omega t - k_y y - k_z z)}\right\} \tag{2}$$

are assumed about an equilibrium which occurs when the fluid surface is at x = 0 and the electric field is $\mathcal{E}_x = \frac{V_0}{d}$. The solution for the perturbation fields which exist when the fluid interface deforms slightly, and for the fluid velocity and pressure is derived explicitly in Melcher's text (14). The resulting dispersion relation is

$$\omega^2 = \frac{k}{\coth k\ell}\left\{k^2 T - \epsilon_0 k\left(\frac{V_0}{d}\right)^2 \coth kd + \rho g\right\} \tag{3}$$

where

$$k = \sqrt{k_x^2 + k_y^2} = \frac{2\pi}{\lambda}$$

the wave number in the x-direction. and demonstrates exchange of stabilities as defined by Chandrasekhar (13). This means simply that for a given real value of k, instability occurs for

$\omega^2 < 0$ and the instability is absolute; that is, it is a growing exponential in time, not a growing oscillation. It is important to note that by definition if even just one mode (i.e., one value of k) leads to an instability for a given disturbance, the system is said to be unstable. Onset of instability occurs for $\omega^2 = 0$ in which case equation (3) becomes

$$x^2 - \frac{\epsilon_0}{T}\frac{V_0^2}{d}\, x \coth x + \frac{\rho g d^2}{T} = 0 \tag{4}$$

(4)

where x = kd. It is interesting to investigate this equation in its two basic limits. They are the short and long wave limits in which case the value of voltage, V_o, necessary for instability, is given as follows:

short wave limit $kd >> 1$ $$V_o = d\left[\frac{4\rho g T}{\epsilon_o}\right]^{1/4} \quad (5a)$$

long wave limit $kd << 1$ $$V_o = d^{3/2}\left[\frac{\rho g}{\epsilon_o}\right]^{1/2} \quad (5b)$$

where ρ is the mass density, T is the surface tension and is the permittivity of free space. The resulting dispersion relations for each limit are shown in Figure 2 as a function of V_o.

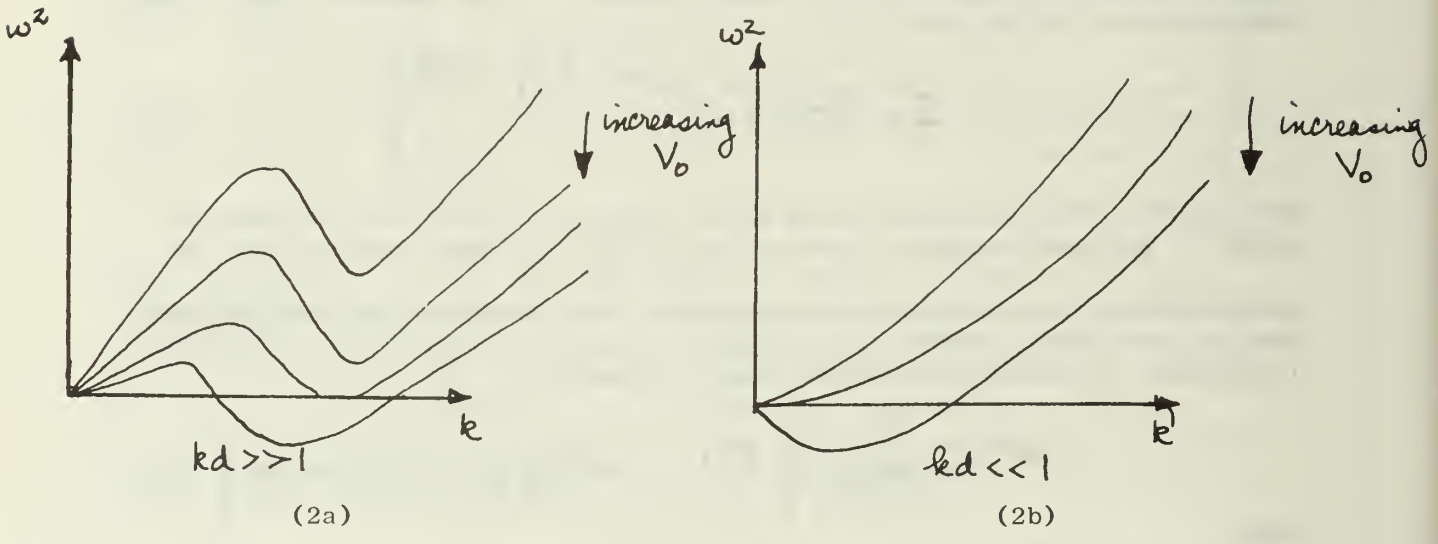

Figure 2.

In an attempt to corroborate this theory the following experiment was performed. A liquid metal, the eutectic fallium-indium alloy*, which is a liquid at room temperature, was stressed by a perpendicular field much as in Figure 1. As the voltage was increased some of the metal was pulled toward the upper plate. This initial disturbance quickly grew into a sharply pointed spout. Instability was assumed to occur when this spout occurred (just before arcing to the upper electrode) since the initial disturbances, when the metal was just pulled toward the upper electrode, would eventually die out with a long time constant. Voltages for the onset of instability are plotted in Figure 3 with the theoretical result from equation (5b). The instability is found to be of the long wave limit since the surface tension of this liquid is so great. Melcher (15) also finds

*This metal had the following parameters in mks units: ρ = 6700, T = .63.

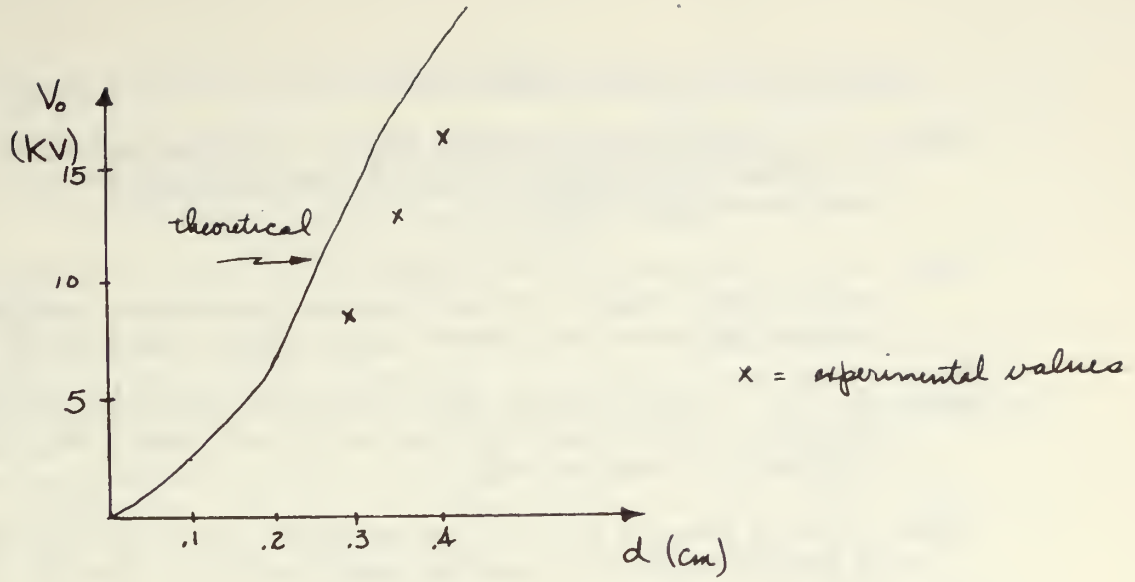

Figure 3.

this type of result because the factor $G = \frac{\rho g d^2}{T}$, which is the ratio of the energy density stored in the gravitational field to the energy stored by surface tension, is less than 3. (It is 2.6 in the case at hand.) In liquids for which this is true, dispersion relations of the kind found in Figure (2b) result.

There are several reasons for the disparity between the theoretical and experimental results as shown in Figure 3. It was assumed initially that equilibrium occurred when the fluid interface was flat and stationary. It was very difficult, however, to maintain this kind of a boundary as the point of instability was approached so that one of the initial assumptions was violated. Also, the surface of the gallium-indium alloy was difficult to keep "clean." Impurities of some kind, perhaps oxides, formed on the surface and were large enough at times to distort the surface of fluid. Thus, these distortions resulted in areas of increased field strength. All attempts at purification failed. As predicted by theory, the first wavelengths to become unstable were long waves. The experiment seemed to predict this since instabilities occurred at only one point on the interface and not at regular intervals which would suggest a shorter wavelength. Since the experimental apparatus was only 2.5 inches square (due to a lack of sufficient gallium-indium alloy for a larger device), the effect of the boundaries on the fluid interface would probably be great. In addition, the experiment was performed in vacuum and the apparatus viabrated slightly along with the vacuum equipment. These viabrations never did allow the surface to be flat and the separation between the initially slightly rippled interface and the upper electrode was effectively less than measured. All of these sources of experimental error would tend to cause the interface to become unstable before the theoretical value.

This paper was supported in part by a grant from the U.S. Air Force, AFOSR-68-1508.

References

1. Owen, D. W., "Electrical Breakdown Between a Plasma and an Electrode at a Negative Potential", United Kingdom Atomic Energy Authority, AWRE Report No. 0-78/67.

2. Meyer, R. X., "Acceleration of cesium ions by means of a negative space charge sheath", Plasma Research Laboratory, Aerospace Corporation Report No. TR-669 (9220-03)-02, March 1966.

3. Meyer, R. X., " A Space Charge Sheath electric thruster", Plasma Research Laboratory, AerospaceCorporation, Report No. TR-1001 (2220-50)-1, November 1966.

4. Meyer, R. X., "Magnetic Field Effect on Space Charge Neutralization in Electric Propulsion", AIAA Journal, Vol. 5, No. 12, December 1967.

5. Redhead, P. A., Can. J. Phys., 36, 255 (1958).

6. Jepson, R. L. and Kelmer, J. C., Proc. IRE, 49, 1920 (1961).

7. Masek, T. D., "Plasma Investigation in a Reversed-Current electron bombardment ion engine", AIAA Journal, 5, 692 (1967).

8. Cobić, B. and Matić, M., "Characteristics of the Gas Ionization In a Magnetron Diode", Ninth International Conference on Phenomena in Ionized Gases, Bucharest, 1969.

9. Cobić, B., Tosić, D., Perović, B., "An Intense Ion Source for High-Melting Point Materials", Nucl. Inst. and Meth., 24, 358 (1963).

10. Gabovich, M. D., "Plasma Ion Sources", Foreign Technology Division, Wright-Patterson AFB, Ohio (1965).

11. Danilov, V. N., "Bipolar Flow in a Special Magnetic Fluid." Treaty of the Moscow Physical Technical Institute, No. 10, Izledovaniye po Fiziki i Radiotechniki, P. 67 (1962).

12. Danilov, V. N. "Using Electrons to Compensate Ion Space Charge in a Magnetic Field", Radiotechniki i Electronica, 1964, No. 8, P. 1262-1265.

13. Chandrasekhar, S. "Hydrodynamic and Hydromagnetic Stability". Oxford Press (1961).

14. Melcher, J. R., "Field-Coupled Surface Waves", MIT Press (1963).

15. Melcher, J. R., ibid., P. 61-66.

16. Pierce, J. R., "Theory and Design of Electron Beams". D. Van Nostrand (1954).

THERMONUCLEAR REACTIONS INITIATED IN PARTICLE-PARTICLE COLLISIONS

C. D. Hendricks, A. W. Dipert and D. Weidenfeld
Charged Particle Research Laboratory
Department of Electrical Engineering
University of Illinois

Introduction

The possible production of a controlled thermonuclear reaction initiated from a solid-solid interaction at extremely high velocity and laser beam irradiation is currently being investigated. The production of a thermonuclear reaction requires that the interacting particles have a temperature equivalent of about 10 KEV per nucleon. Calculations for a realistic accelerating potential will show that there is an upper limit to particle size for a fusion reaction initiated only by high velocity particles. If large size particles are used, or a lower accelerating potential is applied, the additional energy required for a fusion reaction may be supplied by irradiating the particles at the moment of impact with a high power laser beam. Preliminary experiments will be done with a 150 KV power supply. Since the supply potential is not nearly sufficient for obtaining fusion velocities for any reasonable size particles, a high power laser will be used to supply the additional required fusion energy.

Basic Theory

If a charged particle is to ignite a thermonuclear reaction, the atoms involved in the collision must have an energy of at least 10 KEV. If a particle (Lithium Deuteride is to be considered) is acceleraged through a voltage of 10,000 volts, it will have sufficient energy for ignition of a nuclear reaction provided that the particle is 100 per cent ionized. Since this is impossible for a solid particle composed of more than a few atoms, we will calculate a lower limit of ionization given a practical accelerating voltage. Many electrostatic generators are capable of producing a potential of at least 10 million volts, and if we set this value as the upper limit for accelerating voltage, then at least 1 out of a 1,000 atoms must be ionized to achieve sufficient fusion energy.

The required charge-to-mass ratio for a particle with a fraction (f) of its constituent atoms ionized is given by the expression

$$\frac{Q}{M} = \frac{fZN_o q_o}{A}$$

Z = number of protons in a molecule

$N_o = 6.02 \times 10^{26}$ molecules/kg-mole

A = molecular weight

$q_o = 1.6 \times 10^{-19}$ coulombs

Then for an f value of 0.001 for a LiD particle, the charge-to-mass ratio is approximately 2×10^4 coulombs/kilogram.

Next, the electrostatic field E_s at the surface of a spherical

particle is computed for Lithium Deuteride for a set of radii. E_s for a surface of a sphere is given by

$$E_s = \frac{Q}{4 \pi r^2 E_o}$$

Q = total charge = Nq_o

N = Number of ions/particle

Also using the equation for number of atoms per kilogram-mole and the equation for the mass of the particle

$$N = \frac{ZN_o}{A} m \qquad m = \frac{4}{3} = \pi r^3 \rho$$

Combining the above equations, an expression for E_s in terms of the particle size (radius) and physical properties of the particle can be obtained.

$$E_s = \frac{N_o q_o}{3 \quad o} \left[\frac{Z \rho}{A} \right]$$

For fractional ionization, $E_s' = E_s f$, and using the above equation and $f = 0.001$, the surface field for LiD is computed for a range of particle sizes.

R (microns)	E		
0.01	7.16×10^9		
0.05	3.58×10^{10}	Z = 2	
0.1	7.16×10^{10}	P = .883 g/cc	LiD
0.5	3.58×10^{11}	A $\simeq$ 9	
1.0	7.16×10^{11}		

Using a value 10^9 volts/meter given by most references as an upper limit to the electric field at the surface due to field emission effects, we require a particle size of about 0.01 microns.

Development of a Reaction System

The success of a system to produce a reaction depends on the development of a method for obtaining a uniform rate of charged solid particles with a consistent charge-to-mass ratio. Current research efforts are investigating particle charging methods, charge-to-mass ratio selection schemes, and particle containment and ejection systems.

The quadrupole electric field is investigated as a practical method of particle selection and containment. In the device, the particles are held in dynamic equilibrium by alternating electric fields. The

electrode configuration of the device gives sinusodally time varying forces whose strengths are proportional to the distance from a central origin. The governing differential equation of particle motion is a special case of the Mathieu differential equation. The solution of the Mathieu equation for stable motion is dependent on the charge-to-mass ratio of the particle and the applied driving frequency and voltage of the device. By selecting an operating voltage and frequency, a range of stable charge-to-mass values can be calculated.

Experimental Apparatus

A small experimental electric quadrupole chamber was machined from brass (see diagram). For initial experiments, 60 cycle line frequency was used. A high voltage transformer connected to an auto-transformer gave a variable voltage between 0 and 5,000 volts. The chamber was mounted over an electric particle injector. The particle injector is essentially two parallel plates spaced about 1 cm apart. The upper plate has a small aperture for particles to escape. A high voltage is applied between the plates and the electric field charges and attracts the particles to the upper plate. A fraction of them pass through the aperture and enter the quadrupole chamber.

Particles with the correct initial velocity and charge-to-mass ratio should then be retained within the chamber. In the actual experiment, after a few seconds of operation, between 1 and 5 particles were observed to be suspended. By varying the driving potential for a specific value of charging voltage, an optimum value could be found that would give a high suspension rate. By switching a high voltage on the upper plate of the suspension chamber, the suspended particles could be ejected out the small aperture in the upper plate of the quadrupole.

The experiment showed that a relatively simple system could be constructed to select and eject charged particles. Refinements of the system could be made to increase the ejection rate, narrow the charge-to-mass selection, and increase the charge per particle.

Conclusion

The current exploratory experiments have completed the initial design of a solid particle injection system capable of producing a uniform rate of charged particles with a consistent charge-to-mass ratio. The next area of investigation is to refine the system to obtain a higher charge-to-mass ratio and a higher particle ejection rate.

Future charging investigations would use electron beams to increase the charge on a suspended particle. Circuitry would be developed to vary the driving frequency of the device as the charge increased. Studies of high power laser (in the gigi-watt range) characteristics will be conducted. A suitable laser system will then be purchased or constructed. A 150 KV power supply will be used for acceleration of particles. Timing techniques have been developed to synchronize the laser pulse with particle collision.

This paper was supported in part by a grant from the U.S. Air Force, AFOSR-68-1508.

DIAGRAM OF THE PARTICLE SELECTION-EJECTION DEVICE

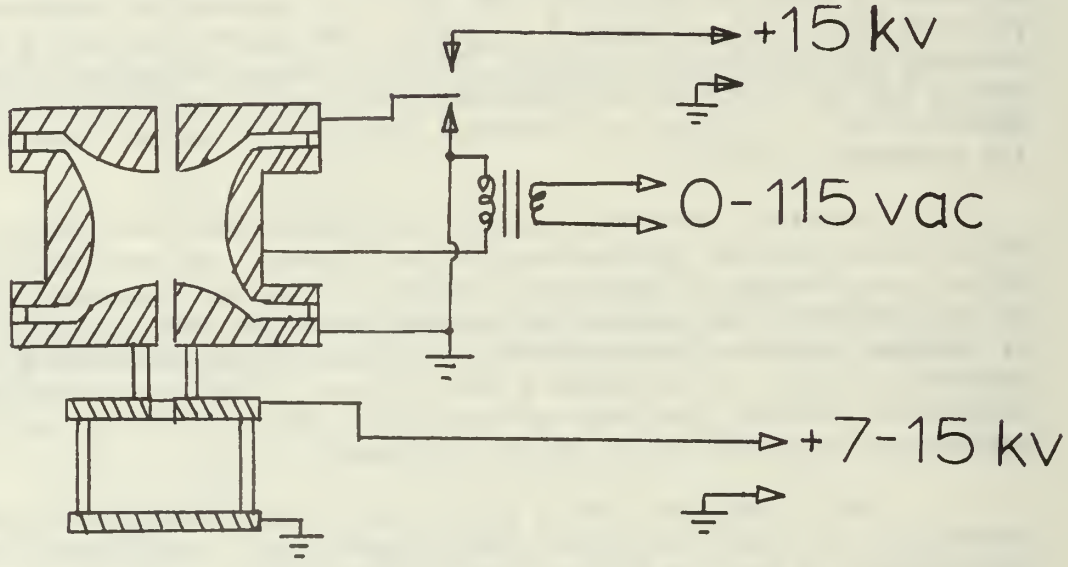

INTERACTION OF LASER PRODUCED PLASMAS WITH A MAGNETIC FIELD

M.J. Lubin and H. S. Dunn
University of Rochester, Rochester, N. Y.

For the past three years the plasma physics group at the University of Rochester has been investigating the interaction of laser produced plasmas with strong magnetic fields in both the collisionless and collisional regimes. Use of the energy of giant pulsed lasers to create a plasma of known and measurable properties, devoid of externally applied driving currents, has proven to be a unique experimental tool for the study of plasma-magnetic field interactions and nonlinear wave propagation. Here we report on two phases of our work, the electromagnetic radiation from a laser produced plasma expanding into a uniform magnetic field and the two-stream instability (and possible collisionless shock wave) created by the expansion of a laser produced plasma into a quiescent background plasma. In both projects, experimental observations have been supported by theoretical studies.

1. Electromagnetic Radiation from a Laser Produced Plasma Expanding into a Uniform Magnetic Field (1). Experimental observations (2) of the radiation field resulting from the expansion of a laser plasma produced from the vaporization and heating of a droplet of lithium hydride in the presence of a uniform magnetic field suggest the existence of strong azimuthal surface currents. A typical oscilloscope trace of the radiated power is shown in figures 1 and 5. The radiation measurements,

all made in a direction normal to the magnetic field as shown in figure 2, were carried out using a submillimeter detector with measurable wavelength response from 70 microns to 8 mm. combined with a rise time of less than 4 nanoseconds.

The result of a computer simulation of a representative experimental situation where the magnetic field is sufficiently weak that the expanding plasma remains spherical during the time interval of interest is shown in figure 3. To calculate the electromagnetic radiation signature of the expanding plasma, it is necessary to consider three separate effects, namely the dipole-like radiation resulting from the induced azimuthal currents, the surface cyclotron radiation and volume cyclotron radiation.

The dipole radiation field is obtained by solving Maxwell's equations both inside and outside the expanding plasma sphere and matching the two solutions at the plasma-vacuum interface, r=R(t). The external solution is easily obtained and the far-field power radiated into a solid angle $d\Omega$ is

$$dI = \frac{B_c^2 \sin^2\Theta}{4\mu_c} \frac{(F'')^2}{c^3} d\Omega \qquad (1)$$

where F is an arbitrary function of the retarded argument t-r/c and the primes on F denote differentiation with respect to the argument. For the internal solution, we use directly the results given by Bernstein and Fader (3) to deduce, after many approximations, that

$$F = R^3 \left\{ 1 - \frac{4}{\pi^{1/2}} \left(\frac{R}{\ell} \right) + \frac{3}{2} \left(\frac{R}{\ell} \right)^2 \right\} \qquad (2)$$

for values of $R < \ell/2$, the length ℓ being given by

$$\ell = \left(2\mu_0 \bar{J}_a R^3 \dot{R}_a \right)^{1/2} \qquad (3)$$

where the subscript "a" refers to the asymptotic phase of the expansion. Inserting this value of F into the far field approximation eq.(1) gives the radiated power.

As the plasma temperature drops during the expansion, penetration of the magnetic field into the plasma volume begins to occur. During this time, a certain number of electrons escaping from the plasma will be reflected back into the plasma volume through helical trajectories. Multiplication of the average intensity of radiation for a single electron in cyclotron motion (4) by the number of electrons escaping from the plasma volume gives, after a detailed calculation, the total intensity radiated into a solid angle $d\Omega$,

$$dI = \frac{63\pi^2 n e^3 B_0 R^2}{2048 \varepsilon_0 m c^3} \left(\frac{2kT}{\pi m} \right)^{3/2} d\Omega \qquad (4)$$

where it has been assumed that observation is normal to the magnetic field and $(v/c)^2 << 1$.

After the magnetic field has diffused into the volume, we would expect volume cyclotron radiation to occur. Integration

of volume cyclotron radiation from an elementary volume dT of plasma (5) over the plasma sphere gives

$$dI = \frac{e^4 B^2 n k T R^3}{12\pi\varepsilon_0 m^3 c^3}\left\{1 + \frac{1}{5}\left(\frac{R}{r}\right)^2\right\} d\Omega \qquad (5)$$

for observation normal to the magnetic field.

The total contributions of the dipole, surface and volume cyclotron radiation are plotted in Figure 4. The conductivity in these calculations has been the scalar conductivity associated with the free expansion. During the peak of the radiation signal, the $\omega\tau$ correction is significant since $1 + (\omega\tau)^2$ is of the order of 10 or higher, thus leading to a smaller value of $\bar{J}$ which should appear in equation (3). This effect is also offered as a tentative explanation for the trend of the measured radiation intensity in figure 5 toward a linear dependence for higher values of magnetic field. The radiation intensity illustrated in figure 4 was obtained by adjusting the relative contributions of the dipole and surface cyclotron radiation to fit the general shape of the experimentally measured form. A detailed fit is difficult. This is understandable in view of the crudeness of the model used to calculate the radiation history, the limited experimental data available, and the lack of knowledge of the surface number density required to calculate the surface cyclotron radiation. A more meaningful problem would involve the study of the interaction with uniform magnetic field when spherical symmetry

of the expanding plasma is not assumed. This is presently being pursued.

2. Two-Stream Instability in Laser Produced Plasmas (6). Freely expanding laser produced have large directed energy to thermal energy ratios. The expansion of such a plasma into a quiescent background plasma is being studied both experimentally and theoretically to investigate the properties of two-stream instabilities and possible existence of collisionless shock waves (7,8).

Our experiment utilizes a cesium, Q-machine plasma, as a background for the expansion of an aluminum plasma formed by focusing a 40 MW, 20 nsec. wide ruby laser pulse onto a 20 micron thick aluminum wire. The hot plasma produced from the vaporization of the aluminum wire rapidly cools as the thermal energy absorbed from the incident radiation goes into directed energy of expansion. After a few nanoseconds the aluminum plasma is expanding with its asymptotic expansion velocity. The Q-machine used in this experiment is a single ended, pulsed emitter type, similar to one built at Columbia University (9). The laser beam is focused onto the wire which is located at the center of the cesium plasma column. Alignment is done by means of an auxilliary gas laser. The expansion of the laser plasma is monitored by floating double probes located along the axis of the Q-machine.

The experiments are conducted in a low axial field (B=100 gauss) in order to minimize the effects of the magnetic field. The results

of the experiment, summarized in figure 6, show four typical probe traces taken at different background conditions. A definite decrease of the peak current was noted as the background density was increased. Apparently the presence of the cesium plasma caused a number of the free streaming aluminum ions to be either deflected or slowed down.

The mean free path for coulomb scattering is given by:

$$\lambda \quad \frac{1.9 \times 10^{12} W^2}{n \ln \Lambda}$$

where W is the energy of relative motion of the two interacting particles and n is the density of scatterers. Since the measured aluminum expansion velocity is about 5 x 10^6cm/sec., the cross section for aluminum-cesium coulomb collisions is very small yielding mean free paths on the order of 10^4cm. Thus the observed particle scattering cannot be explained on the basis of simple Coulomb scattering.

An analysis was undertaken to find out whether the experimental results could be explained on the basis of a two-stream instability. Following Stringer (10) the dispersion relation for a many component, one-dimensional, homogeneous plasma may be written as:

$$k^2 + \sum_j \left(\frac{\Omega_j}{C_j}\right)^2 I\left[\left(\frac{\omega}{k} - U_j\right)/2^{1/2} C_j\right] = 0$$

where $\Omega_j^2 = 4\pi n_j e_j^2 / m_j$ (plasma frequency of each component)

$C_j =$ sound speed of each component

$U_j =$ drift velocity of each component

$$I(z) = 1 + i\pi^{1/2} z\, w(z)$$

where $W(z)$ is the error function of complex argument.

In applying this relation to our experiment the following assumptions were made:

1. The electron and ion-temperatures of the cesium plasma are equal.

2. The electron and ions in the laser plasma are expanding at the same velocity.

3. Since the temperature of the cesium plasma is T=.25ev., the electron thermal velocity of the cesium plasma was taken to be five times greater than the expansion velocity of the aluminum plasma.

The dispersion relation was solved for various electron and ion temperatures in the laser plasma and for several density ratios of cesium plasma to laser plasma. For a given density ratio, plots of the instability regions and various growth rates were made as functions of two parameters, the electron, ion temperature ratio- T_e/T_i, and the ratio of directed velocity to electron thermal speed for the expanding plasma, V/C_e. A typical instability plot is shown in figure 7 for a density ratio (aluminum density/ cesium density) $N_1/N_2 = 10$. For a streaming velocity of 4×10^6 cm/sec., a representative growth rate is $\gamma \sim 5 \times 10^{-5} \Omega_{pe}$ which gives interaction distances of approximately 10 cm. for a streaming density of $4 \times 10^{11} cm^{-3}$. Measured interaction distances are from 6 to 10 cm. this giving reasonable agreement.

From the measured probe currents, we estimate the density of the expanding plasma to be no more than about $5 \times 10^{11}/cm^3$ thus

giving typical density ratios of 10 to 100. The growth rate of the instability versus the density ratio is plotted in figure 8 for the particular case $T_e/T_i = 10^4$ and given V/C_e. As a matter of interest we plotted the number of particles collected in the main peak of the probe traces versus background density, this plot is shown in figure 9. In this plot N refers to the particles collected with background cesium and N_o to the number of particles collected with no background plasma, In figure 9 we see that the number of particles lost roughly follows an $\exp\left(-xn^{1/2}\right)$ dependence characteristic of a two-stream instability rather than the $\exp\left(-\gamma n\right)$ dependence to be expected for coulomb scattering, again re-affirming the fact that coulomb scattering of the ions is not responsible for the observed particle loss.

The experiment then leads us to the following conclusions:

1. Laser produced plasmas can be two-stream unstable even when expanding into much lower density plasmas.

2. Collisionless shock waves will be difficult to produce using laser plasmas unless much higher density background plasmas are used than were used in this experiment. In the case of higher density background plasmas snow plowing can be expected to play an important role.

The effect of a strong axial B-field in the interaction of the two plasmas is presently being studied.

REFERENCES

1. Dunn, H.S., and Lubin, M.J., "Electromagnetic Radiation from a Laser Produced Plasma Expanding into a Uniform Magnetic Field", J. of Plasma Physics (accepted for publication).
2. Lubin, M. J., Dunn, H. S., and Friedman, W., Third Conference on Plasma Physics and Controlled Nuclear Fusion Research, Novosibirsk, U.S.S.R. (1968).
3. Bernstein, I. A., and Fader, W. J., Phys. Fluids 11, 2209 (1968).
4. Landau, L. and Lifshitz, E., Classical Theory of Fields, Addison-Wesley (1960).
5. Bekefi, G., Radiation Processes in Plasmas, John Wiley and Sons (1966).
6. Soures, J., and Lubin, M., "Observation of Two-Stream Instability in a Laser Produced Plasma", submitted for publication in Phys. Fluids.
7. Dawson, J., Phys. Fluids 7, 981 (1964).
8. Koopman, D. W., and Tidman, D. A., Phys. Rev. Lett. 18, 533 (1964).
9. Korn, P., Marshall, T. C., and Schlesinger, S. P., Rev. Sci. Inst. 39, 1085 (1968).
10. Stringer, T. E., Plasma Physics 6, 267 (1964).

FIGURE CAPTIONS

1. Oscilloscope Trace of Far Infrared Radiation Emitted from Laser Plasma Expanding in a Uniform Magnetic Field

2. Geometry of Expanding Plasma for Dipole Calculations

3. Computed Time-History of Expanding Laser Plasma

4. Computed Radiation History

5. Measured Values of Far Infrared Radiation Intensity in a Uniform Magnetic Field

6. Typical probe signals due to laser produced plasma expanding against background Cesium Plasmas. Sensitivity is 10 ma/division, .5 sec/division, (a) no background plasma, (b) background density of $4 \times 10^9/cm^3$, (c) background density of $1.2 \times 10^{10}/cm^3$, (d) background density of $2.7 \times 10^{10}/cm^3$.

7. Stability conditions for aluminum streaming into a background cesium plasma, density ratio (aluminum/cesium) = 10. The parameters V/C_e and Ti/T_e and the plasma frequency, , refer to values for the streaming aluminum plasma, is the growth rate of the fastest growing waves.

8. The maximum growth rate for $T_e/T_i = 2.5 \times 10^3$ plotted as a function of the ratio N_2/N_1 = (cesium/density/ aluminum density).

9. Measured particle loss versus background cesium plasma density.

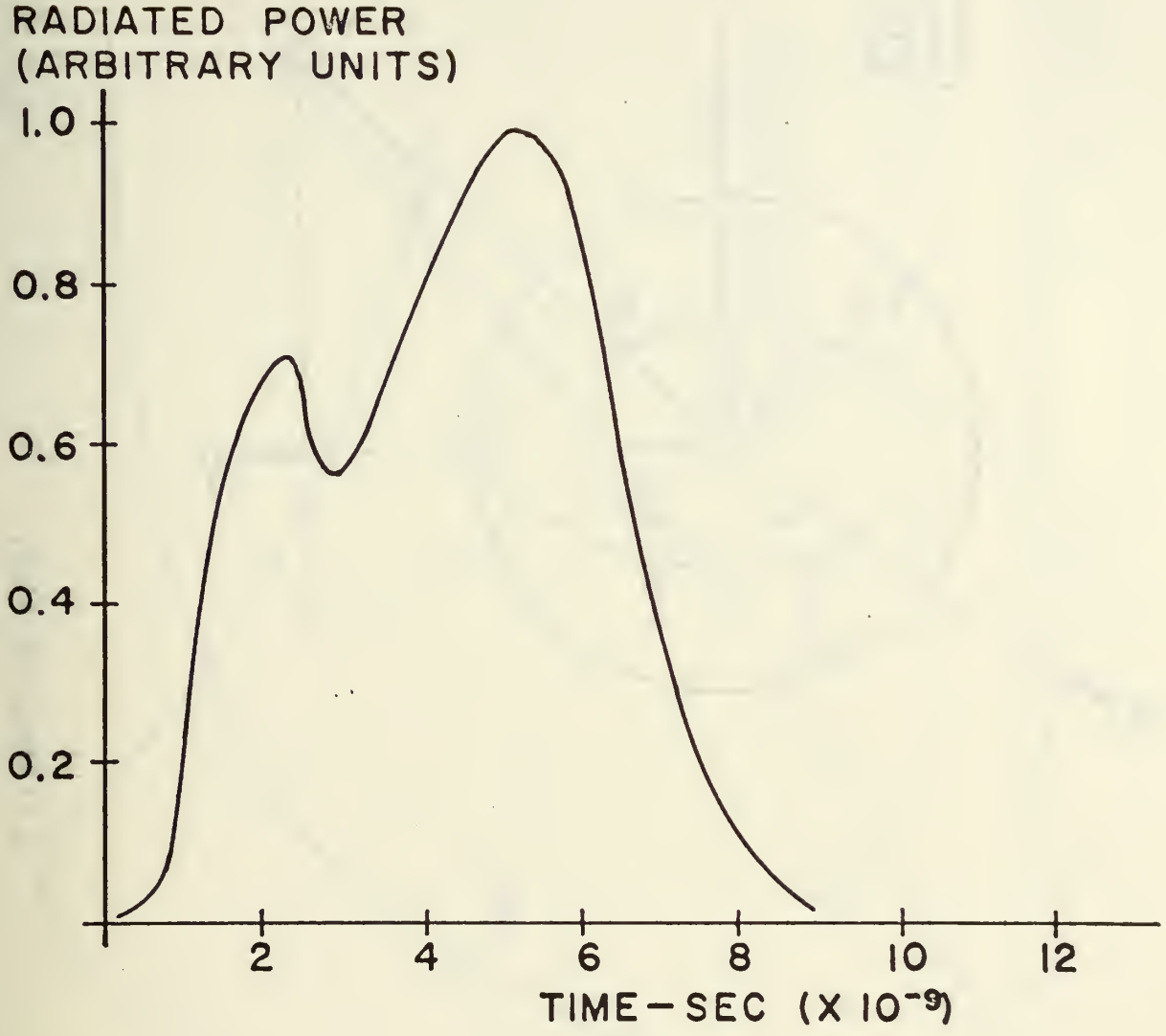
RADIATED POWER
(ARBITRARY UNITS)
1.0
0.8
0.6
0.4
0.2
2
4
6
8
10
12
TIME – SEC (X 10⁻⁹)

Figure 1.

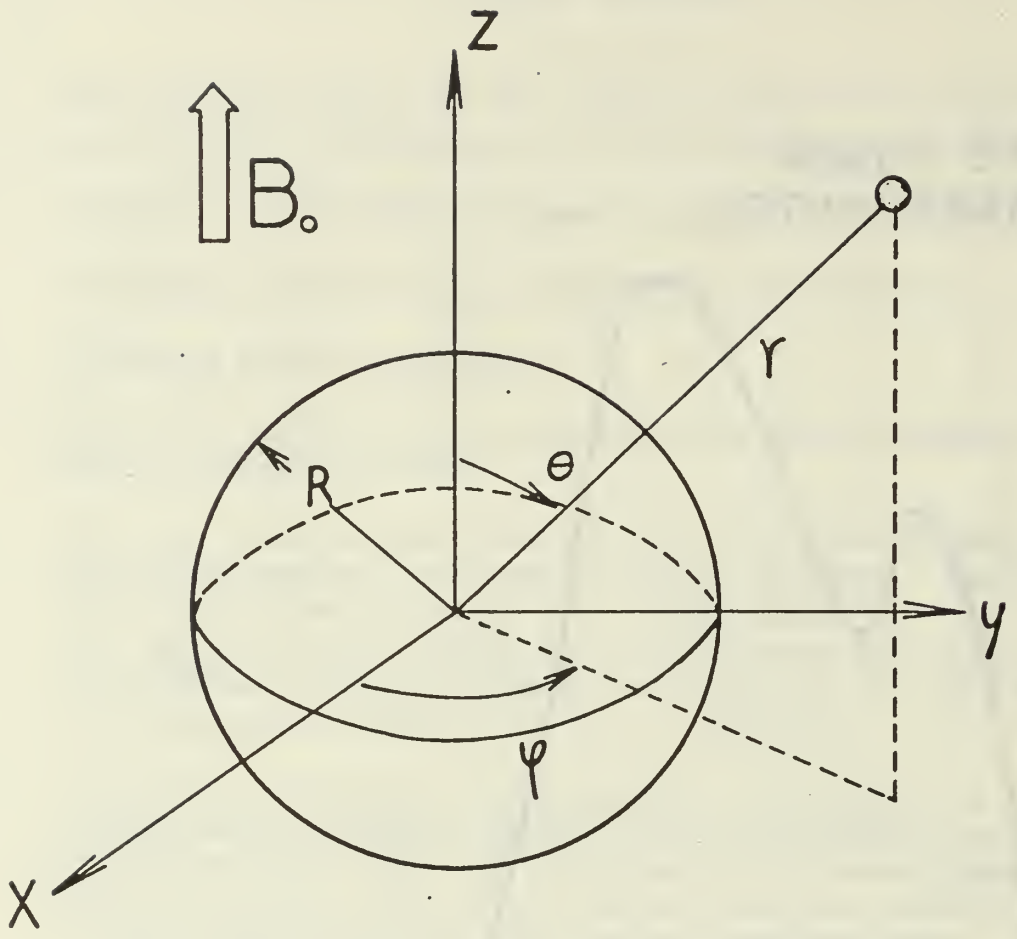

FIG. 2

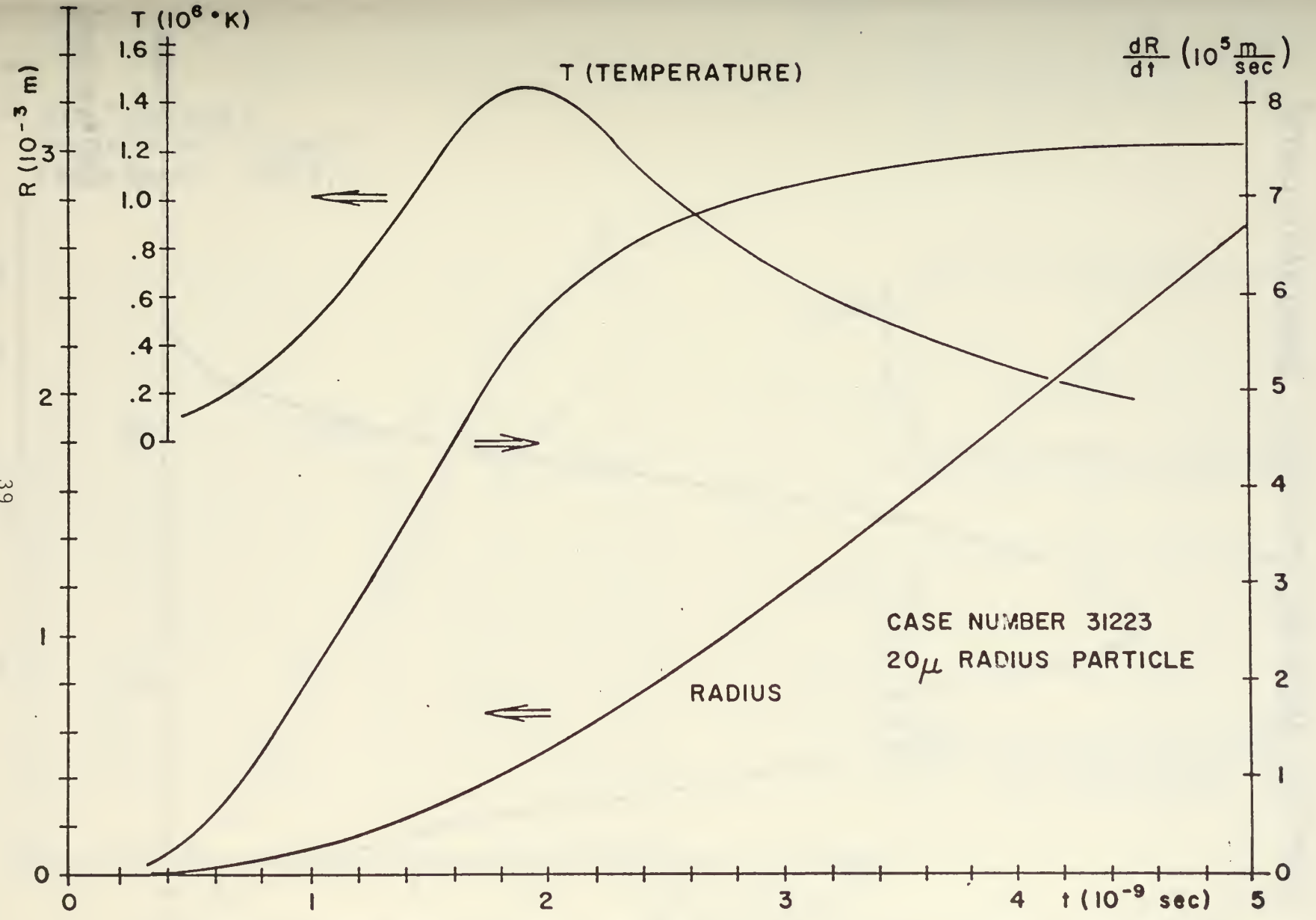
T (10^6 °K)
T (TEMPERATURE)
$\frac{dR}{dt}$ ($10^5 \frac{m}{sec}$)
R (10^{-3} m)
CASE NUMBER 31223
20μ RADIUS PARTICLE
RADIUS
t (10^{-9} sec)

Fig 3

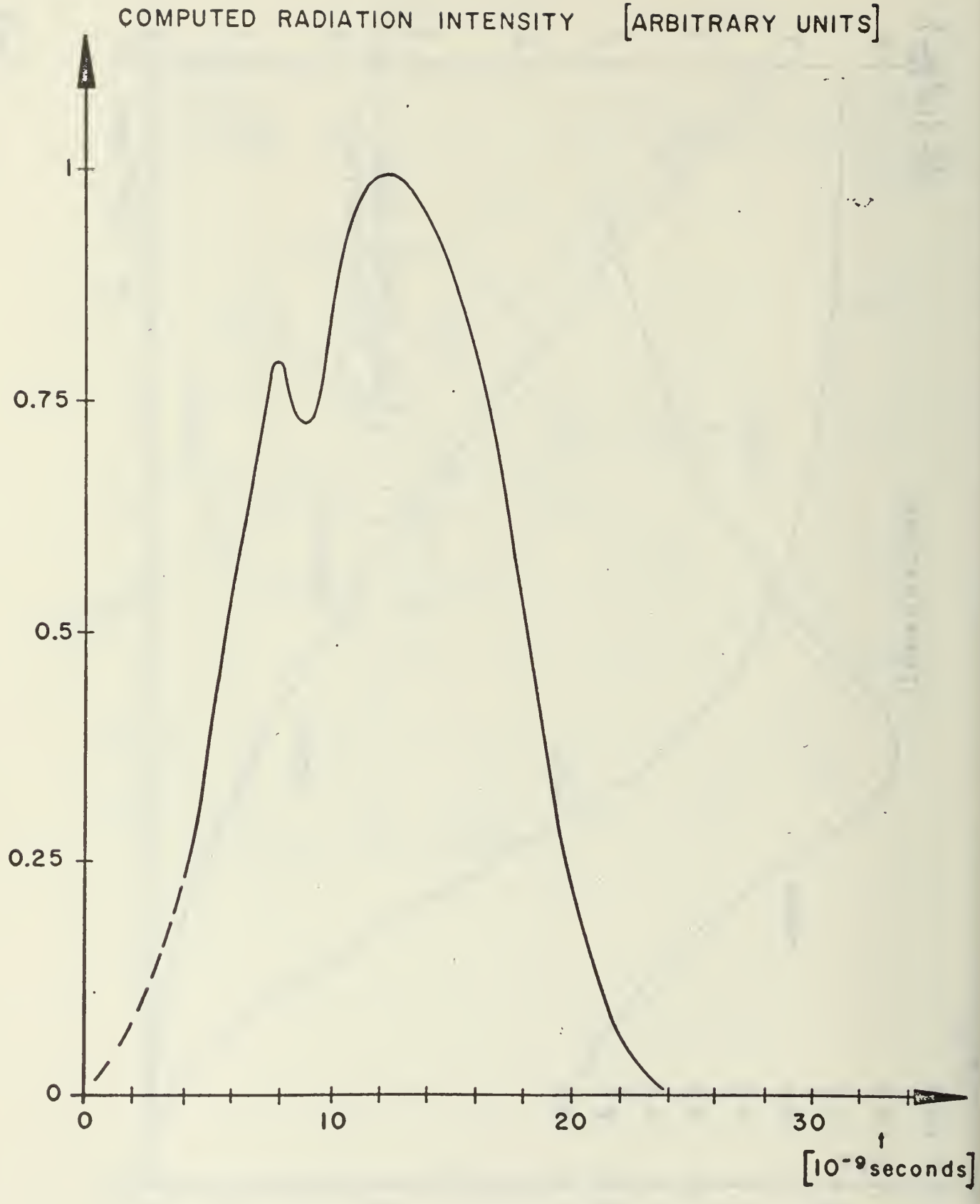
COMPUTED RADIATION INTENSITY [ARBITRARY UNITS]
1
0.75
0.5
0.25
0
0
10
20
30
t
[10⁻⁹ seconds]

Fig. 4

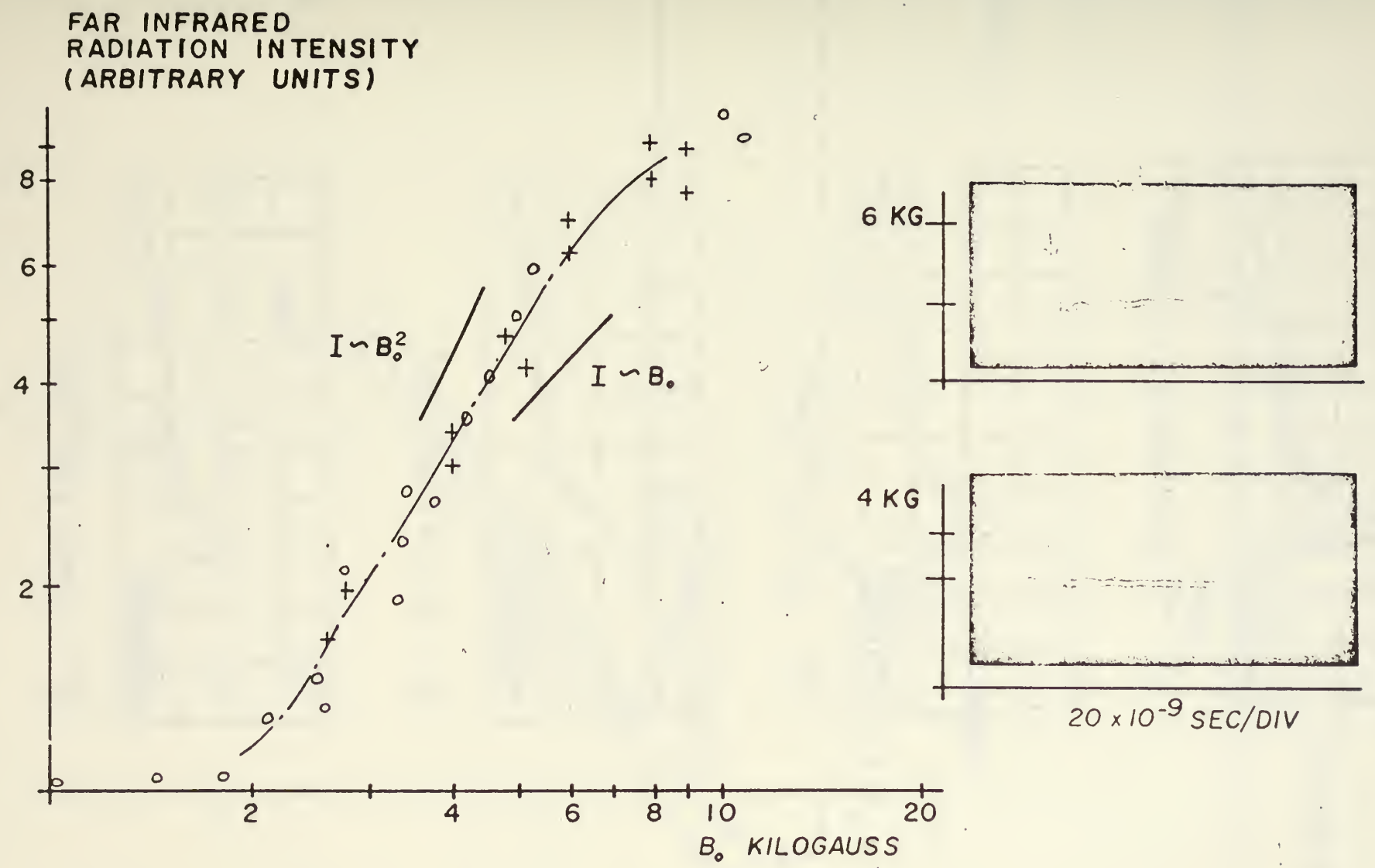
FAR INFRARED
RADIATION INTENSITY
(ARBITRARY UNITS)
8
6
4
2
I ~ B₀²
I ~ B₀
2
4
6
8
10
20
B₀ KILOGAUSS
6 KG
4 KG
20 x 10⁻⁹ SEC/DIV

Figure 5

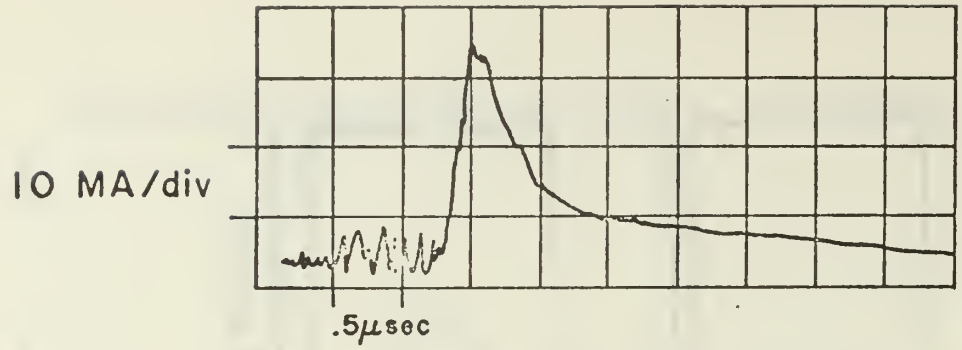

(a) NO BACKGROUND PLASMA

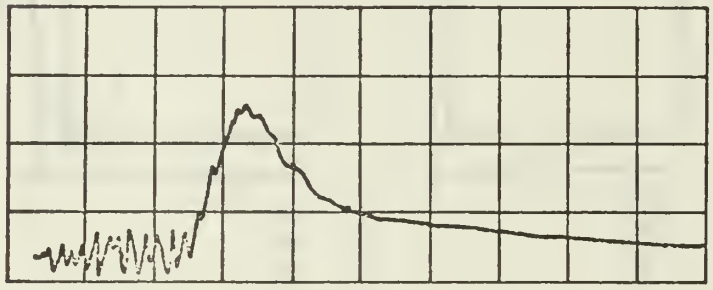

(b) $N_e = 4 \times 10^9/cm^3$

(c) $N_e = 1.2 \times 10^{10}/cm^3$

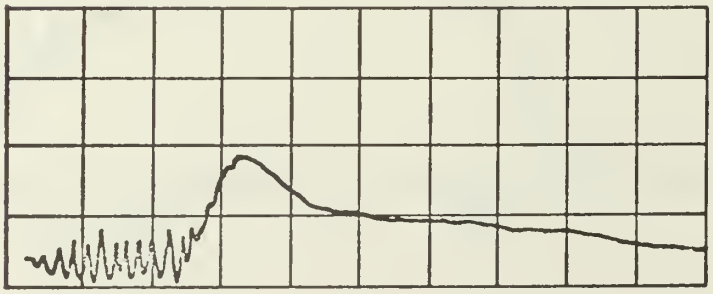

(d) $N_e = 2.7 \times 10^{10}/cm^3$

FIG. 6

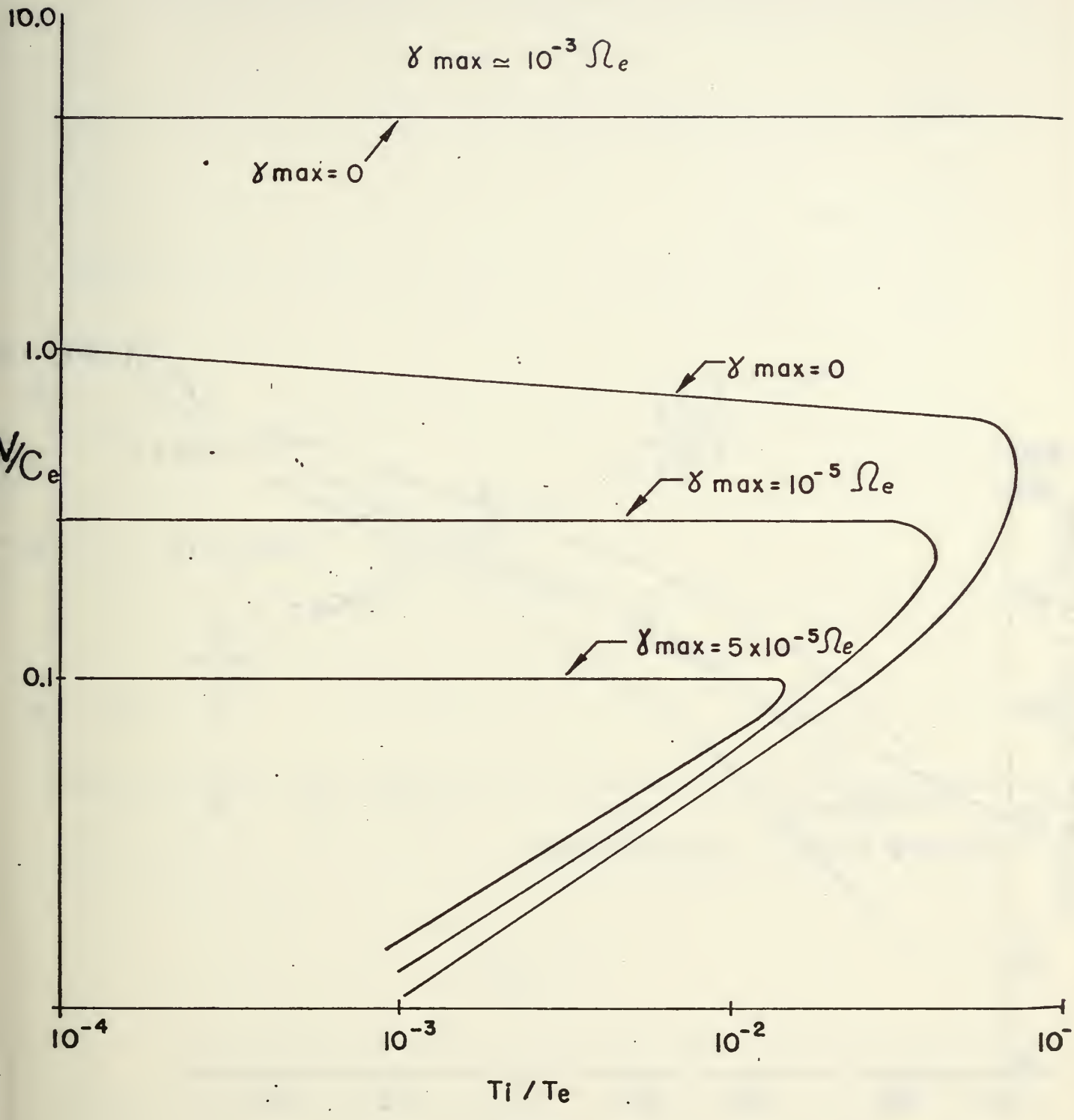
10.0
1.0
0.1
γ max ≃ 10⁻³ Ωe
γ max = 0
γ max = 0
γ max = 10⁻⁵ Ωe
γ max = 5 x 10⁻⁵ Ωe
V/Ce
10⁻⁴
10⁻³
10⁻²
Ti / Te

Figure 7

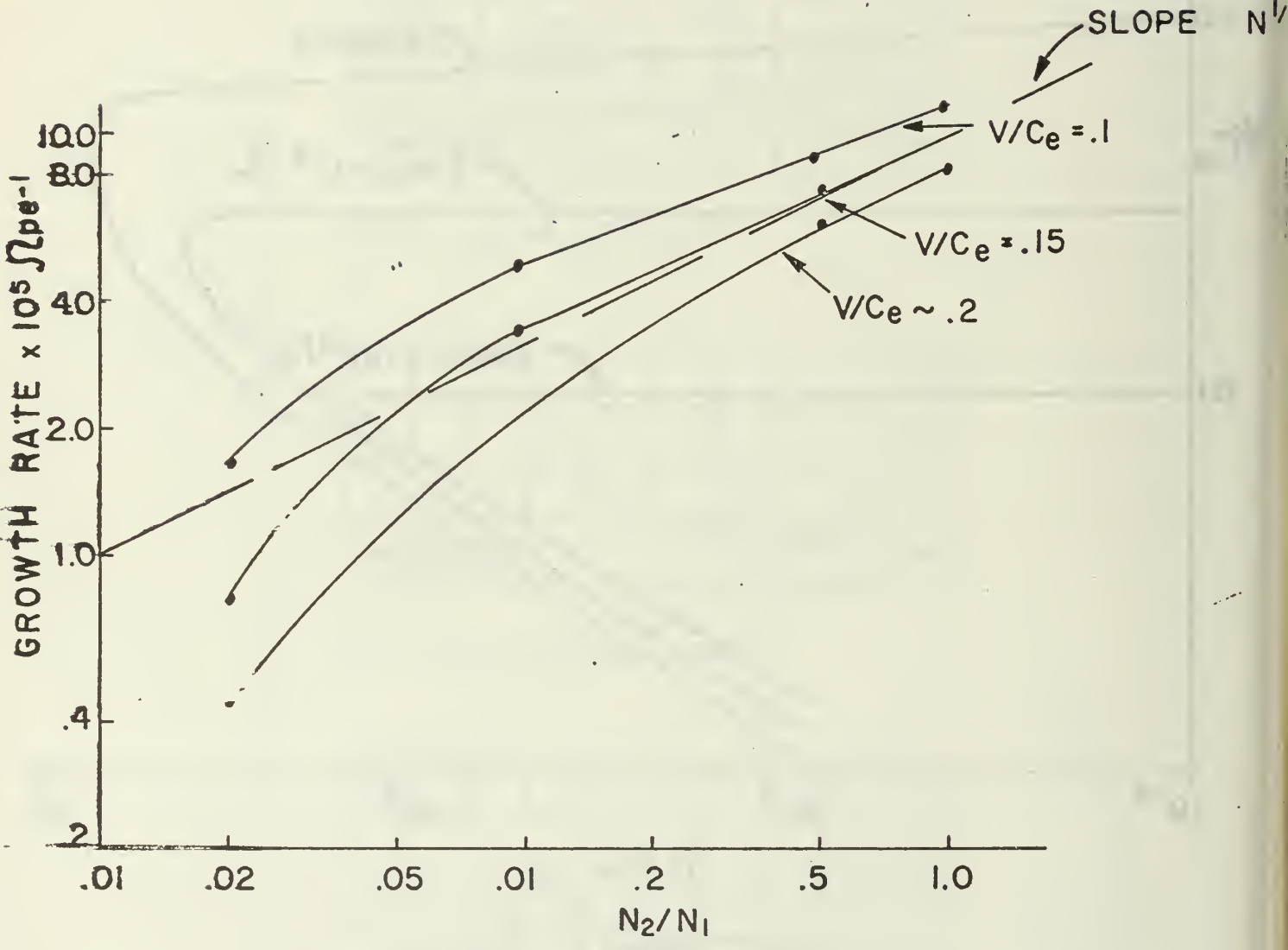
SLOPE N1/
V/Ce = .1
V/Ce = .15
V/Ce ~ .2
GROWTH RATE x 10^5 Ωpe^-1
10.0
8.0
4.0
2.0
1.0
.4
.2
.01
.02
.05
.01
.2
.5
1.0
N2/N1

Figure 8

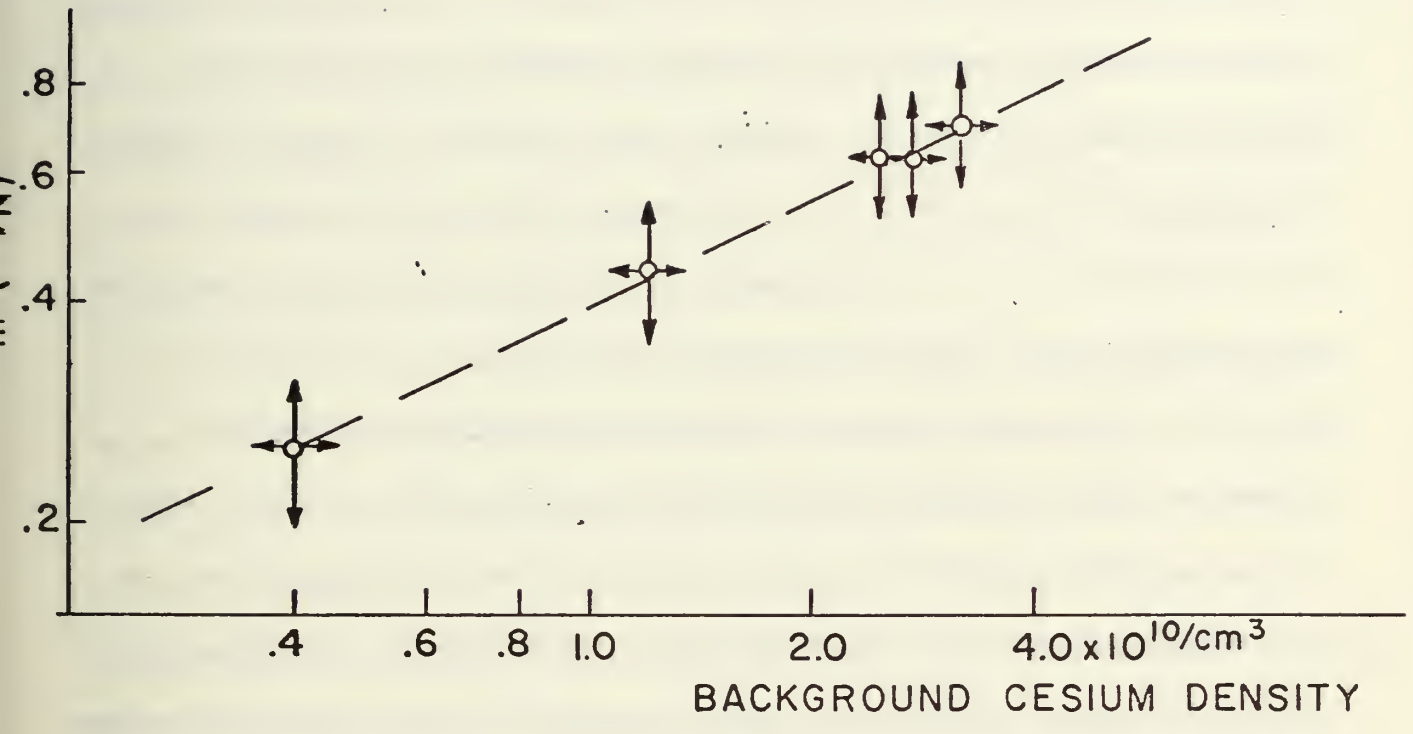

Figure 9.

LASER CREATED PLASMA AND COLLISIONLESS SHOCK WAVE PHENOMENA

by

F. Schwirzke and A. W. Cooper
Naval Postgraduate School, Monterey, California

1. Introduction

Collisionless shock waves are an important mechanism in heating plasmas to temperatures and densities of thermonuclear interest. Laser production of plasma is now being applied to the problem of investigating collisionless shocks in a laboratory plasma. A steady state collisionless plasma is formed in a hollow cathode arc facility. Collisionless shocks are produced by the rapid expansion of a hot plasma obtained by focusing a giant laser pulse on the tip of a small target. The expanding laser plasma acts as a very fast piston to produce the collisionless shock. The adjustable experimental parameters include background plasma density, external magnetic field, ion mass, Alfvén velocity, electron temperature, and the velocity of the expanding plasma. By thus varying the magnetic Mach number the structure and damping mechanisms of the collisionless shock can be studied in an effort to deduce the collisionless mechanisms of energy dissipation and its effectiveness in thermalizing the ordered wave motion.

2. Dynamics of a Laser Created Plasma Expanding in a Magnetic Field

The two problems of creating and confining a high temperature plasma in a magnetic field configuration are usually closely linked together and a laser produced plasma is no exception. Theoretical calculations[1-3] and experimental

results[4-10] show that energy from a giant laser pulse can be absorbed by a small target within a few nonoseconds, thus creating a high temperature plasma. Obviously the next step is then to investigate the interaction of the expanding plasma with a magnetic field. This interaction is of special importance in the controlled thermonuclear research program where the purpose is to confine a thermalized hot plasma in a stable magnetic field configuration. In the experiments to be discussed[10] the plasma was produced by impact on a 30 micron glass fiber of a 20 nsec, 150 MW pulse from a neodynium glass laser with no background plasma. About one joule of energy was absorbed in a plasma of 10^{16} atoms, giving an expansion velocity of about 10^7 to 10^8 cm/sec, and initially a plasma-to-magnetic pressure ratio of order 10^7.

a. The expansion of the $\beta \approx 10^7$ plasma can be described by hydrodynamic theory. The temperature decreases rapidly according to the form $T_r = T_o(r_o/r)^2$, where T_o and r_o are the temperature and radius of the plasma when it ceases to absorb laser energy. Most of the energy content of the plasma appears as kinetic energy of expansion. The rapid decrease of the plasma temperature implies that an asymptotic plasma expansion velocity is reached in a rather short time while $\beta >> 1$. This explains the observed asymptotic expansion velocity being the same with and without a magnetic field.

b. The expansion of a plasma in the presence of a magnetic field has been treated theoretically, and an oscillation or bounce of the plasma against the field predicted at the condition of $\beta \approx 1$[11]. Experimental observations are in approximated agreement with this result[10]. An expanding plasma of infinite conductivity

would repeatedly bounce off the compressed B where $\beta \approx 1$. With finite resistivity, diffusion across B will also occur. Hence, the bounce radius and the characteristic width for the pressure gradient in the wave front are determined by the effective resistivity. This means a laser produced plasma which expands across a magnetic field also reveals extensive new possibilities for the investigation of instabilities and turbulence in the wave front[12,13].

c. Resistive effects associated with surface currents in the wave front form the most effective means of rethermalization of the directed kinetic energy of expansion. In addition, if the growth rate becomes greater than the electron Coulomb collision frequency ν_e, instabilities may develop in the front and also contribute very effectively to the energy dissipation process.

The two-stream instability will start where the current-associated mean ordered velocity of the electrons in the wave front becomes larger than the mean thermal velocity. The current is in the direction perpendicular to B and to the normal of the wave front. The two-stream instability has a large growth rate $\gamma \approx \omega_{pe}(m/M_i)^{1/3}$ and may develop if $\nu_e < \gamma$, where ω_{pe} is the plasma frequency and m and M_i are the electron and ion mass. The growth time of the two-stream instability is rather small in comparison with the propagation time of the wave which is in the order of

$$\tau \approx 10\ (c/\omega_{pe}V_A)$$

Here V_A is the Alfvén velocity, $d \approx 10\ c/\omega_{pe}$ is of the order of the characteristic width of the front when the resistivity of the plasma is determined by the presence of the instability, c is the volocity of light. If $\gamma\tau >> 1$ a steady state will exist

within the wave front and the onset of the instability can be studied locally by considering the perturbed motion of the ions and electrons by means of the equations of the two-fluid theory.

Considering a stationary wavefront which is common to shock theory, (see figure), propagating in the r-direction across the magnetic field, the electric current is perpendicular to B and r in the θ direction and is given by Maxwell's equation

$$j = -enV_{e\theta} = -(c/4\pi)dB/dt.$$

Substituting $\omega^2_{pe} = 4\pi ne^2/m$ and $K = |(1/B)dB/dr)|$ where K is inversely proportional to the width of the front d, the criterion for the onset of the two-steam instability, $V^2_{e\theta} > kT_e/m$,

becomes: $$d < (\pi c/\omega_{pe})(2/\beta)^{1/2} \qquad (1)$$

where $\beta = (8\pi nkT_e/B^2)$. Criterion (1) will be satisfied at a certain radius since n and T_e decrease rapidly during the expansion of the laser produced plasma. In agreement with these discussions the measurements[12,13] indicate that the two-stream instability enhances the resistivity in the wave front by more than two orders of magnitude and thus determines the width of the wave front of about $d \approx 13c/\omega_{pe}$. The discrepancy between the values of T obtained from the magnetic probe signal and from the effective conductivity as estimated from the width of the front also indicates that a collisionless mechanism is contributing to the energy dissipation.

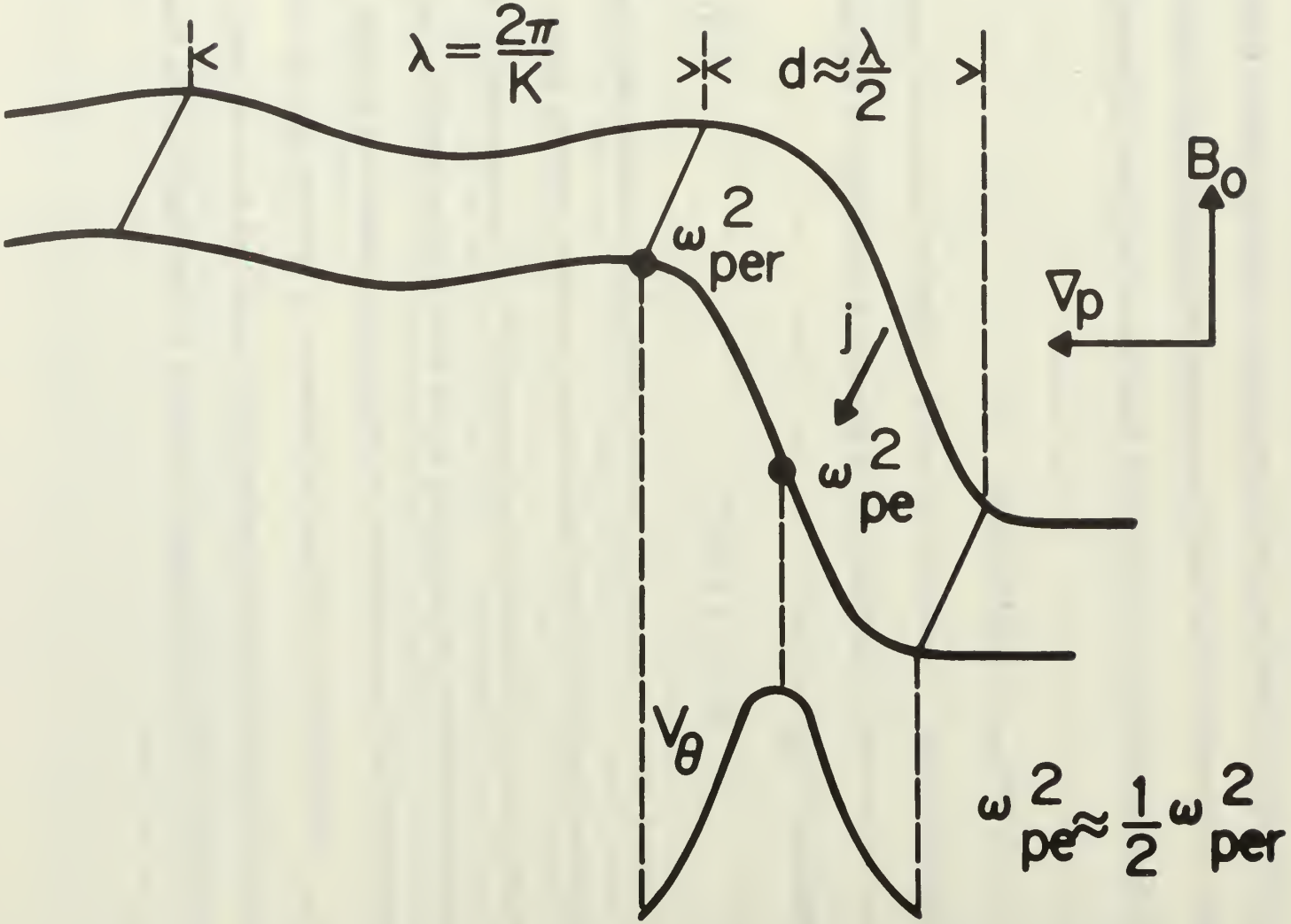

STRUCTURE OF THE WAVE FRONT (SCHEMATIC)

3. Conclusions

Theory and experiment have shown that a laser produced plasma can be used to study turbulent energy dissipation mechanisms and collisionless shock wave phenomena. However, experimentation requires higher power levels, and therefore the laser system is now being expanded to about 1 GW by addition of an amplifier stage.

4. References

1. Basov, N. G. and Krokhin, O. N., Proceedings of the Conference on Quantum Electronics, Paris, Vol. 2. 1373 (1963).

2. Dawson, J. M., Phys. Fluids 7, 981 (1964).

3. Hora, H., Institut fur Plasmaphsik, Garching bei München, IPP/6/23 (1964).

4. Ascoli-Bartoli, U., et. al., Plasma Physics and Controlled Nuclear Fusion Research, Vol. II, 941 (1965).

5. Haught, H. F. and Polk, D. H., Phys. Fluids 9, 2047 (1966).

6. Lubin, M., Bull. Am. Phys. Soc. 13, 320 (1968).

7. Tuckfield, R., and Schwirzke, F., Bull. Am. Phys. Soc. 13, 320 (1968).

8. Schwirzke, F., and Tuckfield, R., Bull. Am. Phys. Soc. 13, 1553 (1968).

9. Sigel, R., Buchl, K., Bulser, P. and Witkowski, S., Phys. Letters, 26, 498 (1968).

10. Tuckfield, R. G., Schwirzke, F., Plasma Phys. 11, 11 (1969).

11. Bhadra, D. K., Phys. Fluids 11, 234 (1968).

12. Schwirzke, F., Tuckfield, R. G., Phys. Rev. Letters, 22, 1284 (1969).

13. Schwirzke, F., Proc. III Europ. Conf. on Controlled Fusion and Plasma Phys., Utrecht, The Netherlands, 114 (1969). Wolters - Noordhoff Publ. - Groningen.

STREAMING PLASMA INTERACTION WITH LONGITUDINAL MAGNETIC FIELDS

J. G. Siambis
Carnegie-Mellon University
Pittsburgh, Pennsylvania 15213

It is well known that plasmas produced in theta pinches satisfy thermonuclear power requirements in two respects, density and ion temperature but not confinement time. In this work the transfer and flow of a plasma from a 5 KJ conical theta pinch gun is studied as it enters a rising longitudinal magnetic field. The maximum value of the single mirror magnetic field can be raised to 7 KG. The following diagnostics have been utilized, 70 GH microwave interferometer, STL image converter camera, spectroscopy, diamagnetic loops, photomultipliers and probes. Measurements have been carried out at the location of maximum magnetic field gradient. We find that the electron density rises from 10^{15} per cc for zero field to 7×10^{15} per cc for 3 KG at the measurement location. The electron temperature rises at first from 6.7 ev to a maximum of 12 ev at 1 KG and then falls to a value of 2 ev for the maximum field of 3 KG, while the ion temperature as obtained from the diamagnetic loop measurement increases throughout this range. The front velocity of the plasmoid is found by probe measurements to be 5×10^{6} cm/sec. One of the objectives of these measurements is to establish the occurance of a shock wave in the transition from supersonic to subsonic flow in the plasmoid. (see Figure 1) Further modifications in

the system will incorporate a guide field between the gun and the mirror field and thus minimize the interaction with the tube walls.

The theoretical work is concerned with the propagation and stability of drift waves in realistic magnetic field configurations. Results have been published[1] which elucidate the effect of shear on the stability of drift waves in stellarator and levitron type geometries. Further work in progress takes into account the variation of magnetic field along the field lines and drift-Alfven waves are also considered.

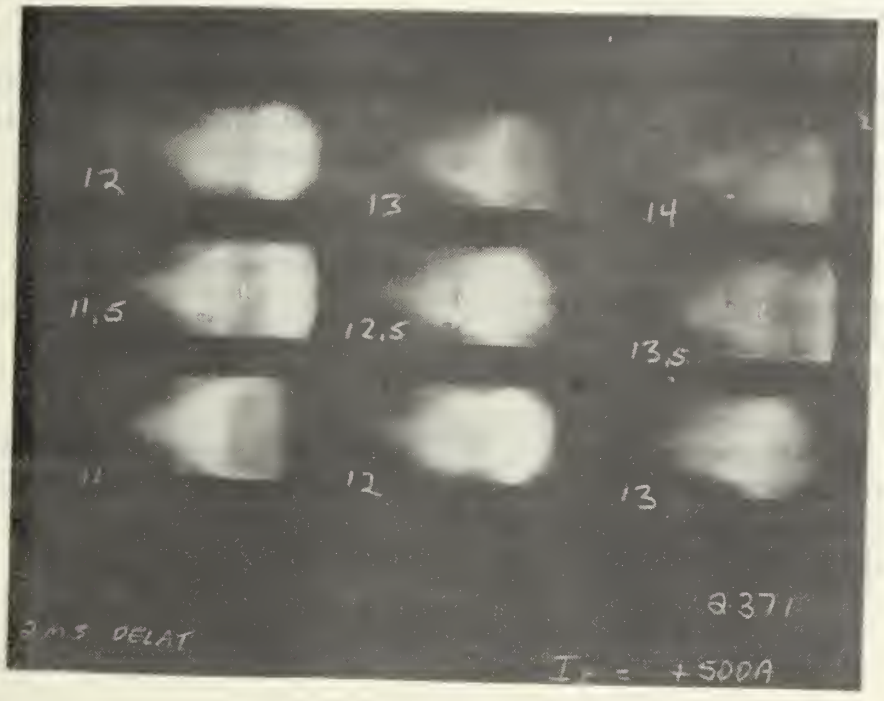

Figure 1. Image converter camera pictures of plasma flow from plasma gun (right) to converging longitudinal magnetic field (left). The time is shown in microseconds with each picture. The converging magnetic field to the left has a value of 3 KG, and is the location of maximum magnetic field gradient.

[1] J. G. Siambis, Phys. Fluids 12, 1971 (1969)

PANEL 2. TURBULENCE AND WAVES

Name	Topic
Dr. A. Anastassiades Nuclear Research Center Greek Atomic Energy Commission Aghia Paraskevi, Attikis Athens, Greece	
Dr. Winston Bostick Department of Physics Stevens Institute of Technology Hoboken, New Jersey 07030	Vorticity and Neutrons in the Plasma Focus
Dr. Robert A. Gross Dept. of Applied Science & Engineering Columbia University New York, N. Y. 10027	Hydromagnetic Heating of Plasma for Production of Controlled Fusion Reactions
Dr. Norman C. Jen City College Research Foundation City University of New York New York, N. Y. 10031	Plasma Turbulence Research
Professor O. K. Mawardi Department of Engineering Case Western Reserve University Cleveland, Ohio 44106	Heating and Accelerating Mechanisms in the Plasma Focussed Discharge

Vorticity and Neutrons in the Plasma Focus

W. H. Bostick, L. Grunberger, V. Nardi, and W. Prior
Stevens Institute of Technology, Hoboken, N.J., U. S. A.

Image converter photographs (5-nanosecond duration)of the current sheath in a plasma coaxial accelerator operated with D_2 at 8 torr show that the current sheath is corrugated and that there are imbedded in this sheath dense plasma filaments (see figures 1 and 2). Five-nanosecond time-and space-resolved spectroscopy shows that the light from these filamentary structures appears primarily as a continuum. The degree of broadening of the Hβ in the filaments places the electron density there > $10^{18}/cm^3$. The stream velocity $\underline{v}$ (relative to the current sheet) for mass flow ahead of and on the current sheath is of the same order of magnitude of the current sheet velocity in the laboratory frame ($\simeq 0.5 \times 10^7$ cm/sec). Evidence has been adduced[1] to suggest that these filaments, which are produced in pairs, coincide in space with regions where the magnitude $|\underline{\omega}|$ of the vorticity $\underline{\omega} = 1/2$ curl $\underline{v}$ assumes very high values. We refer to these filaments as plasma vortex filaments. Mass flow along the filaments from center conductor to outer conductor has been observed. Magnetic fields parallel and anti-parallel to this flow along the filaments have been measured. These magnetic fields occupy regions of space comparable in extent to the size of the filaments and are associated with the filaments. Magnetic probe measurements indicate that a large portion of the total current in the plasma coaxial accelerator is carried in the current sheath, and that the current sheath is about 2.5 mm. thick as compared with the filament diameter, which is about 1mm. The corrugated shape of the current sheath (figures 1 and 2) is an indication that a large fraction of the current carried by the sheath is actually carried by the filaments.

Schlieren photographs taken with a giant pulsed laser with an exposure time of about 25 nano-seconds show essentially the same features as the image converter camera shows and place the electron density in the filaments at a value of about 10 times the background density, or a filament density of $3 \times 10^{18} cm^{-3}$.

When the spacing between the vortex filaments is small enough, they annihilate in pairs, and at the plasma focus (figure 3) near the axis a general region of annihilation (enhanced illumination) starts at the end

of the center conductor and moves away from the center conductor along the axis at a speed of 1.5×10^7 cm/sec.

Two main neutron pulses occur: the first during the vortex annihilation along the axis while the bright region moves from the center conductor to the crown of the "umbrella". The second main neutron pulse is associated in time with the vortex annihilation occurring in the crown of the umbrella as the vortices "burn" pair by pair as a shock wave moves radially outward in the crown. This observed vortex annihilation is the authors believe, the laboratory scale version of the solar flare phenomenon. With this relatively small scale apparatus the neutron yield per pulse is about 5×10^8 neutrons. This yield is much less than that obtained by other experimenters[6,7] who use much higher energy storage.

On the basis of the experimental observations it seems reasonable to conclude that the observed "optical front" represents very well the geometric configuration of the region (of thickness $d \sim 1$mm) of sharp transition for mass density ρ pressure (isotropic) P, fluid velocity $\underline{v}$, and magnetic field $\underline{H}$.

Specifically, by considering as usual the shock front in the limit $d \to 0$, i.e. as a surface of discontinuity Σ (say) for these quantities, the most appropriate location of Σ is obtained by identifying Σ with the foremost face of the optical observed layer. The filaments which appear embedded in the optical front, i.e. immediately behind Σ, can be related closely theoretically, as we show here, to the shape of Σ.

Since the equations for the magnetic field and for the vorticity become the same under some circumstances[2] and even a relationship of proportionality between magnetic field and vorticity can be deduced for finite-conductivity compressible plasma[3] it is suggested that a similar relation can exist also for different or more general conditions and in particular for our flow-carrying filaments and the magnetic fields parallel or anti-parallel to the filaments.

The vorticity, $\underline{\nabla} \times \underline{v}_1$, behind the shock front (suffix o denotes conditions ahead of the shock, suffix 1 conditions behind it) can be evaluated in terms of the two "principal curvatures" of Σ; in terms of two shock strength parameters $\zeta = \frac{\rho_1}{\rho_o}$, $\alpha(H)$; and in terms of $\underline{v}_o$, $\underline{H}_o$.

A convenient form of the Newton's equation for stationary conditions ($\partial_t = 0$) and infinite conductivity ($\underline{E} = \underline{H} \times \underline{v}$ = the electric field in the plasma) is

$$(1)\quad (\underline{\nabla} \times \underline{v}_1) \times \underline{v}_1 = -\frac{1}{\rho_1} \underline{\nabla} P_1 - \frac{1}{2} \underline{\nabla} v_1^2 - \frac{1}{4\pi\rho_1} \underline{H}_1 \times (\underline{\nabla} \times \underline{H}_1)$$

The system of orthogonal curvilinear coordinates with unit vectors $\underline{\tau}_a$, $\underline{\tau}_b$, tangential to the "curvature lines" of Σ and $\underline{n}$ normal to Σ, is introduced ($\underline{A}_\tau$, $\underline{A}_n$ then indicate respectively the tangential and normal components of a vector $\underline{A}$ with respect to Σ).

Since $[(\underline{\nabla} \times \underline{v}_1) \times \underline{v}_1]_\tau = (\underline{\nabla} \times \underline{v}_1) \times \underline{v}_{1,n}$ and

$$(2)\quad \underline{\nabla} \times \underline{v}_1 = -[(\underline{\nabla} \times \underline{v}_1) \times \underline{v}_{1,n}] \times \frac{\underline{n}}{v_{1,n}} \text{ , the tangential component } \lambda\underline{\tau}_a + \mu\underline{\tau}_b \text{ of}$$

the right hand side of (1) is first estimated in order to obtain $\underline{\nabla} \times \underline{v}_1$.

All quantities $\rho_1, \underline{v}_1, \underline{H}_1, P_1$ can be expressed in terms of $\rho_o, \underline{v}_o, \underline{H}_o, P_o$, expressed by the jump (shock) conditions on Σ (deHoffman, Teller relations[4]). The leading contributions to λ, μ (the differential operators are transformed to curvilinear coordinates and "strong shock" conditions are assumed, $P_o \sim o$, enthalpy $i_o \sim 0$) have the form

$$\lambda \overset{\sim}{=} F(\rho_o, \underline{v}_o, \underline{H}_o, \alpha, \zeta) \frac{1}{R_a}, \mu \overset{\sim}{=} G(\rho_o, \underline{v}_o, \underline{H}_o, \alpha, \zeta) \frac{1}{R_b}$$

where $\frac{1}{R_a}$ and $\frac{1}{R_b}$ are the "principal curvatures" of Σ (at a point $\underline{x}$ the curvatures are taken positive when they are convex to the incoming flow) and

$\alpha = \frac{H_{1,a}}{H_{o,a}} = \frac{H_{1,b}}{H_{o,b}}$ if $\zeta > 1$. By substituting in (2) we have

$$(3)\quad \underline{\omega} = \frac{1}{2} \underline{\nabla} \times \underline{v}_1 \overset{\sim}{=} -\underline{\tau}_a \frac{\zeta}{2v_{o,n}} \frac{G}{R_b} + \underline{\tau}_b \frac{\zeta}{2v_{o,n}} \frac{F}{R_a}$$

If $\underline{\tau}_a$ is the vector with projection on the orthogonal-to-z plane, which is(approximately) collinear to the electrode radius R then, we have by experimental observation (see figures 1 and 2), that $\left|\frac{1}{R_b}\right| > \left|\frac{1}{R_a}\right|$ up to and during the first stage of the "rolling off" of the optical front onto the face of the center conductor. Here the filaments which are perpendicular to the azimuthal magnetic field predominate. Later at the final stage of collapse $\left|\frac{1}{R_a}\right|$ increases and $\left|\frac{1}{R_b}\right|$ decreases and it is now possible to see filaments in both the azimuthal and radial-axial directions (figure 3, note, "spider web" type of filamentary pattern). Correspondingly, during the earlier period, ω_a, which is collinear with the radial-

axial filaments, as dominant, but later both ω_r, which is parallel with the azimuthal filaments, and ω_z are influential.

The algebraic signs of the ω components depends on the signs of R_a, R_b (and also on the functions F,G). Both signs are certainly present behind S with a relative frequency apparently in agreement with the empirical observations.

In summary, equation (3) (which has a corresponding analogue in gas dynamic shocks[c]) shows that the existence of vorticity parallel to the observed filaments can be predicted as a direct consequence of the corrugated nature of the observed shock front.

In addition to the MHD solution one of the authors has obtained a solution to the Vlasov equation which gives the pairs of filaments with the expected mass flow structure and magnetic structure.

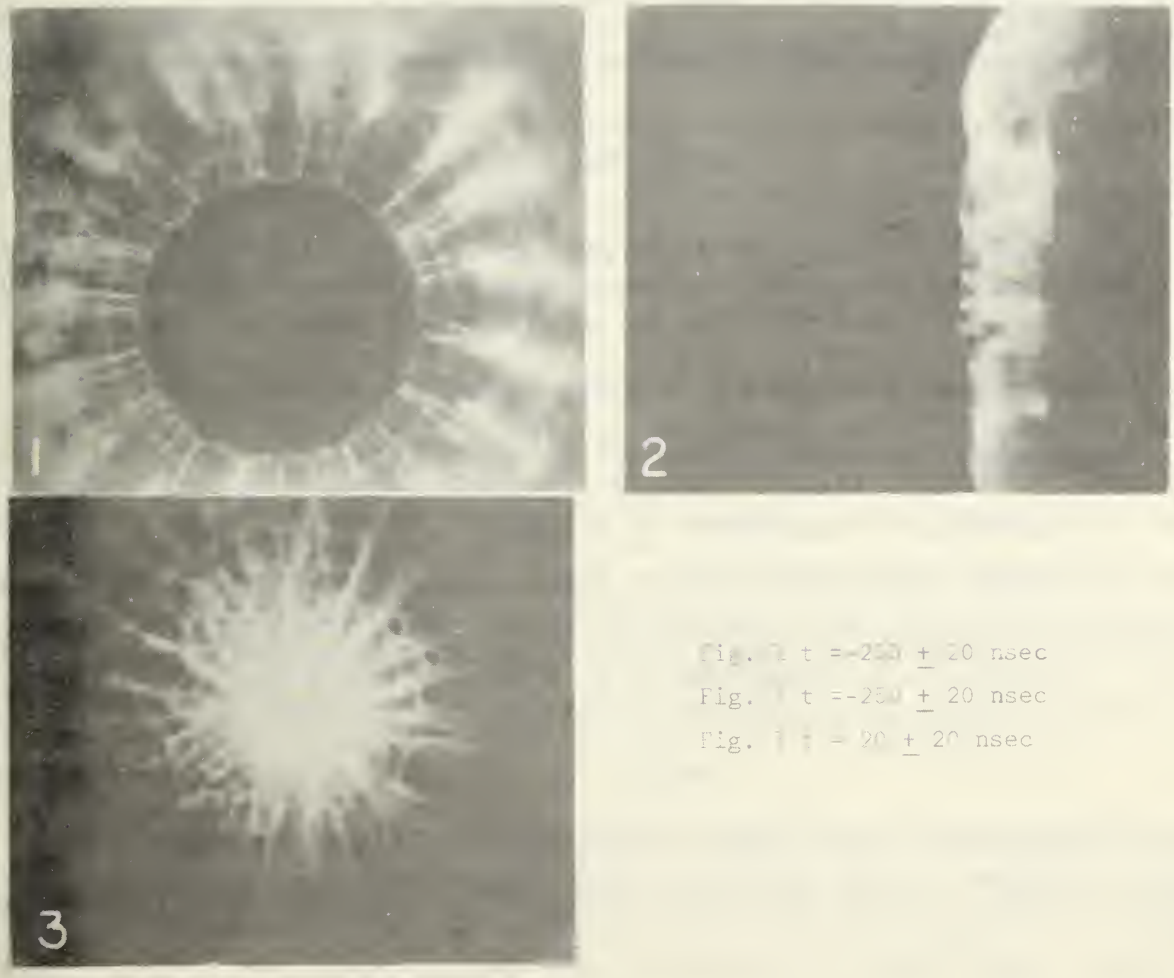

Fig. 2 t =-250 ± 20 nsec
Fig. 1 t =-250 ± 20 nsec
Fig. 3 t = 20 ± 20 nsec

Figure Captions

Figs. 1, 2. and 3 are 5-nanosecond exposure IC photographs of the PCA operated with 8 mm of deuterium. The time at which each picture was taken is indicated in terms of t = 0 coinciding with the first peak in the $\frac{dI}{dt}$ signal. Figures 1 and 3 are taken along the electrode axis z. Figure 2 is a profile. Note that the "scallope appearance of the current sheath in figures 1 and 2 is evidence that even at this early time the vortex filaments are carrying a large fraction of the total current in the sheath. The PCA has inner and outer conductor diameters of 3.4 and 10 cm, and an inner conductor length of 13.6 cm. It is driven by a 45 μf capacitor bank capable of 25 kv. The PCA is usually operated at 11 to 14 kv with deuterium at 8 torr. At 13 kv the energy storage is 3.5 kj, the peak current 500 ka. The half cycle time is 2 μ sec.

Figs. 1, 2, and 3 are all taken at a time when the discharge current is flowing from the face of the center conductor to the outside conductor.

References

[1] W. H. Bostick, W. Prior, L. Grunberger, and G. Emmert, Phys. Fluids 9, 2079 (1966) also Third European Conference on Controlled Fusion and Plasma Physics, Utrecht 1969.

[2] G. K. Batchelor, Proc. Roy. Soc. A201, 405 (1950).

[3] E. A. Vitalis, Plasma Physics 10, 747 (1968)

[4] F. de Hoffmann, E. Teller, Phys. Rev. 80, 692 (1950).

[5] M. J. Lighthill, J. Fluid Mech. 2, 1 (1957).

[6] N. J. Peacock, Third Conference on Plasma Physics and Controlled Nuclear Fusion Research, Novosibirsk, USSR, August 1968 CN-24/G-4.

[7] P. J. Bottoms, J. W. Mather and A. H. Williams, ibid G-5.

Credits

Research sponsored by the Air Force Office of Scientific Research, Office of Aerospace Research, United States Air Force, under AFOSR Grant No. AF-AFOSR-465-67.

23 February 1970

For the 13th AFOSR Contractors Meeting - Physical Energetics;
Naval Postgraduate School, Monterey, California; 5-7 May 1970.

Hydromagnetic Heating of Plasma For Production of Controlled Fusion Reactions

Robert A. Gross
Columbia University
New York, N.Y. 10027

This research is directed at creating a high temperature, fusion reacting gas by means of a very strong shock wave, and understanding the resulting plasma properties and behavior. The shock speed required to create a thermonuclear reacting plasma in room temperature deuterium gas is 1 to 3×10^8 cm/sec, with corresponding plasma temperature of 1 to 10 keV.

A small, one meter long, coaxial, electromagnetic shock tube has been used for many years at Columbia University to study ionizing shock waves in hydrogen at speeds up to about 2×10^7 cm/sec ($T \sim 40$ eV). During the past year, this device has been used principally for developing better plasma shock diagnostic techniques, and, in particular, laser phasographic and holographic nanosecond photographic methods.

A higher energy electromagnetic shock tube was completed in 1969. This new device is 3 meters long and has an outer diameter of 22.5 cm. Its shock waves are driven by a 2×10^6 amp. current delivered from a 3×10^5 joule, 100 keV capacitor bank. A preshock

magnetic field up to 10 kG. is applied usually in the azimuthal plane. This high energy shock tube is now operating and some preliminary results obtained in it are:

1. The experimental results are very reproducible.
2. Ionizing shock speeds of 70 cm/μsec have been created in hydrogen with a preshock pressure of 25 mTorr. This shock speed correspondes to an acoustic Mach number ~ 550 and an Alfven Mach number ~ 4. A laser interferometer measurement showed a shock compression ratio of ~ 4 indicating a post shock plasma density of $n \sim 6 \times 10^{15}$ cm^{-3}.
3. At 100 mTorr initial pressure, shock speeds of 30-50 cm/μsec have been obtained. At 30 cm/μsec, the magnetic shock structure thickness is 35 cm. The shock wave is followed by a current free, hot, uniform plasma about 45 cm long (at the 150 cm tube position). This plasma is followed by a diffusing contact surface current. The volume of shock heated plasma is approximately 10^4 cm^3.
4. The shock heated plasma produces copious X-rays. Preliminary X-ray spectra indicate that at M ~ 400, the electron temperature $T_e \approx 500$ eV and an energy analyzer indicates an ion temperature $T_i \approx 300$ eV.

An improved vacuum system has just been installed so that the device can be operated with room temperature hydrogen at pressures as low as 1 mTorr ($n = 3 \times 10^{13}$ cm^{-3}) with an impurity level less

than one percent. Correspondingly higher shock speeds and higher plasma temperatures should be obtainable.

These strong shock wave experiments are being simulated on a computer by solving the corresponding shock tube hydromagnetic initial value problem. Comparison between the test data and computer predictions has provided considerable insight into shock formation time, diffusing current layers and other nonsteady phenomena.

A theoretical study is in progress of the dynamics and properties of the plasma created by a giant laser pulse heating a solid deuterium-tritium sphere. Preliminary results indicate that for very short, high power laser pulses, the fusion energy released exceeds the laser light input energy for laser pulses of greater than $\sim 7 \times 10^{15}$ ergs. The possible benefits of surrounding the fuel with a heavy Z material are being investigated.

A theoretical study is in progress to determine the behavior of a D-T fuel pellet injected into a fusion temperature plasma.

Publications concerning our work during this past year are:

P. Koch and R. A. Gross, "Effect of Radiation Upon the Post Shock State" Phys. Fluids, 12, 1182 (1969).

B. P. Leonard, "Electron Temperature Effects in Fast Magneto-hydrodynamic Shock Waves" Phys. Fluids 12, 1816 (1969).

C. K. Chu and R. A. Gross, "Shock Waves in Plasma Physics" Advances in Plasma Physics, Vol II, ed. W. Thompson and A. Simon, John Wiley and Sons, 1969.

B. Miller, "Theta Pinch Behavior for Very Early Times" Phys. Fluids, in press.

D. A. Bout and R. A. Gross, "Interaction of an Ionizing Shock Wave with a Transverse Magnetic Field" Phys. Fluids, in press.

D. A. Bout, R. S. Post, and H. Presby, "Ionizing Shocks Incident Upon a Transverse Magnetic Field" Phys. Fluids, in press.

P. Goldberg, "The Structure of Collisionless Shock Waves in a High Beta Plasma" Phys. Fluids, in press.

R. A. Gross and B. Miller, "Shock Heating of Plasmas" Vol IX, Methods of Experimental Physics, ed. H. R. Griem & R. H. Lovberg, Academic Press, 1970

R. A. Gross, "Physics of Strong Shock Waves" in Vol. "High Energy Density" Academic Press, Series of Varenna International School of Physics, Enrico Fermi, in press.

Plasma Turbulence Research

by

Norman C. Jen

The City University of New York

In recent years, one of the most important problems in the field of plasma research and the development of thermonuclear fusion control is the understanding of the characteristics of plasma turbulence. Due to the lack of physical pictures of the turbulence and the inadequacy of the non-linear mathematical method for describing the complicated dynamics, significant progress in plasma turbulence research becomes nearly impossible. The objectives of this research are (a) to obtain the actual physical pictures of the turbulent plasma through experimentation, (b) to understand the interactions and energy transmission mechanisms among particles and waves by the quasi-linear theory, and (c) to develop a computer program for such a problem with the feeding of the experimental results as input data.

A set of systematic experiments has been conducted in the specially constructed quiescent plasma device with a magnetic field, ranging from 50 to 6,000 gauss. The highly ionized plasma column, which is 0.75 inch in diameter by 20 inches in length, has a density of 10^{10} - 10^{11} particles per cu. cm. at a temperature of 2,400 Kelvin degrees. The dynamics of the turbulent plasma has been successfully recorded by the newly developed high speed plasma camera at one end of the plasma column. The results obtained are as follows:

(1) At a low magnetic field of approximately 200 gauss, the instability sets in and gives a symmetrical pattern of convective cells. The convective cell has the characteristics of zero frequency of oscillation, and maximum efficiency of confinement. The convective cell is shown in Figure 1.

(2) At a magnetic field of moderate strength of approximately 1000 gauss, the frequency spectrum shows coherent waves with a predominant frequency in the order of 10,000 cycles per second. The value of the frequency agrees with theoretical predictions.

(3) At a higher magnetic field above 3000 gauss, the plasma column with a longitudinal current becomes unstable in the form of Kadomtsev helix. At the same time, the plasma column gives a continuous frequency spectrum similar to the spectrum in ordinary hydrodynamic turbulence. The photographic pictures show the rotation of the plasma column and the pitch of the helix as a function of the magnetic field. In addition, the pictures also indicate the continuous change of density distribution and the collective oscillations of the plasma across the plasma column. This oscillation is the primary factor for the continuous spectrum and the most important element for the plasma turbulence. The pictures are shown in Figure 2.

The theoretical studies on the quasi-linear theory lead to following results:

(1) The collision term in the Boltzmann equation, in the form of Krook model or Fokker-Plank model, has significant meaning in the regime of medium density plasma which is the case in this research.

(2) The disturbed distribution function of plasma column can be

excited into a turbulent state or can be transformed into a Maxwellian state through the interaction or the energy transmission mechanism among particles and waves.

For a computer program, the time dependent magnetohydrodynamic equations in the Lagrangian system with two space coorinates have been written and successfully tested. This program has a number of defense applications.

By using the newly developed plasma camera technique in the quiescent device, combined with the theoretical analyses and the Lagrangian computer program, the research on plasma turbulence has been productive in many areas and a much better understanding of plasma turbulence is likely to be attained in the near future.

Figure 1

Figure 2 (B = 5000 gauss)

Heating and Accelerating Mechanisms in the Plasma Focussed Discharge

O. K. Mawardi, Plasma Research Laboratory
Case Western Reserve University, Cleveland, Ohio

Introduction

The production of hot dense plasmas by means of focussed discharges has been known for some time.[1] The early accounts on plasma focussing investigations reported in the literature referred to two distinct electrode configurations: the coaxial accelerators[2] and the metal-walled discharges.[3]

The usual explanation for the formation of a dense focus by a coaxial accelerators has rested on the assumption that the dynamics of the plasma consists of an initial acceleration phase of the plasma in the "barrel" of the gun, followed by a fast z-pinch effect. Experimental observation of the plasma focus by means of optical framing pictures and x-ray photographs[4] seem to indicate that the above proposed explanation for the plasma focus is perhaps correct since it describes the appearance of the discharge in its broad lines. Upon close scrutinity, however, this model either breaks down or is unable to account for several puzzling features of the plasma focus.

The time associated with a hydromagnetic instability is often associated with the ratio of pinch diameter to the local ion speed. When this criterion is used it turns out that this time is almost two orders of magnitude shorter than the lifetime of the plasma focus.[5,6] Even when due consideration is given to shock heating and compression it is evident that the simplified picture of the linear pinch is unable to account for the observed life time and rate of heating of the plasma.

Other features of the plasma focus which are still not understood are:

1) The remarkable flatness of the front of the discharge
2) The mechanism for the neutron production
3) The shape of the x-ray spectrum
4) The sensitive dependence of the discharge characteristics on the shape of the electrodes.

Proposed Research Program

1) Theoretical Work

Two problems are proposed to be investigated

a) Dynamics of Focussed Discharge

There are two features of the focussed discharges which are very important to clarify. In many experiments the discharge takes place in a static neutral gas background. This is in contradistinction to the pulsed gas discharges where the background gas pressure is very low. Now, it was pointed out by Kunkel and Gross[7] that the dynamics of an ionizing front resembles that of a detonation wave. This is because, the Lorentz forces are sensed by charged particles only. Consequently, in an ionizing front the charged particles can be visualized as sensing the electromagnetic forces as soon as the front overtakes the particles. A parallel situation occurs in a detonation front where the energy is released at the front, i.e., as the unburnt gas crosses the front it burns thus releasing the energy. An immediate consequence, of this analogy is that the ionizing fronts have a limiting velocity (the analog of the Chapman-Jouguet criteria). The collapse of the discharge will therefore be set by the hydromagnetic counterpart of the Chapman-Jouguet condition.

Another very interesting feature of the focussed discharge was discussed by Morozov.[8] He suggested that the high temperatures and densities found in the plasma focus may be explained on the basis of hydromagnetic arguments when the component $(\underline{B}\cdot\nabla\underline{B})$ of the magnetic pressure is retained in the calculations. Morozov was able to demonstrate that for purely azimuthal magnetic fields as encountered in focussed discharges, conservation of momentum of the plasma requires it to be compressed mainly by the $(\underline{B}\cdot\nabla\underline{B})$ terms as it flows towards the focus.

Density compressions of the order of $(M_A^2(\gamma-1))^{\frac{1}{\gamma-1}}$ can be obtained, where M_a is the Alfvenic Mach number for the plasma flow. For an initially cold plasma (of the order of 1 ev.) M_A can be quite large ($\sim 10^2$). It is readily estimated that for this case a proton temperature of 5 kev can be reached.

A model for the dynamics of the plasma flow which incorporates both of the aforementioned features and is able to account for most of the observed characteristics viz.,

a) the formation of the bubble,
b) the flatness of the front of the discharge,
c) the jet-like character of the focussed discharge and
d) the sensitive dependence of the appearance of the focussed discharge on the shape of the central electrode (hollow or solid)

is the hydromagnetic analogue of the collapsing cavity produced by the penetration of a jet in a liquid.

There are more subtle reasons for the parallel between the two phenomena. The discharge proceeding in a neutral gas, the front will become an ionizing front and these fronts are known to be fairly stable and behaving like a detonation wave. The use of a hollow electrode, allows the forward moving jet to appear. Actial time integrated photograph for this phenomenon clearly demonstrates this effect.

It is thus proposed to develop the hydromagnetic theory for this model taking into account the compressibility of the plasma. The properties which are proposed to investigate in order are i) the flow pattern, ii) stability of the flow, iii) expected heating in the "pinched" region.

b) Theoretical Study of Electron-Heating

A characteristic feature of the focussed discharge is the appearance of discontinuity in the current. This discontinuity is accompanied by neutron-production. It is often stated that the resulting electric associated with this discontinuity is responsible for the local acceleration of the deutrons.

It is reasonable to expect that this strong electric field appearing in the focus may lead to onset of instabilities and turbulence. This in turn causes the turbulent heating of the electrons. Since the electrons appear to be colder than the ions, ion-acoustic instabilities are strongly Landau damped[9] and an other instability has to be invoked to explain the anomalous electron heating.

It is proposed to examine, the turbulent behavior of the electrons under the assumption of magneto-acoustic instabilities. The electron heating is proposed to be estimated from simple linearized turbulence theory. The temperature thus predicted will be compared with those measured experimentally as described in the section on experiments.

2) Experimental Work

In addition to the routine monitoring of the focussed discharge by measuring the current voltage, probing of the magnetic field and visual observation of the discharge by means of an STL image converter camera, it is proposed to conduct the following investigations

A) Measurement of Electron Density

Average values and spatial distribution of the electron density in the discharge are proposed to be measured by means of two separate techniques

a) Spectroscopic Techniques

The mean value of the electron density in the focus or elsewhere in the discharge will be estimated by the following standard techniques

1) Doppler shift
2) Line broadening
3) Continuum and discrete line intensity.

The measurements will be made with a McPherson spectrometer. Eight channels are available in the instrument for time resolved spectroscopy.

b) Laser Interferometry

A laser interferometer suited to the measurement of transient plasma density fluctuations has been constructed[10] through the modification of an Ashby-Jephcott interferometer.[11] The increased sensitivity results from a technique introduced by Hooper and Bekefi[12], but unlike their design our interferometer works well on one shot experiments. Our interferometer can respond to electron density fluctuations as short as 15nsec.[13]

B) Neutron Production Mechanism

The purpose of this part of the experimental program is to clarify the mechanism of neutron production. In particular the aspects that will be investigated will be the total neutron production and their angular distribution. The effect of the design parameter (condenser voltage, gas density, electrode configuration and discharge period) on the neutron flux will also be studied.

The angular distribution of the neutrons emitted from the focus has been used in the past as a criterion to corroborate or disprove the validity of the "boiler" theory of Filipov. Although we too will check this angular distribution we feel that the mechanism of neutron production may be better understood by examining the deuteron energy-spectrum. The neutrons will be detected by means of a neutron activation counter similar to the one developed by Lanter and Bannerman.[14]

The deutron energy spectra will be inferred from a time of flight technique. A drift tube will be attached to the coaxial accelerator and the arrival of the particles will be detected by a solid state detector and counted with a high-speed single channel analyzer (Hewlett-Packard Models 5583 and 5590).

References

1. See for instance J. W. Mather "Proceedings of Conference on Pulsed High Density Plasmas" 1967, Los Alamos Report LA-3770.
2. J. W. Mather Phys. Fluids 8, 366, (1965).
3. N. V. Filippov et al., Nucl. Fusion Suppl. Pt 2, 577, (1962).
4. J. W. Long, et al., "Proceedings of Conference on Pulsed High Density Plasmas," 1967 Los Alamos LA-3770.
5. Ref. 4
6. J. W. Mather Phys. Fluids 11, 611, (1968).
7. W. B. Kunkel and R. A. Gross "Plasma Hydromagnetics" (Stanford University Press, 1962) p. 58 ff.
8. A. I. Morozov Soviet Phys. Technical Phys. 12, 1580 (1968).
9. J. Lawson Phys. Fluids 3, 786, (1960).
10. D. L. Rode and J. E. Hammel Bull. Ameri. Phys. Soc. II, 12, 793 (1967).
11. D. E. Ashby, et al., J. Appl. Phys. 36, 29, (1965).
12. E. B. Hooper and G. Bekefi J. Appl. Phys. 37, 4083, (1966).
13. D. L. Rode, Non Linear Plasma Heating Case Plasma Research Program Tech. Rep. A-59 (1968).
14. R. Lanter and D. Bannerman, "Detector for Bursts of Neutrons" Los Alamos Report LA-3498-MS.

PANEL 3. CONFINEMENT AND INSTABILITIES

Name	Topic
Professor F. Cap University of Innsbruck Institute for Theoretical Physics Innsbruck, Austria	General Methods to Investigate Nonlinear Plasma Instabilities Resistive Drift Waves Driven by a Density Gradient Dissipative Magnetohydrodynamic Instabilities Microinstabilities in Arbitrary Plasma Configurations Overstable Modes Due to Resistivity Gradients
Dr. G. S Janes Avco Everett Research Laboratory AVCO Corporation Everett, Massachusetts 02149	Research on the Production and Containment of Electron Rich Plasmas
Professor M. Kristiansen Dept. of Electrical Engineering Texas Technological University Lubbock, Texas 79409	Fast Plasma Heating Research
Professor A. J. Lichtenberg Dept. of Electrical Engineering & Computer Sciences University of California Berkeley, California 94720	Ion Heating and Confinement of Neutral-Free Plasmas
Professor James E. McCune Dept. of Aeronautics and Astronautics Massachusetts Institute of Technology Cambridge, Massachusetts 02139	Kinetic Theory of Unstable Plasmas
Dr. M. L. Pool Ohio State University Physics Department Columbus, Ohio 43212	Rotating R-Field Plasma for Thermonuclear Power Reactors
Professor D. R. Wells Department of Physics Miami University Coral Gables, Florida 33124	Broken Symmetries and CRT Confinement

GENERAL METHODS TO INVESTIGATE NONLINEAR PLASMA INSTABILITIES

F. Cap, D. Floriani, F. Herrnegger, N. Ortner

Institute for Theoretical Physics
Innsbruck University, A-6o2o Innsbruck, Austria

A. Thermodynamic potential and nonlinear stability in magnetohydrodynamics, F. Herrnegger

The stability of a plasma system in a stationary equilibrium depends essentially on nonlinear effects due to the interaction between the variables determining the evolution of the system or due to the dependence of the phenomenological transport coefficients on the instantaneous state of the plasma. Prigogine /1/ introduced the concept of a thermodynamic local potential into the equations of an electrically nonconducting nonequilibrium fluid. In the following this concept of local potential has been applied /2/ to the magnetohydrodynamic Benard problem. The applicability of this method to the investigation of the stability behavior of dissipative flows is due to the fact that convective terms appear in the functional of the local potential besides the dissipative terms (viscosity, heat conductivity, etc.). This is the feature which makes it possible to construct a thermodynamic theory of hydromagnetic stability.

The Benard problem consists in a horizontal layer of plasma in which a temperature gradient is maintained by heating it from below in a constant gravitational field.

We are concerned with magnetohydrodynamic systems that satisfy the ideal MHD basic equations including heat conductivity and viscosity /1/.

We construct a negative semidefinite function Φ by multiplication of the momentum equation by $\frac{1}{T_o}\frac{\partial \vec{v}}{\partial t}$, the equation of heat conduction by $\frac{\rho_o c_v}{T_o^2}\frac{\partial T}{\partial t}$, the equation of induction by $\frac{\partial \vec{B}}{\partial t}$, and by adding the resulting equations the left hand side defines the

function Φ:

$$\Phi = -\left[\frac{\rho_o c_v}{T_o^2}\left(\frac{\partial T}{\partial t}\right)^2 + \frac{\rho_o}{T_o}\left(\frac{\partial \vec{v}}{\partial t}\right)^2 + \left(\frac{\partial \vec{B}}{\partial t}\right)^2\right] \qquad (1)$$

This expression contains only derivatives with respect to time t and represents a negative semidefinite function which vanishes identically in the steady state and is smaller than zero otherwise:

$$\Phi \leq 0 \qquad (2)$$

We integrate the result (1) over the volume V, use the principle of local potential /2/ of the steady state (characterized by bared quantities $\bar{q}(\vec{x})$) and together with the condition (2) we get the result

$$\int_V \Phi dV = \frac{\partial}{\partial t}\, \phi\{\bar{q}(\vec{x}), q(\vec{x},t)\} \qquad (3)$$

where ϕ is a very complicate functional of the time-independent quantities $\bar{q}$ (standing for $\vec{v}$, $\vec{B}$, etc.) and of the analogous instantaneous quantities $q(\vec{x},t)$. In the steady state the left-hand side of (3) vanishes, this means the first variation of ϕ is zero. The Euler-Lagrangian differential equations resulting from this variational principle are the steady-state equations from which we have started. Thereby a variational principle containing convection and dissipative terms has been given (to treat the MHD Benard problem). The principle is useful for numerical treatment of stability problems.

B. Lyapunov's stability theory in plasma physics, F. Cap, N. Ortner

The classical stability theory of Lyapunov is successfully used for mechanical systems with a finite number of degrees of freedom. This theory describes the stability behavior of solutions of ordinary differential equations (or systems) without knowledge of the explicite solutions. These informations are obtained from functional-theoretical investigations of the Lyapunov function. In order to evaluate the conditions for stable domains of the solutions, the knowledge of the Lyapunov function and of the form of the differential equations is sufficient. The effective

determination of the Lyapunov function is the main problem. However, the governing differential equations in plasma physics are partial differential equations /3,4/. In order to apply the Lyapunov theory to stability problems in plasma physics we have transformed the MHD basic equations in ordinary differential equations by the help of similarity transformations /5/. These transformed ordinary differential equations are then the starting point for stability search using the Lyapunov criteria /4/. This way of treating the stability of a system has the advantage that no linearization of the problem has been undertaken (for more details of our preliminary investigations on this problem see Ref. /5/).

C. A general algorithm for the investigation of plasma instabilities, D. Floriani

The treatment of the full non-linear equations of any plasma theory implies considerable mathematical effort. For this reason approximate solutions are searched by simplifying the equations or by using iterative procedures. The usual linearization can be interpreted as the first step of such an iteration. On analysing this linearisation one easily perceives the close relationship with Taylor series expansion in time t /6/. We assume that every quantity can be expanded in a Taylor series:

$$\vec{f}(\vec{r},t) = \sum_{n=o}^{\infty} \vec{f}_n(\vec{r})\, t^n/n!,$$

$\vec{f}_n$ being the vector with components $\rho_n(\vec{r})$, $v_{x,n}(\vec{r})$, $v_{y,n}(\vec{r})$, $v_{z,n}(\vec{r})$, $T_n(\vec{r})$, $B_{x,n}(\vec{r})$, ... Introducing this into the MGD equations we get recurrence formulas for the coefficient functions $\vec{f}_n(\vec{r})$:

$$\vec{f}_{n+1}(\vec{r}) = \vec{f}_{n+1}\{\vec{f}_o(\vec{r}),\vec{f}_1(\vec{r}), \ldots ,\vec{f}_n(\vec{r})\}.$$

Instead of differential equations one now has equations containing only algebraic operations and applications of the del-operator ∇ to already known functions; approximations of arbitrary order can be obtained in a systematic manner. If one starts from

a configuration near equilibrium the recurrence formulas can be simplified. It also seems possible to use this method in statistical mechanics /7/. The most interesting application may be the computation of the initial time behavior of a system near equilibrium by help of high-speed computers.

References:

/1/ R.I. Donnelly, R. Herman, I. Prigogine, Nonequilibrium Thermodynamics, Variational Techniques and Stability, University of Chicago Press, 1966

/2/ F. Herrnegger, Report UNICP-SR64, Institute for Theoretical Physics, Innsbruck University (197o)

/3/ T.K. Fowler, J.Math.Physics 4, 559 (1963)

/4/ V. Zubov, Methods of Lyapunov, Noordhoff 1964

/5/ F. Cap et al., Report UNICP-HWB69, Institute for Theoretical Physics, Innsbruck University (1969)

/6/ D. Floriani, Nucl.Fusion 9, 77 (1969) and Report UNICP-SR62 Institute for Theoretical Physics, Innsbruck University (1969)

/7/ J.W. Weil, Nucl.Fusion 9,171 (1969).

RESISTIVE DRIFT WAVES DRIVEN BY A DENSITY GRADIENT

G. Auer

Institute for Theoretical Physics
Innsbruck University, A-6o2o Innsbruck, Austria

Drift waves and drift instabilities may arise in a plasma whenever gradients exist. Since such gradients, e.g., of density, temperature, magnetic field, etc., occur in any plasma device and since drift instabilities have a strong influence on plasma losses the problem of drift waves is of fundamental importance for the problem of plasma containment.

A suitable device for studying oscillations and waves in a plasma is the Q-machine. A great number of experiments in these quiescent plasmas was dealing with spontaneous oscillations which under certain conditions could be identified as density-gradient driven drift waves /1/. The usual theory of these drift waves /1,2/ which is based on a two-fluid model assumes isothermal behavior of ions and electrons, i.e. infinite thermal conductivity. We wanted to examine the other extreme, the case of zero heat conductivity and thus of adiabatic oscillations and to see what changes are brought about by this assumption.

The analysis is based on the first two moments of the Boltzmann equation, i.e. the equation of continuity and the equation of motion for both, ions and electrons. Finite electron inertia, ion motion parallel to the magnetic field, and parallel electric resistivity are taken into account /3/. Since we consider a low-ß plasma variations of the magnetic field resulting from plasma motion may be neglected. The electric field is derived from a potential (electrostatic waves). As the frequency of the oscillations we are dealing with is much smaller than the plasma frequency quasineutrality of the plasma is a good approximation.

The equilibrium (zero order state) is assumed to be as follows: the magnetic field is homogeneous and has only a component in the z-direction, a density gradient lies in the x-direction, and

ions and electrons drift oppositely directed in the y-direction. The linearization of the problem is carried out in the well known manner, by superposing a slight perturbation onto the equilibrium quantities and neglecting terms of second order in perturbations.

It is convenient to assume the zero order density to have an exponential shape. In this case the resulting partial differential equations have constant coefficients and we may look for solutions of the form exp $i(k_y y + k_z z - \omega t)$. The condition that the determinant of a set of homogeneous equations must vanish for a non-trivial solution leads to the desired dispersion relation. It is a polynomial of 7th degree in the frequency as a function of the wavenumber. The dispersion relation was discussed for zero and for large parallel wave number. It was solved numerically for the range of small parallel wave numbers. The result of numerical computation is shown in the diagram, fig. 1a and 1b, where we have plotted the normalized phase velocity against the parallel wavenumber.

The results we have obtained are as follows: The modes which are already present in the isothermal case and which are labeled 1 to 5 in the dispersion curves are only sightly changed by our assumption of adiabatic plasma behavior. They were already discussed by F.F. Chen /2/. Besides them two new modes occur: For vanishing parallel wavenumber the mode labeled 6 in the diagram propagates with the γ-fold ion drift velocity (where the adiabatic exponent $\gamma = c_p/c_v$). The electrons oscillate in the x-direction, the ions in the y-direction. The mode number 7 travels for $k_z = 0$ with the γ-fold electron drift velocity. For the limit of vanishing electron mass the perturbations of the ion velocity, the density and the electric potential vanish. Thus this wave is the propagation of a perturbation of the electron velocity and electron pressure, respectively. When the parallel wavenumber increases from zero the two modes keep up their identity over a large range until they turn over into acoustic waves propagating with the adiabatic sound velocity, of course. As concerns their growth rate the imaginary part of

their frequency is so small compared to the real one that they are practically stable.

The investigations will be continued by inclusion of ion viscosity and thermal conductivity.

References:

/1/ H.W. Hendel, T.K. Chu, P.A. Politzer, Phys.Fluids 11,2426(1968)

/2/ F.F. Chen, Phys.Fluids 7, 949 (1964)

/3/ G. Auer, Proceedings of Conf. on Phys. of Quiescent Plasmas (Paris, Sept. 1969), Vol.II, p.3, and Report UNICP-SR69, Institute for Theoretical Physics, Innsbruck University (1969)

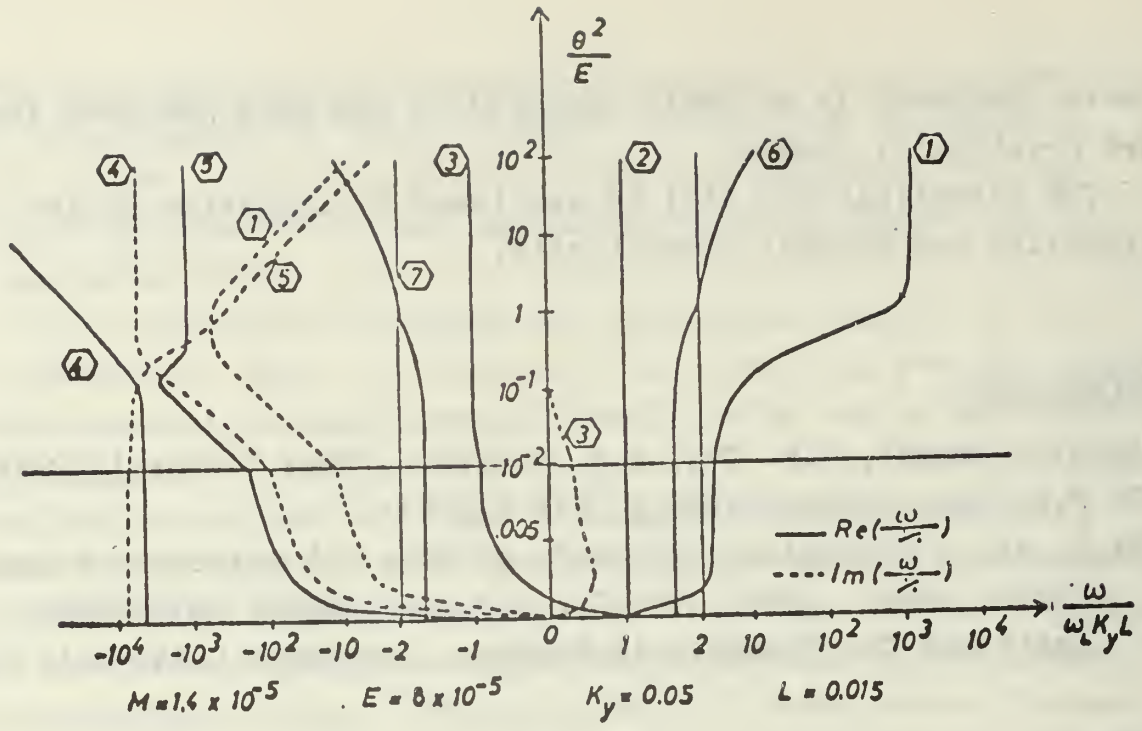

Fig.1a. Variation of the normalized wave velocity $\omega/\omega_L K_y L$ with the parallel wave number : $L < K_y$ (reciprocal density decay length smaller than perpendicular wave number)

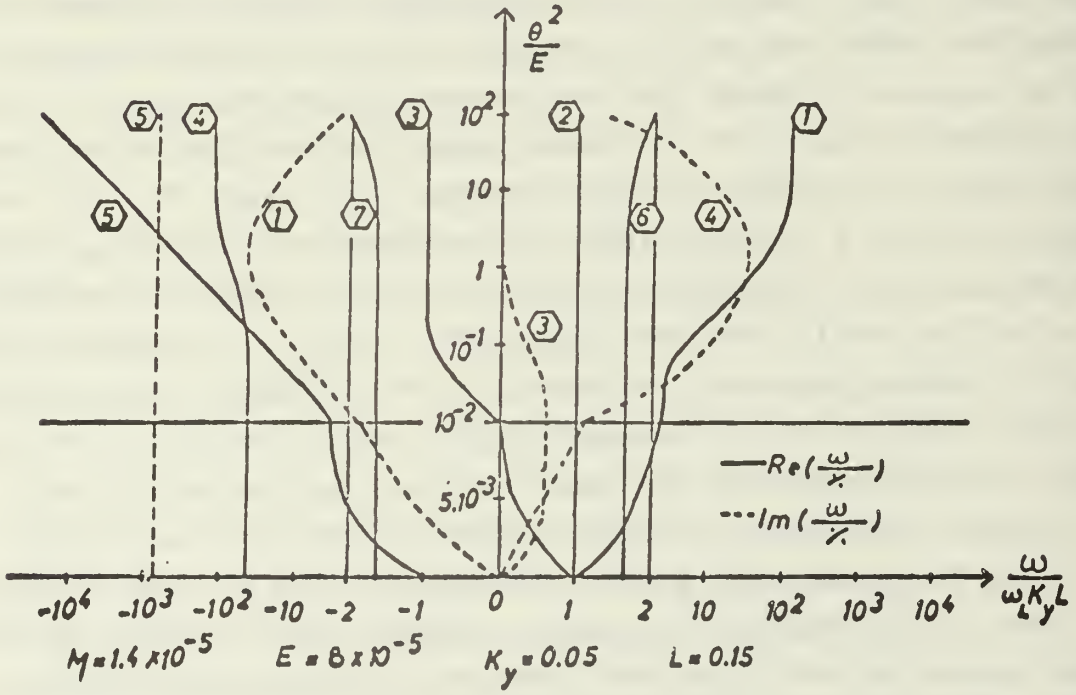

Fig.1b. Variation of the normalized wave velocity $\omega/\omega_L K_y L$ with the parallel wave number: $L > K_y$ (reciprocal density decay length greater than perpendicular wave number)

DISSIPATIVE MAGNETOHYDRODYNAMIC INSTABILITIES

E.H. Jager, P. Unteregger

Institute for Theoretical Physics
Innsbruck University, A-6o2o Innsbruck, Austria

It is well known that finite electrical resistivity and finite viscosity may cause and drive important classes of MHD instabilities, the so-called "dissipative" instabilities. As an understanding of these instabilities is of crucial importance for the mastering of plasma containment a considerable deal of work has been done on this problem.

The combined effects of non-zero flow velocity, resistivity, viscosity, of a sheared magnetic field on the stability of an incompressible plasma sheet being in a state of steady equilibrium flow has been investigated by E.H. Jager /1/. Starting from the basic MHD equations, the convective equations for gravitational force and resistivity, and from the perfect-gas equation of state, we consider an infinite horizontal slab of a quasi-neutral, incompressible plasma. The equilibrium magnetic field $\vec{B}_o$ is a sheared field which depends only on y but is oriented perpendicular to the y direction which is defined as the vertical direction. The equilibrium velocity $\vec{v}_o$ depends on y but is perpendicular to the y direction as well. The gravitational force per unit mass, $\vec{g}_o$, which simulates geometrical effects has only a y component depending on y, whereas the equilibrium pressure p_o is a function of x, y, and z. Viscosity is assumed to be constant throughout the slab, and the Boussinesq approximation is used. On linearizing the basic equations with respect to the perturbed quantities $q_1(x,y,z,t)$, with $q_1(x,y,z,t) = q(x,y,z,t) - q_o(x,y,z,t)$, we obtain a system of linear differential equations the coefficients of which either are constant or depend on y only. These equations are satisfied by solutions of the form $q_1(x,y,z,t) = q(y) \exp\left[i(\bar{w}t + lx + nz)\right]$. Substitution of this expression into the linearized equations yields

a set of ordinary differential equations which after some tedious calculations can be reduced to an ordinary differential equation of 6th order for the y component of the perturbed velocity $\vec{v}_1$. The involved coefficients of this equation depend on the equilibrium quantities, the frequency $\bar{w}$, and the wave numbers l and n. They can be found in the original paper /1/. Several special cases have been discussed.

If we assume that magnetic shear, resistivity, gravitational force, fluid velocity are constant and viscosity vanishes we obtain a fourth-order differential equation for v_y. In the limit of vanishing resistivity we find the so-called "Alfvén modes" for a moving plasma, with $w^2 = w_A^2 = (lB_x + nB_z)^2/\rho$. For non-vanishing resistivity there essentially appear two modes one of which is damped by resistivity only.

Now consider a viscous fluid of zero resistivity with a uniform velocity field in a magnetic field of constant shear and in a constant gravitational field. In this case the dispersion relation yields a mode damped by viscosity.

Next the dispersion relation for a viscous resistive fluid shows the combined influence of constant resistivity and viscosity.

Finally, preliminary estimates seem to indicate that a variable flow velocity changes the non-dissipative as well as the dissipative modes but leaves the growth rates of the dissipative modes unchanged. A more accurate investigation of this subject is under way.

Jager's research represents a generalization of the work done earlier by P. Unteregger /2/. Unlike Jager, Unteregger assumed a static equilibrium with $\vec{v}_o = 0$. He showed that the hydromagnetic modes of an inhomogeneous, incompressible plasma are strongly influenced by the dependence of the Alfvén frequency on the magnetic field. For the case that the field of the equilibrium configuration is perpendicular to the wave vector of the perturbation he found out that the magnetic field has no influence on all possible oscillatory-mode eigenfunctions

of the above form. Unteregger finally pointed out that finite electrical conductivity and viscosity give rise to new modes which do not appear in ideal magnetohydrodynamics.

References:

/1/ E.H. Jager, Report UNICP-SR65, Institute for Theoretical Physics, Innsbruck University (1969)

/2/ P. Unteregger, Report UNICP-SR6o, Institute for Theoretical Physics, Innsbruck University (1968)

MICROINSTABILITIES IN ARBITRARY PLASMA CONFIGURATIONS

S. Kuhn

Institute for Theoretical Physics
Innsbruck University, A-6o2o Innsbruck, Austria

Because of the considerable mathematical difficulties arising with the use of the Boltzmann or Vlasov equations in microinstability research the relevant analyses were for a long time confined to geometrically simple plasma configurations (e.g., one-dimensional plane slab). It has, however, been shown /1,2/ by Taylor, Hastie, and Haas that it is possible to treat the problem in a much more general manner and to account for all geometrical effects from the outset. Now, though the stability theory devised by Taylor and Hastie /1/ holds for geometrically arbitrary plasma configurations it is specified to the case of a c o l l i s i o n l e s s plasma undergoing l o w - f r e q u e n c y oscillations with long wavelengths in the direction of the magnetic field. Beside these so-called flute and drift modes there can, however, arise also high-frequency modes as has been pointed out, e.g., by Rosenbluth /3/. This now is the point where we tried an application of Taylor's and Hastie's theory to the range of h i g h - f r e q u e n c y o s c i l l a t i o n s , additionally taking into account a c o l l i s i o n t e r m which might give us an estimate of collisional damping.

Given an equilibrium described by the distribution function $F(\vec{r},\vec{v})$, the electric potential $\Phi(\vec{r})$, and the magnetic field $\vec{B}(\vec{r})$. We require the ratio $r_L/L = \lambda$ to be much less than unity, where r_L is a typical Larmor radius and L is a typical macroscopic length of the system. Apart from this assumption the geometry of the configuration under consideration is left arbitrary. On this equilibrium we now superimpose small perturbations

$$\tilde{f} = \hat{f}(\vec{r},\vec{v})\exp i\left[S(\vec{r})/\lambda+\omega t\right], \quad \tilde{\Psi} = \hat{\Psi}(\vec{r})\exp i\left[S(\vec{r})/\lambda+\omega t\right]$$

of the distribution function and of the electric potential, resp.

These expressions are inserted into the Boltzmann equation which is then linearized. The collision term is assumed to be of the Krook form $-\nu_{coll} f$. Now it has proved convenient to introduce "natural" coordinates as follows. On each magnetic line of force (labeled by two parameters α, β such that $\vec{B} = (\partial\alpha/\partial\vec{r})\times(\partial\beta/\partial\vec{r})$) one can define in any point (determined by some arc length s along the line of force) an accompanying coordinate frame consisting of $\vec{e}_1 = \vec{B}/B$ and two unit vectors $\vec{e}_2$, $\vec{e}_3$ perpendicular to $\vec{e}_1$ and to each other. Then the velocity may be expressed in terms of the variables $\mu = \vec{v}_\perp^2/2B$ (magnetic moment), $K = \vec{v}^2/2 + e\phi/m$ (equilibrium particle energy), $\phi = \tan^{-1}(\vec{e}_3.\vec{v}/\vec{e}_2.\vec{v})$ (azimuthal angle of $\vec{v}_\perp$ about $\vec{B}$), and $\sigma = \vec{e}_1.\vec{v}/|\vec{e}_1.\vec{v}|$ (sign of $\vec{v}_\parallel$ with respect to $\vec{e}_1$). Introducing $\vec{x} = \lambda\vec{r}$, $\nabla = \partial/\partial\vec{x}$, and expanding the quantities involved in simple power series in λ the Boltzmann equation reads in the lowest order in λ

$$i\frac{\bar{\omega}}{\omega_c} f_o + i\frac{mc}{e} f_o D' S_o - i\frac{c}{B} \Psi_o \nabla S_o.(\sigma q\vec{e}_1 \frac{\partial}{\partial K} + \vec{v}_\perp D_1)F_o = \frac{\partial f_o}{\partial\phi}$$

where D' and D_1 are complicated operators /4/.

The solution to this equation is found to be

$$f_o = b_1 - b_2\int_o^{2\pi} d\phi'\left[\frac{1}{b_3} + \Theta(\phi'-\phi)\right]\exp\left[I(a_1,\phi) - I(a_1,\phi')\right]$$

where b_1, b_2, b_3, a_1, and I are complicated functions depending on known quantities. From Poisson's equation we obtain

$$Q(\omega) = \int d^3\vec{r}\left[\Psi_o^2(\nabla S_o)^2/4\pi - \Psi_o \sum_j e\int d^3\vec{v} f_o\right] = 0.$$

Stability analysis now requires to find out under what conditions this equation may have a solution ω lying in the "unstable" lower ω half-plane. This question may in principle be answered by means of a Nyquist plot of $Q(\omega)$. By a Nyquist plot in our case we understand the mapping of a closed contour (consisting of a straight line just below the real axis and of a half-circle in the lower ω half-plane with its radius tending to infinity) into the complex Q plane.

We were able to prove the following properties to hold generally for $Q(\omega)$:

a) $Q(\omega)$ has no poles located in the lower half-plane since the only poles that possible arise can be shown to lie above or (for the collisionless case) on the real axis.

b) $Q(\omega)$ has no branch points located in the lower ω half plane for this function can be shown to be a simple power series in ω in the lower ω half-plane.

Because of properties a) and b) we are able to apply the Nyquist theorem which states that there are no unstable modes if the Q contour does not encircle the origin.

c) The infinite half-circle of the ω contour maps onto one single point $Q(\omega)$ located on the real Q axis. This statement is proved by some more detailed calculations.

Finally, to complete the formal part of our work, Q has been calculated for the collisionless case /4/ in which it appears to be slightly more concise than in the case of collisions.

Given the expressions for $Q(\omega)$, our stability problem is in principle solved. We have to substitute the specific parameters and functions of the system under consideration for their general counterparts in these expressions and to calculate the shape of the Nyquist plot. Such an investigation will yield sophisticated criteria necessary and sufficient for stability.

Our present work is dedicated to discussing the physics standing behind the method under consideration.

References:

/1/ J.B. Taylor, R.J. Hastie, Plasma Phys. 1o, 479 (1968)

/2/ R.J. Hastie, J.B. Taylor, F.A. Haas, Annals Phys.41, 3o2 (1967)

/3/ M.N. Rosenbluth, Phys.Fluids 8, 547 (1965)

/4/ S. Kuhn, Report UNICP-SR68, Institute for Theoretical Physics, Innsbruck University (1969)

OVERSTABLE MODES DUE TO RESISTIVITY GRADIENTS

F. Herrnegger

Institute for Theoretical Physics
Innsbruck University, A-6o2o Innsbruck, Austria

In a sheet pinch in a plasma of variable electrical resistivity the following types of instabilities occur:

a) the tearing instability in which the sheet breaks up under the action of the magnetic field into filaments parallel to the direction of the current,
b) the rippling instability in which the locally variable electrical resistivity changes the current density.

A coupling occurs between the transverse variation of resistivity and the steady current associated with the main magnetic field.

The purpose of this paper is to study these problems /1/, especially the effect of resistivity gradients perpendicular to the main magnetic field on the generation of overstable modes in a current-carrying inhomogeneous plasma sheet which is in the presence of a magnetic shear field and of a constant gravitational field $\vec{g}$. It will be shown that overstable modes may exist. These solutions are connected with the second derivative of the mean resistivity ($\bar{\eta}''$) i.e. they depend on whether the course of the resistivity curve $\bar{\eta}(x_2)$ in the plasma sheet is convex or concave. Furthermore it is shown that the region of neutral stability depends essentially on the resistivity gradient and on $\bar{\eta}''$, the second derivative, except in the case of homogeneous plasmas.

We consider a current-carrying plasma sheet supported by a gravitational field where the following assumptions are made:

a) the main magnetic field depends on x_2: $\vec{B}(x_2) = [B_1(x_2), 0, B_3(x_2)]$
b) neglecting the thermal conductivity along the magnetic field lines, the perturbation in electrical resistivity, η, results only from convection: $\partial\eta/\partial t + \vec{v}.\nabla\eta = 0$ ($\vec{v}$ flow velocity)

c) no zero-order diffusion velocity exists and the Boussinesq-approximation is assumed to be valid.

Starting from the linearized MGD basic equations and looking for solutions of the form

$$f^*(\vec{x},t) = f^*(x_2)\exp\left[i(\vec{k}.\vec{x} - \omega t)\right]$$

we determine the criteria for overstable solutions. This problem can be reduced to a selfadjoint differential equation of second order with respect to b ($b = B_2'' - k^2 B_2$, the prime denotes d/dx_2, $s = (\vec{k}.\vec{B})$)

$$(\bar{\eta}^{-2}b')' + b\left[-k^2\bar{\eta}^{-2} + \bar{\eta}\bar{\eta}'' + i\omega\mu\bar{\eta} + (s^2\bar{\eta}/i\rho\omega)\right] = 0 \qquad (1)$$

Multiplying this equation by the complex conjugate of b, integrating over the plasma volume, and assuming homogeneous boundary conditions we get from (1) a quadratic equation for ω which has complex solutions only when the condition

$$\left|\frac{\int\bar{\eta}^{-2}|b'|^2dx_2}{\int\bar{\eta}^{-2}|b|^2dx_2} + k^2 - \frac{\int\bar{\eta}\bar{\eta}''|b|^2dx_2}{\int\bar{\eta}^{-2}|b|^2dx_2}\right| < 2\sqrt{\frac{\mu}{\bar{\rho}}}|s|\left|\frac{\int\bar{\eta}|b|^2dx_2}{\int\bar{\eta}^{-2}|b|^2dx_2}\right| \qquad (2)$$

is satisfied. Therefore oscillatory increasing or decreasing modes exist. This condition shows that overstable modes are associated with the second derivative of the resistivity and consequently depend on whether the curve $\bar{\eta}(x_2)$ has a positive or negative curvature. Therefore we see that, since the left-hand-side of (2) is positive semi-definite, overstable modes occur where s is not zero. Thus the absence of overstable modes found by other authors is due to the fact that making an expansion of the solution about the point where s = 0 and breaking off after the first or second term, results in losing the effect of resistivity curvature. Furthermore for s = 0 no overstable modes can exist, as can be seen from Eq. (2). When local mean quantities are denoted by <> the condition for overstability derived from (2) reads

$$\left|\left\langle\frac{|b'|^2}{|b|^2}\right\rangle + k^2 - \left\langle\frac{\bar{\eta}''}{\bar{\eta}}\right\rangle\right| \leq 2\sqrt{\frac{\mu}{\bar{\rho}}}\left\langle\frac{s}{\eta}\right\rangle \qquad (2')$$

The inequality (2') contains the unknown function b. In order to make quantitative conclusions we have to solve (1). An

approximate solution of (1) which is also valid in the case of high resistivity gradients, provided the wavenumber k is sufficiently high, reads

$$b(x_2) = \frac{1}{\bar{n}q^{1/4}}\left[c_1 \exp\left\{i\int_{\bar{x}_2}^{x_2}(1+\frac{\varepsilon}{2})\sqrt{q}\,d\xi\right\} + c_2 \exp\left\{-i\int_{\bar{x}_2}^{x_2}(1+\frac{\varepsilon}{2})\sqrt{q}\,d\xi\right\}\right] \qquad (3)$$

with $q(x_2) = -k^2 + \frac{\omega\mu}{i\bar{n}} + \frac{s^2}{i\omega\rho\bar{n}}$ and $\varepsilon = \bar{q}^{3/4}\frac{d^2}{dx_2^2}(q^{-1/4})$

(c_1, c_2 constants of integration). This approximate solution holds in a region where $q \neq 0$ and where the further condition

$$\frac{1}{2}|\varepsilon| << \frac{1}{2}\left|\frac{d}{dx_2}\left(\frac{1}{q}\right)\right| << 1$$

is fulfilled. When the solution (3) is inserted into the derived stability criterion (2) or (2'), then we get particular information as to how the course of the resistivity in the sheet may be changed in order to reduce the amplitude of the instabilities.

References:

/1/ F. Herrnegger, Proc. 3rd Europ. Conf. Contr. Fusion Plasma Physics, Utrecht 1969, p. 52

RESEARCH ON THE PRODUCTION AND CONTAINMENT OF ELECTRON RICH PLASMAS

(Contract No. F44620-69-C-0095)

J.D. Daugherty, J.E. Eninger, G.S. Janes and R.H. Levy
Avco Everett Research Laboratory, Everett, Massachusetts

I. INTRODUCTION

An electron rich plasma is defined as a plasma in which the space charge density of positive ions is significantly lower than the space charge density of electrons. Under these conditions, space charge effects play a more important role in controlling plasma behavior than do thermal and kinetic effects. The intrinsic stability shown by electron rich plasmas under properly controlled conditions is of fundamental importance to plasma physics, and has stimulated a great interest in a number of new applications.* A Landau damping effect due to the strong electric fields in electron rich plasmas has been predicted, and offers new possibilities to stabilize flute type phenomena in plasmas.

The production of such plasmas is accomplished in two steps. First, a cloud of electrons is injected into a toroidal vacuum chamber by means of the so-called inductive charging scheme; this scheme is described in Section II. Second, the ion component of the plasma is formed through progressive ionization of the neutral background gas in the chamber. This ability to control the density of ions and electrons independently allows a new and a different experimental approach to stability problems.

In Section III, we discuss a number of instability mechanisms of importance in electron rich plasmas, their effect on plasma production and containment, and how they can be avoided. Section IV contains a description of the toroidal devices and experimental procedures used in the present research. The basic understanding of injection and containment gained with our Mark I apparatus is summarized in Section V, where also the progress of subsequent Mark II experiments is presented. Section VI contains concluding remarks with an outline of important problems that remain to be studied in this field.

II. INDUCTIVE CHARGING AND EQUILIBRIA

The inductive charging scheme[6, 7], which we used to establish the initial electron space charge cloud, is based on the adiabatic transport of electrons in a time-dependent (increasing) magnetic field. This principle is best described by considering the guiding center motion of an individual

*Three novel devices have so far been invented in the course of the present research: 1) the solar flare plasma radiation shield[1, 2], 2) a heavy ion accelerator[3] and 3) a source of highly stripped ions.[4, 5]

particle under the influence of crossed electric and magnetic fields, as shown in Fig. 1 for an infinite cylindrical geometry with a uniform, axial magnetic field $\overline{B}$. It is evident that a steady magnetic field leads to an equilibrium situation, since the drift caused by the radial space charge electric field E_r is purely azimuthal. When B increases, a radial motion due to the induction field E_θ is added to the azimuthal drift, thus causing the electrons to spiral inward. An electron beam launched at the cylindrical wall will, therefore, be accumulated within the cylinder, producing a negative space charge cloud and a potential well. The adiabatic approximation assumes that $E_\theta \ll E_r$, which implies that the total number of electrons in a magnetic flux tube is conserved during the process of electron injection. Under these conditions, it is possible to establish various radial electron density profiles by controlling the time history of the injected current. This knob is of major importance in experimental studies of electron rich plasma stability, since geometrical factors are critical.

The principles of inductive charging can be extended to toroidal geometries. We have demonstrated, both theoretically[8] and experimentally[7], the existence of toroidal electron cloud equilibria without the necessity for a magnetic field rotational transform.*

III. STABILITY THEORY

In dealing with the macroscopic stability of an electron rich plasma, one can distinguish between effects that are related to the electron component alone, and effects associated with interactions of the electron component with the ion component.

Regarding the first of these two categories, we have demonstrated[10] that the high frequency, short wavelength stability of magnetically confined electron clouds can primarily be described in terms of a single, dimensionless parameter: $q \equiv \omega_p^2/\omega_c^2 = n_e m_e/\epsilon_o B^2$. Although stability against short wavelength perturbations does not exist in a strict sense for any value of q, theoretical[10] as well as experimental[6] evidence shows that the stability required for all practical purposes (such as the familiar Penning discharge and the applications studied here) can be ensured if $q \leq 0.1$.**

A long wavelength instability has also been identified and analyzed theoretically. This is the diocotron or slipping stream instability[11,12] which occurs due to the electrostatic interaction between two surface waves propagating on each side of a crossed-field electron beam of finite thickness. The diocotron instability exhibits a high growth rate even for low values of q, but it can be avoided completely by the selection of electron beam and electrode configurations, in which the unstable long wavelengths are suppressed. Re-entrant beam configurations, like those in cylindrical and toroidal geometries, can easily be stabilized, since the beam circumference is an upper limit to the possible wavelengths.

---

*In a recent paper,[9] T. H. Stix has applied these results to C.T.R. conditions.

**The growth rate for this gyro-resonance type instability is $\sim 1/2\, q\omega_c \exp(-2/q)$, which becomes vanishingly small for $q \leq 0.1$. There are important devices, however, based on the highly unstable conditions prevailing for $q \approx 1$, e.g., the microwave magnetron.

The diocotron waves are negative energy waves. This implies that any perturbing influence that removes energy from the wave will cause the wave to grow. The flow of currents induced in nearby walls with a finite conductivity, such as in the present experiments, could provide enough dissipation to drive an electron rich plasma unstable. This resistive wall instability[10, 13] should have a growth rate which varies as $n_e^3/\sigma^{1/2} B^2$ and could be serious for devices with useful electron densities ($n_e = 10^{10}$-10^{11} cm^{-3}). It has been suggested, however, that there should be a Landau type coupling[13] between the higher mode diocotron waves and the outer electrons in a radially decreasing density gradient which would serve to damp the waves at a rate sufficient to overcome the resistive wall instability.

In the second instability category, we have predicted[14] and observed[7] an ion-electron resonance instability due to coupling between the diocotron wave and ion oscillations in the potential well of the electrons. This instability is only present in devices where ions are accumulated (it is not found in Penning discharges, for instance), but it has been shown that it can be avoided by keeping the ion density below a critical limit. If the ion is very massive (m_i/Z large), the ion motion will involve frequencies far below those characterizing the electron cloud, and the two systems are essentially decoupled. But as m_i/Z gets smaller (e.g. through progressive stripping of a given element) the ion frequencies increase and the coupling becomes stronger, implying the possibility of an instability. Unstable conditions can also be approached by slowing down the diocotron wave. This is the primary cause of an instability that occurs in the present experiments, when the ion space charge density produced through ionization of the background neutrals reaches a critical value of 10 - 20% of the electron density, in good agreement with the theoretical predictions.

IV. EXPERIMENTAL DEVICES

Figure 2 shows the Mark I apparatus,[7] which is constructed of aluminum and can be evacuated to $\approx 10^{-7}$ Torr. The major radius of this torus is 46 cm, the minor radius 10 cm. The magnetic field is induced by a capacitor bank discharge through the field coils shown. The rise time of the field is $\leq 50\mu$sec, and on this time scale all magnetic flux enters the containment chamber through the indicated injection slot, where the field lines get "loaded" with electrons emitted from a hot tungsten filament. Accumulation of negative space charge then takes place according to the principles of inductive charging described in Section II. Subsequent containment of the injected electron cloud is accomplished by "crowbarring" the field coils, thus causing the magnetic field to stay nearly steady for a length of time determined by the L/R time constant of the coils, typically about 1 msec. This simple way of producing a relatively steady magnetic field was quite adequate for the Mark I experiments, since the containment time was found to be limited to ≤ 60 μsec by the relatively poor vacuum conditions.

The Mark II torus, shown in Fig. 3, is an all-stainless steel, 10^{-10} Torr ultra-high vacuum system designed for long term containment studies. In addition to its superior vacuum, the containment chamber in the Mark II device is entirely separated from the vacuum envelope, thus permitting a great deal of freedom in selecting the size and shape of this chamber. The

present insert has a square cross-section, and high injection voltages can be applied, since ample space has been reserved for electron gun structures. Observe that the electron gun is placed at the outside radius in the Mark II, in contrast to its inside location in the Mark I. The choice of location is associated with the effects of finite electron temperature on injection, and will be discussed below in more detail.

A method has been developed for producing a magnetic field with both the short rise time ($\approx 5\ \mu$sec), required for good injection performance, and a long steady state time duration for containment. This "ring-down-up" scheme is illustrated in Fig. 4 while Fig. 5 shows the resulting time dependence of the magnetic field.

The primary diagnostic tool is the image current button, shown in Fig. 3, which can be used in different modes, both to measure the total injected charge and electric field fluctuations associated with waves and instabilities. Typical image current button signals are shown in Fig. 5.

V. EXPERIMENTAL RESULTS

Since the initial results obtained with the Mark I torus have been published elsewhere[7], we shall only list the major achievements of this work:

1) Development of semiempirical scaling laws for electron injection. It was shown that the limit on total charge derives from a natural energy limitation in combination with an anomalous noise or electron heating mechanism.

2) Experimental demonstration of the existence of theoretically predicted[8] toroidal electron cloud equilibria.

3) Stable containment of ion densities of up to 20% of the electron density, and identification of the ion-electron resonance instability[14] as the limitation on containment time.

The most important result of the subsequent experiments with the Mark II apparatus is the achievement of high plasma densities in combination with long containment times. Thus, we have contained an electron density of 3×10^9 cm^{-3} for 3 msec, yielding a figure of merit $n_e \tau \approx 10^7$ cm^{-3} sec (compared to $\approx 10^5$ cm^{-3} sec for the Mark I). The longest containment time observed is 5 msec. Fig. 5 shows a set of oscillograms from these containment experiments. The quiescent period preceding the rapid onset of the ion instability shown by trace c) in Fig. 5, is convincing evidence of toroidal plasma equilibrium. The diocotron frequency of oscillogram d) is a direct measure of the average electron density, and proves that no charge has been lost through non-adiabatic processes.

In the Mark I, as well as in early Mark II experiments we used a diode type electron gun. A serious drawback was that this gun had to be operated space charge limited in order to give acceptable injection results. This condition leads to extremely severe requirements on filament emission

even for moderate filament voltages, and results in poor injection efficiency. Those problems were circumvented with a new triode gun, whose current can be controlled independently of the filament potential.

Contrary to the diode, the triode also launches the electrons with a relatively low temperature, i.e., kinetic energy in the cycloidal motion perpendicular to the magnetic field, $W_\perp$, as well as in the motion parallel to the field, $W_\parallel$. This reduction of the thermal energy permitted an increase in the electron density in the Mark II by a factor of four. The decision to locate the electron gun of this device at the outside radius was based on criteria for the generation of anomalous noise[7] (which occurs when the magnetic field strengths reaches a certain critical value), in addition to the advantages of having a longer filament. Although we were aware of the fact that the thermal effects would be amplified with this filament location ($W_\perp$ increases due to the conservation of magnetic moment, and $W_\parallel$ due to the conservation of angular momentum), there was then no reason to believe that the temperatures produced by the diode would be large enough to have an inhibiting effect on the injection. At the present time, however, it is clear that the most favorable conditions for electron injection should be with a triode gun located at the inner radius of a torus with such a shape, that the ratio of outer to inner radius is as close to one as possible.

Finally, the long containment times have been achieved primarily as a result of the improved injection efficiency; this has reduced the gas desorption caused by wasted electrons, and therefore delayed the onset of the ion instability.

VI. CONCLUSIONS

We have given a review of our research on electron rich plasmas, and presented the latest experimental results in a strongly condensed form. Although several fundamental wave and instability phenomena have been satisfactorily covered, there remain questions that need to be examined theoretically and/or experimentally. In particular, the predicted Landau type damping should be investigated in more detail. The overall evidence suggests that a number of interesting applications should be feasible as a consequence of the somewhat unusual stability properties of these plasmas.

As far as it can be judged at the present time, two important problems have to be solved before long term containment can be achieved. One problem is wall outgassing that occurs in the Mark II torus in connection with the injection process, however, a straightforward solution to this seems to exist (involving prebombardment of the walls with electrons from a separate gun). A somewhat reduced outgassing is required for the burnout condition, that should keep the ion density below the critical level of about $0.1\ n_e$, in which case the ion-electron resonance instability cannot occur.

The second problem is of a more fundamental nature and has to do with the theoretically predicted but not yet observed resistive wall instability.

Whether this wave growth effect exists in the present experiments or not, can only be determined subsequently to the elimination of the much more powerful ion instability. If the resistive wall instability is found to be present, one should investigate different methods to control it. A distinct possibility is that the suggested Landau type coupling will provide sufficient damping to completely cancel the wave growth. This result would be of major significance because it demonstrates that one can take advantage of an intrinsic plasma phenomenon for the suppression of flute type instabilities.

REFERENCES

1. Levy, R.H. and Janes, G.S., AIAA J. 2, 1835 (1964).

2. Levy, R.H. and Janes, G.S., Space/Aeronautics 45, 106 (1966).

3. Janes, G.S., Levy, R.H., Bethe, H.A. and Feld, B.T., Phys. Rev. 145, 925 (1966).

4. Daugherty, J.D., Grodzins, L., Janes, G.S. and Levy, R.H., Phys. Rev. Letters 20, 369 (1968).

5. Daugherty, J.D., Eninger, J.E., Janes, G.S. and Levy, R.H., Transactions on Nuclear Science of the IEEE NS-16, 51 (1969).

6. Janes, G.S., Phys. Rev. Letters 15, 135 (1965).

7. Daugherty, J.D., Eninger, J.E. and Janes, G.S., Phys. Fluids 12, 2677 (1969).

8. Daugherty, J.D. and Levy, R.H., Phys. Fluids 10, 155 (1967).

9. Stix, T.H., "Toroidal Fusion Plasma with Powerful Negative Bias," to be published.

10. Buneman, O., Levy, R.H. and Linson, L.M., J. Appl. Phys. 37, 3203 (1966).

11. Levy, R. H., Phys. Fluids 8, 1288 (1965).

12. Levy, R.H., Phys. Fluids 11, 920 (1968).

13. Briggs, R.J., Daugherty, J.D. and Levy, R.H., "The Role of Landau Damping in Crossed-Field Electron Beams and Inviscid Shear Flow," Avco Everett Research Laboratory Research Report 317, to be published in the Physics of Fluids.

14. Levy, R.H., Daugherty, J.D. and Buneman, O., Phys. Fluids 12, 2616 (1969).

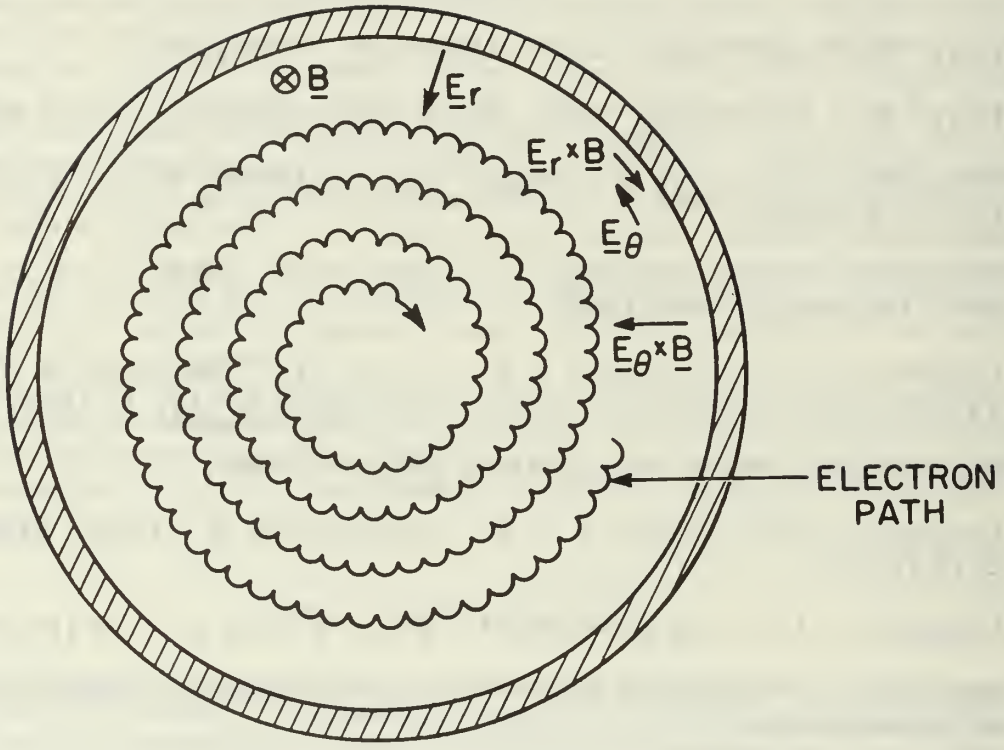

Fig. 1 This figure illustrates the principle of inductive charging. When the magnetic field is steady the only electric field is the radial field E_r due to space charge, and the only drift is the azimuthal drift E_r/B. When B is time varying an induced azimuthal electric field appears, $E_\theta = rB/2$, at radius r. This electric field yields a radial drift speed $E_\theta/B = r\dot{B}/2B$. This drift is inwards when B is increasing and vice versa. Since this radial speed will normally be small compared to E_r/B, the electron paths will resemble tightly wound spirals.

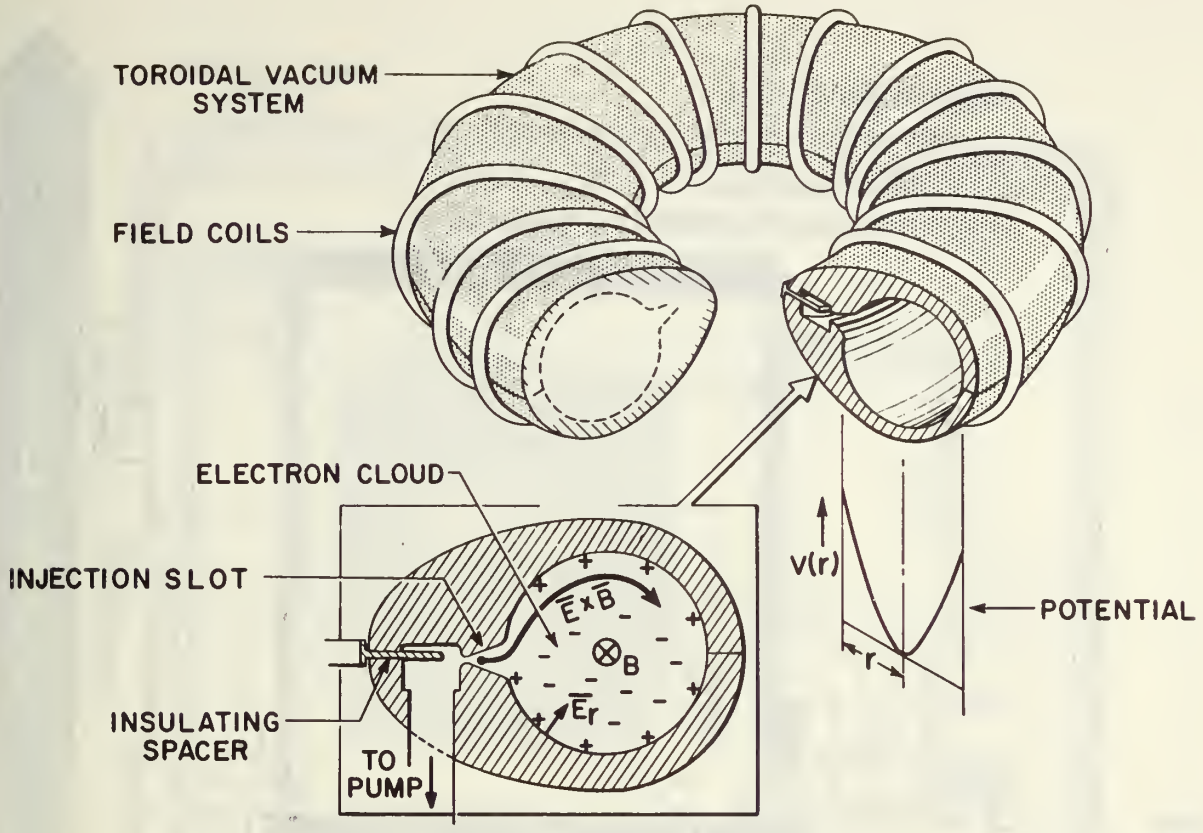

Fig. 2 Schematic diagram of the Mark I torus.

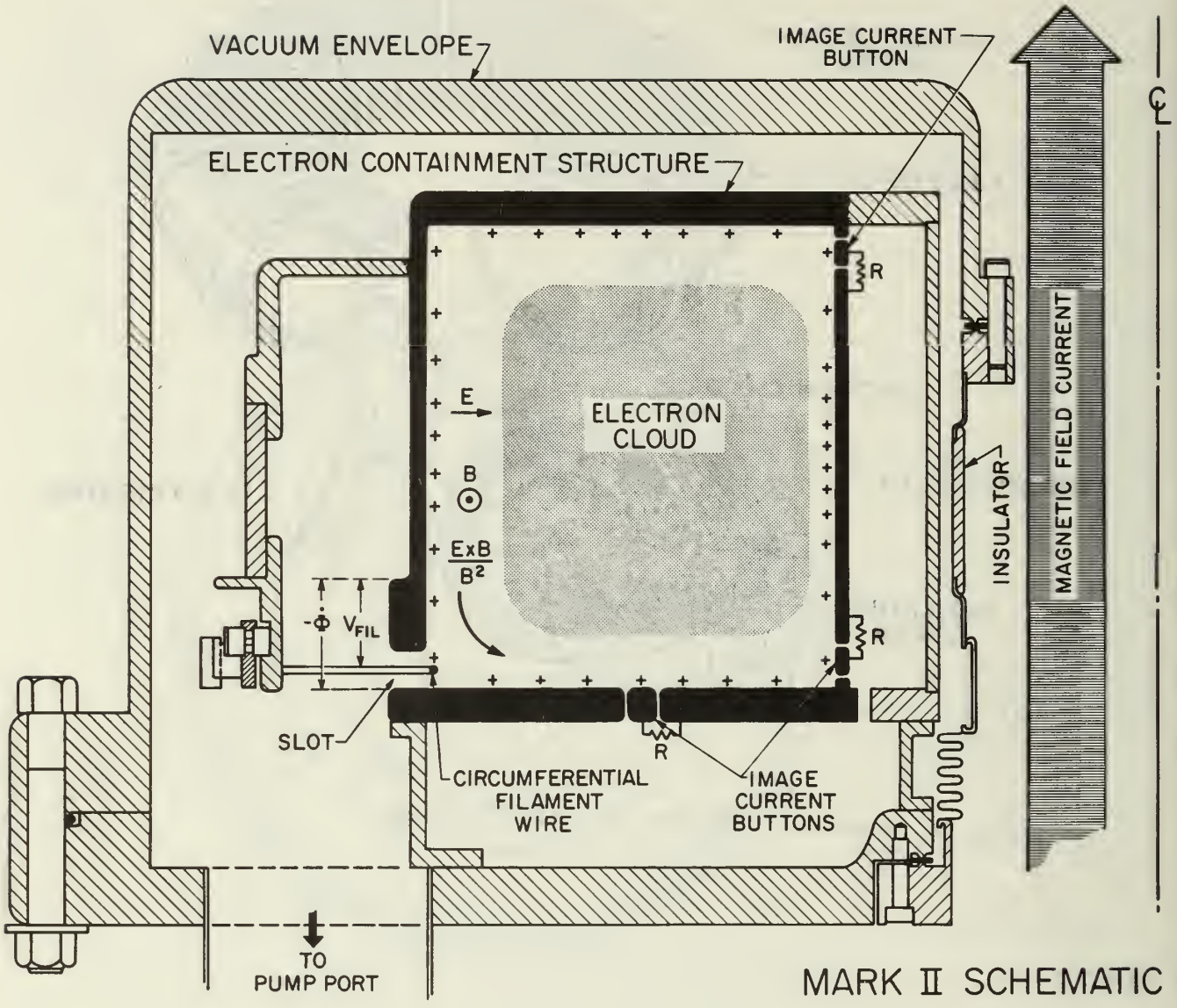

Fig. 3 Schematic cross-section of the Mark II toroidal system.

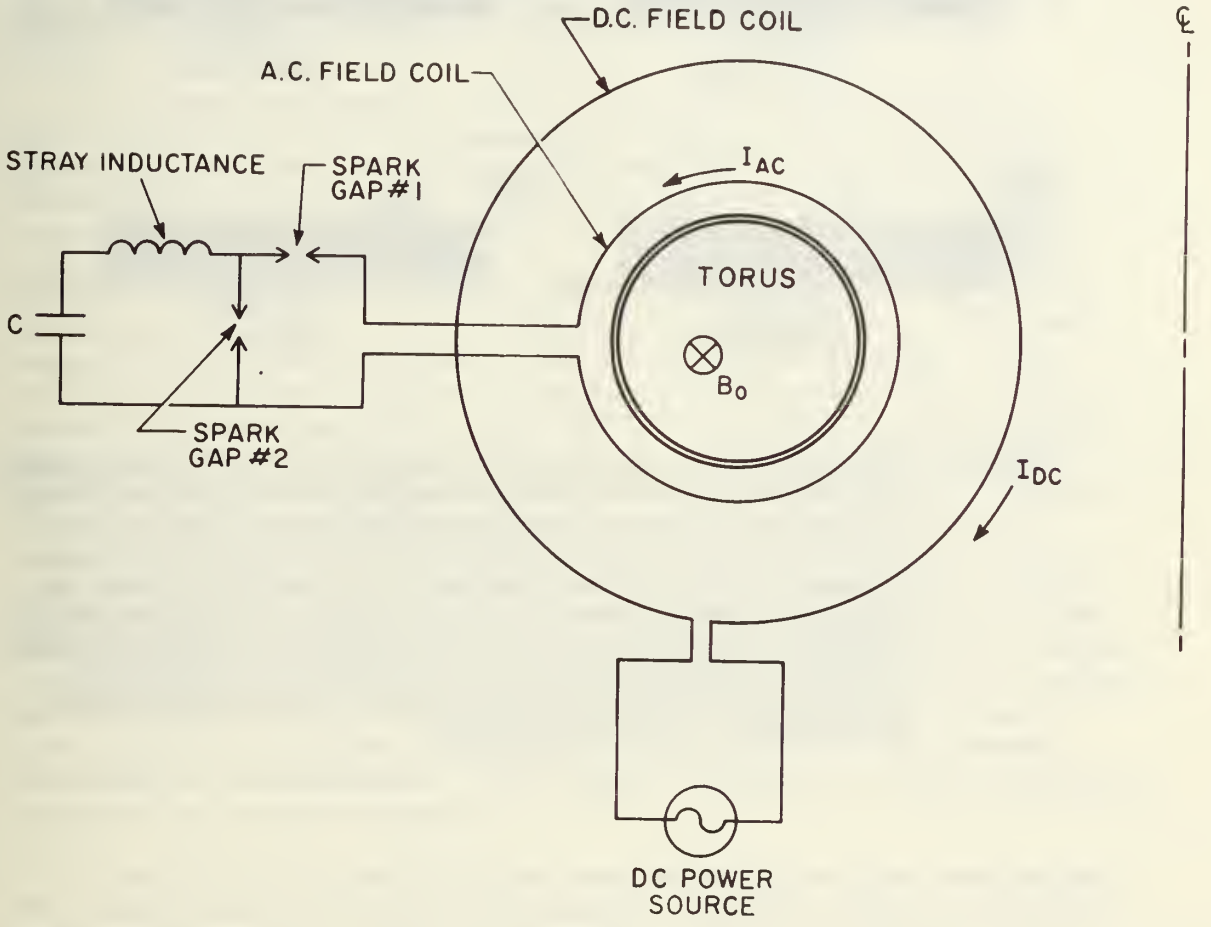

Fig. 4 Schematic illustration of the "ring-down-up" method used for producing a magnetic field with both a short rise time and a long, steady state time duration. The system consists of a D.C. field coil inside of which is located an A.C. coil, that is pulsed for one half of a cycle in order to reduce the D.C. field to zero for a short period of time. Long term containment requires a true D.C. source, e.g. a battery bank, but it is more convenient to use a capacitor bank for containment times $\leq$ 10 msec.

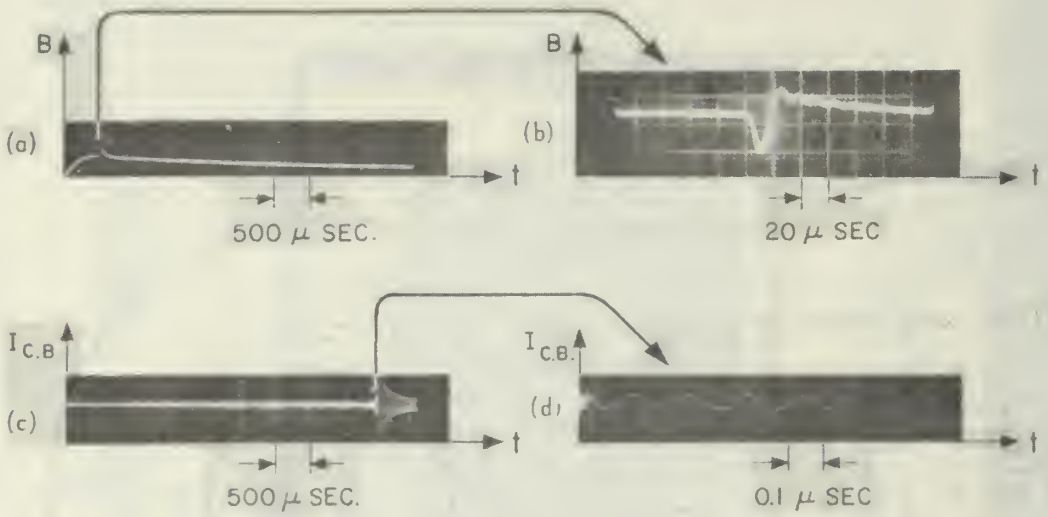

Fig. 5 This set of oscilloscope traces shows the result of an experiment with the Mark II containment apparatus operating in the "ring-down-up" mode of magnetic field programming. In this case a "crowbarred" capacitor bank was used to create a semi D.C. field, shown by traces (a) and (b). Trace (c) is a signal from an image current button, showing the onset of the ion instability about 4 msec after the electron injection. The frequency of the resulting diocotron wave, shown by trace (d), is a direct measure of the average space charge density; here $\approx 1.5 \times 10^9$ cm^{-3}.

FAST PLASMA HEATING RESEARCH

M. Kristiansen and M. O. Hagler

Department of Electrical Engineering
Texas Tech University
Lubbock, Texas 79409

The research under grant AFOSR-69-1757 is divided in four major parts: Fast Theta Pinch Plasma heating, CO_2 laser plasma heating simulations, theoretical investigations of solid-fusion plasma interactions, and exploding wires in external magnetic fields.

The major experimental effort is concerned with a very fast theta pinch (TEP-PEE 1). The system will have a 120kV, 24kJ capacitor bank and uses stripline feed plates and a dielectric switch to minimize the inductance. The figure shows a schematic of the system and the firing sequence.

At the present time the system is being tested for high voltage breakdown with only one of the four capacitors in place. With one capacitor the quarter period of the current ($\tau/4$) is 500ns. With all four capacitors in place it will be approximately 700ns. The plasma is preionized with a 45W, 120MHz rf generator; a slow rising bias magnetic field can also be applied. Preheating of the plasma is achieved by switching a low inductance, low capacitance, uncharged capacitor across the switch. This causes the system to ring and forms an approximately 2ev, fully ionized plasma. The main capacitor bank is charged in approximately 1 msec with a swinging Marx generator. Present investigations are primarily concerned with equipment performance, such as current rise times, peak magnetic fields, switch firing time and jitter, etc. Future investigations will be concerned with studies of shock compression and with end losses and possible end stopping mechanisms. Diagnostic tools include, among others, holographic interferometry, fast cameras, neutron and x-ray detectors, magnetic and electric probes.

A 50W, CW, CO_2 laser is being used in plasma heating simulations. The basic idea is to locate the plasma inside the laser cavity or in a 3-mirror, coupled cavity arrangement. Stacks of sodium chloride flats are used to simulate the plasma and provide the cavity loss mechanism. Theoretical and experimental investigations indicate that both these techniques cause enhanced heating as compared to the simple single pass heating scheme. The final success of the coupled cavity technique appears to depend upon the ability to design a center mirror with very special properties. The experimental investigations have been made on a CW basis but it is felt that the results can be interpreted in terms of pulsed systems. Current theoretical calculations are concerned with the optimum mirror configuration and with the effects of refraction and self-focusing.

A theoretical study of solid-fusion plasma interaction is underway. The motivation for the study is, among others, the problem of

fusion reactor fuel injection and also the possibility of creating a powerful UV source. The theoretical problem is quite complex and the models used in the preliminary calculations appear to be much too simpleminded. The present effort is concerned with formulating a satisfactory and yet tractable model. The model involves the nonlinear heat diffusion equation and includes the criteria for establishing strong, thermal shocks in the solid as well as the effects of surface phenomena. Calculations will be made using both a uniform plasma slab model and also the case of injecting the solid both parallel and perpendicular to the magnetic field into an increasingly dense plasma.

The exploding wire experiment employs a 20kV, 4.5 μf, 4nh capacitor and a low inductance switch and coaxial wire holder system. The exploding wire can be placed in an axial magnetic field. The purpose of the investigation is to study the effect of axial magnetic fields on the pauses (or "dwell" times) in the discharge. This system is also comparatively fast and no pauses have been observed when the wire is brought to explode at the peak current. The current interruption when the wire explodes appears to be very fast. The axial magnetic field currently used appears to be too weak (few thousand Gauss) to cause more than a minor change in the I-V characteristics of the discharge.

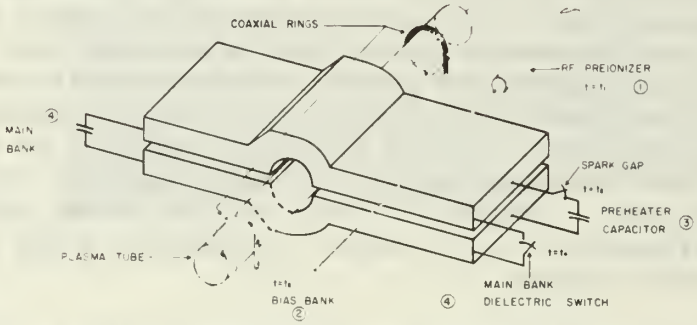

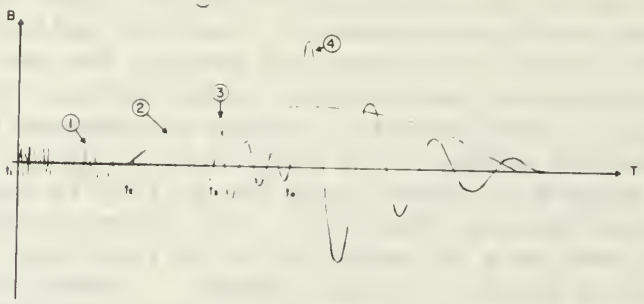

ION HEATING AND CONFINEMENT OF NEUTRAL-FREE PLASMAS

A. J. Lichtenberg and M. A. Lieberman

Department of Electrical Engineering and Computer Sciences
Electronics Research Laboratory
University of California, Berkeley, California 94720

The heating and confinement of a dense ($\omega_{pi} >> \omega_{ci}$), hot-ion ($T_i > 1$ keV) lithium plasma are the objects of the experimental research. Lithium is chosen because: (1) it has a small ion Larmour radius for a given magnetic field; (2) it has a very low vapor pressure at room temperature; (3) its ion charge-exchange cross section is low for most contaminant gases; and (4) source techniques (contact ionization or photoionization) are available to provide a consistent and controllable initial plasma for subsequent heating and confinement experiments.

Generation and Confinement

The basic research facility is a pulsed, magnetic mirror compression experiment[1] (BME-II) with a peak magnetic field of the order of 50 kG and a mirror ratio of 1.5. The field rises to its peak value in 0.5 msec and decays on a time scale of 10 msec. At present, the initial lithium plasma is produced by a contact ionization source and is trapped and heated by adiabatic magnetic compression.

The source produces a two inch diameter column of lithium plasma of density $n = 10^9$ cm^{-3} and temperature $T_i = 0.2$ eV. Langmuir probes and a recently developed microwave cavity technique have been used to measure the density and temperature. To guide the lithium plasma into the high-field compression region, a large volume, d.c. solenoid, producing a peak magnetic field of 800 gauss, has been constructed.

Operating with adiabatic magnetic compression, radial probe measurements show that after an initial stable period of 100-200 microseconds, radial loss occurs in several bursts and continues for as long as a millisecond. Ion energies of 40 eV, consistent with adiabatic compression theory, have been measured[2]. Work has been completed on the task of formulating a set of coupled, first order differential equations describing the dynamics of the lithium plasma in the magnetic mirror compression experiment.

The production of a lithium plasma by photoionization is now under investigation. An experiment to measure the photoionization, using a Xenon flashtube uv source, is now under construction.

Plasma Heating

A broad range of heating mechanisms are being studied for the heating

Research sponsored by the Air Force Office of Scientific Research, Office of Aerospace Research, United States Air Force under AFOSR Grant AF-AFOSR-69-1754.

of both ions and electrons in the lithium plasma magnetic compression experiment. Because of the low initial ion temperature, in addition to the adiabatic heating from magnetic compression, another ion heating mechanism must be employed to obtain ions in excess of 1 keV. Separate electron heating is necessary if the electrons are to be independently confined, and may also be required to stabilize the confined ions. The heating experiments are also viewed as a means of testing heating mechanisms in an environment in which there is little background plasma.

Theoretical and experimental investigations of electron-cyclotron resonance heating in magnetic mirrors is a continuing program. Analytical and numerical work[3,4] indicates that an electron moving in and out of resonance due to its longitudinal motion is stochastically heated by a single frequency r.f. source. A simple, stochastic theory has been confirmed both by exact orbit computations and by experimental results[5]. The experiments have demonstrated that a short pulse (0.2 μ sec) of 3 cm wavelength microwaves of high power (250 kw) can heat electrons above 10 keV. Subsequent adiabatic heating creates an electron plasma with temperature above 100 keV. A second mechanism, which heats both ions and electrons is "turbulent" heating which is initiated by accelerating the electrons through the ions by means of a ringing discharge. The subsequent electron-ion instability has been found to strongly heat the electrons and probably heats the ions also[6]. However, the experiment was performed with a pulsed source, producing a large gas load, causing any hot ions to be lost by charge exchange.

Current theoretical work centers on an understanding of the basic resonant mechanism by which adiabatic invariance is destroyed, and the mechanism which generates stochastic behavior. The Fermi acceleration process is being studied as a simple example exhibiting the transition to stochastic behavior. The transition from a purely stochastic region to one in which adiabatic regions also exist can be predicted analytically. The results of this investigation are being applied to both ion and electron heating. An apparatus to produce a modulated high power (10 kV, 2amp) electron beam has been constructed to resonantly heat the ions in the lithium plasma experiment. The beam serves as a mechanism to allow the accelerating fields to penetrate the plasma, in contrast to external fields which are subject to electron shielding. The collective behavior of the plasma is taken into account in choosing the heating frequency. The turbulent heating experiment will also be repeated in the neutral free, lithium plasma environment.

References

1. M. A. Lieberman and A. J. Lichtenberg, "Plasma Density Measurement by Cavity Perturbation in High Density Plasma," Phys. Fluids, 12, 2109-2116.

2. J. Kim, A. J. Lichtenberg and M. A. Lieberman, "Magnetic Mirror Compression and Heating of a Contact Ionization Lithium Plasma," Bulletin of the A.P.S., 14, 1053 (1969).

3. A. J. Lichtenberg and F. Jaeger, "Modification of Adiabatic Invariance Due to Resonances I: The One-Dimensional Oscillator," Bulletin of the A.P.S., 14, 1074 (1969).

4. F. Jaeger, A. J. Lichtenberg and M. Seidl, "Modification of Adiabatic Invariance Due to Resonances II: Magnetic Mirror with r.f. Perturbation," Bulletin of the A.P.S., 14, 1074 (1969).

5. A. J. Lichtenberg, M. J. Schwartz, and D. T. Tuma, "Non-Adiabatic and Stochastic Mechanisms for Cyclotron Resonance Trapping and Heating in Mirror Geometries," Plasma Phys., 11, 109 (1969).

Kinetic Theory of Unstable Plasmas (Grant No. 69-1697)

J.E. McCune and J.D. Callen
Department of Aeronautics and Astronautics, M.I.T.

I. Program and Objectives

The general objective of this study is to provide more extensive information than is yet available concerning properties of plasma instabilities of the type for which there is as yet no clear-cut means of stabilization in devices aimed at plasma containment in the fusion regime. Outstanding examples include a variety of ion-cyclotron modes (of special concern in mirror machines) and "drift-universal " instabilities (of special concern in toroidal devices). Common to these modes is the necessity of a kinetic description (as opposed to a fluid or MHD description) even in the linear regime.

Our current effort is divided into four parts: 1) Examination of the integral equation for electrostatic perturbations in axisymmetric mirror machines[1], with particular emphasis on the effects of finite geometry on electron Landau damping[2]; 2) Study of the linear theory of drift-universal modes (not stabilized[3] by min-B), with emphasis on determining the complete unstable spectrum[4] -- these results provide the necessary information for use in the non-linear kinetic theory of these modes[5]; 3) Evaluation of the importance of coupling between electrostatic and electromagnetic modes[6]; and 4) Analysis of wave-particle energy transfer with emphasis on wave-amplitude limiting effects for ion-cyclotron instabilities[7]. Much of this work is in collaboration with other groups and is partially supported elsewhere. Because of space limitations we describe below some specific results only for item 2).

II. Some Unfamiliar Properties of Drift-Universal Modes

Using the "slab" model of plasma equilibria with gradients perpendicular to $\underset{\sim}{B}$, we have obtained specific results[4] for the marginal-stability properties of collisionless drift modes (driven by density gradient only). No magnetic shear or curvature effects are included in these preliminary results. Typical results are shown in Figs. 1 and 2 for a proton plasma with $T_e/T_i = 1$. These results extend the earlier results of Krall and Rosenbluth[8] by providing

marginal stability curves over a wide range of $k_\perp a_i$; application to the Wendelstein (WII) experiment is discussed elsewhere[4].

The marginally stable modes divide into three groups (Fig. 2). For small $k_\perp a_i$ ($\lesssim 0.4$) there is a "low-density" branch and a "high-density branch" (i.e., increasing the density eventually stabilizes modes of this type). For $k_\perp a_i \gtrsim 0.4$, there is only one marginally stable branch. For the latter modes the threshold frequency is drastically modified by departure from quasi-neutrality and is roughly proportional to k_z (Fig. 1). Since in this case ω/k_z (threshold) is of the order of or less than the ion thermal velocity, α_i , the usual approximation relating drift waves (generically) to ion-acoustic modes is not useful. An accurate analytic formula for the threshold frequency is shown on Fig. 1.

The vastly different properties of the three groups of marginally stable drift modes shown in Fig. 2 maintain themselves in the unstable regime $[k_z/\varepsilon' < k_z/\varepsilon')_{crit}$ at fixed $k^2\lambda_D^2]$. Figs. 3 and 4 show the growth rates (γ) and real frequencies (ω_r) for unstable modes with $k_\perp a_i = 5$ and $k_\perp a_i = 0.1$, respectively. On each figure the effect of density ($k\lambda_{Di}$) is illustrated.

For $k_\perp a_i = 5$ (Fig. 3) the real part of the frequency takes on its "classical" value[9] (modified for finite $k\lambda_{Di}$) only at one value of k_z ; this formula is therefore not useful in describing any significant part of the unstable spectrum. On the other hand, the estimate of the maximum growth rate (and the k_z at which it occurs), given in Ref. 8, is fairly accurate. We also show on Fig. 3 the behavior of ω_r and γ for very small k_z . Analytic formulas for this behavior are shown on the figure.

For $k_\perp a_i = 0.1$ (Fig. 4), by contrast, the real part of the frequency and the growth rate take on their "classical" values[8] over a fairly significant range of unstable k_z's , particularly at "low" densities (curve (1)) and "moderate" densities (curve (2)). However, no single formula, describing either $\omega_r(k_z)$ or $\gamma(k_z)$ over the full unstable range is yet available.

The behavior of a $k_\perp a_i = 0.1$ mode at very high density (curve (3), Fig. 4) is particularly interesting. At the critical (maximum) $k_z a_i$ for onset, ω_r is very close to (but slightly less than) ω_* . As we move into the unstable regime ω_r drops slightly as γ approaches its first maximum. Then, at about the point at which $\omega/k_z\alpha_e$ approaches unity, ω_r <u>exceeds</u> ω_* ,

the electrons get out of resonance with the wave, and γ accordingly drops dramatically. The growth rate then recovers, rising sharply to a second maximum near $0.3\omega_*$. This second maximum is almost 30 times the first! This is a "nonresonant" instability, first noted by Kadomtsev and Timofeev[10], and, if it can occur, could lead to very large cross-field diffusion. This mode requires, however, a very long wave length along $\underset{\sim}{B}$ (Fig. 4) and probably can occur, if at all, only in certain toroidal devices (for example, in a high-symmetry stellarator with a small, but rational, rotational transform).

More extensive results concerning the properties of drift-universal modes will be reported elsewhere. Effects of departure from slab geometry are under investigation.

References

1. C.W. Horton, J.D. Callen and M.N. Rosenbluth, "Microinstabilities in Axisymmetric Mirror Machines" (to be published).

2. C.C. Damm, J.H. Foote, A.H. Futch, Jr., A.L. Hunt, K. Moses, R.F. Post, J.B. Taylor, "Evidence for Collisionless Damping of Unstable Waves in a Mirror-Confined Plasma", Lawrence Radiation Laboratory, Preprint U.C.R.L. - 72201 (1970).

3. M.N. Rosenbluth and N.A. Krall, Phys. Fluids 8, 5, 1004, (1965).

4. J.E. McCune and K. von Hagenow, "Properties of Marginally-Stable Collisionless Drift-Universal Modes with Application to the W-II Stellarator", Institut für Plasmaphysik Report, Garching, Germany (in press).

5. T.H. Dupree, Phys. Fluids 11, 12, 2680 (1968).

6. J.D. Callen and G.E. Guest, "Electromagnetic Corrections to the Electrostatic Dispersion Relation" (to be published).

7. D.J. Sigmar and J.D. Callen, "Wave-Particle Energy Transfer and Wave Amplitude Limiting Effects" (to be published).

8. N.A. Krall and M.N. Rosenbluth, Phys. Fluids 8, 8, 1488 (1965).

9. B.B. Kadomtsev, Plasma Turbulence, Academic Press, London (1965).

10. B.B. Kadomtsev and A.V. Timofeev, Dokl. Akad. Nauk SSSR 146, 3 581 (1962); Translation: Sov. Phys. - Doklady 7, 9, 826 (1963).

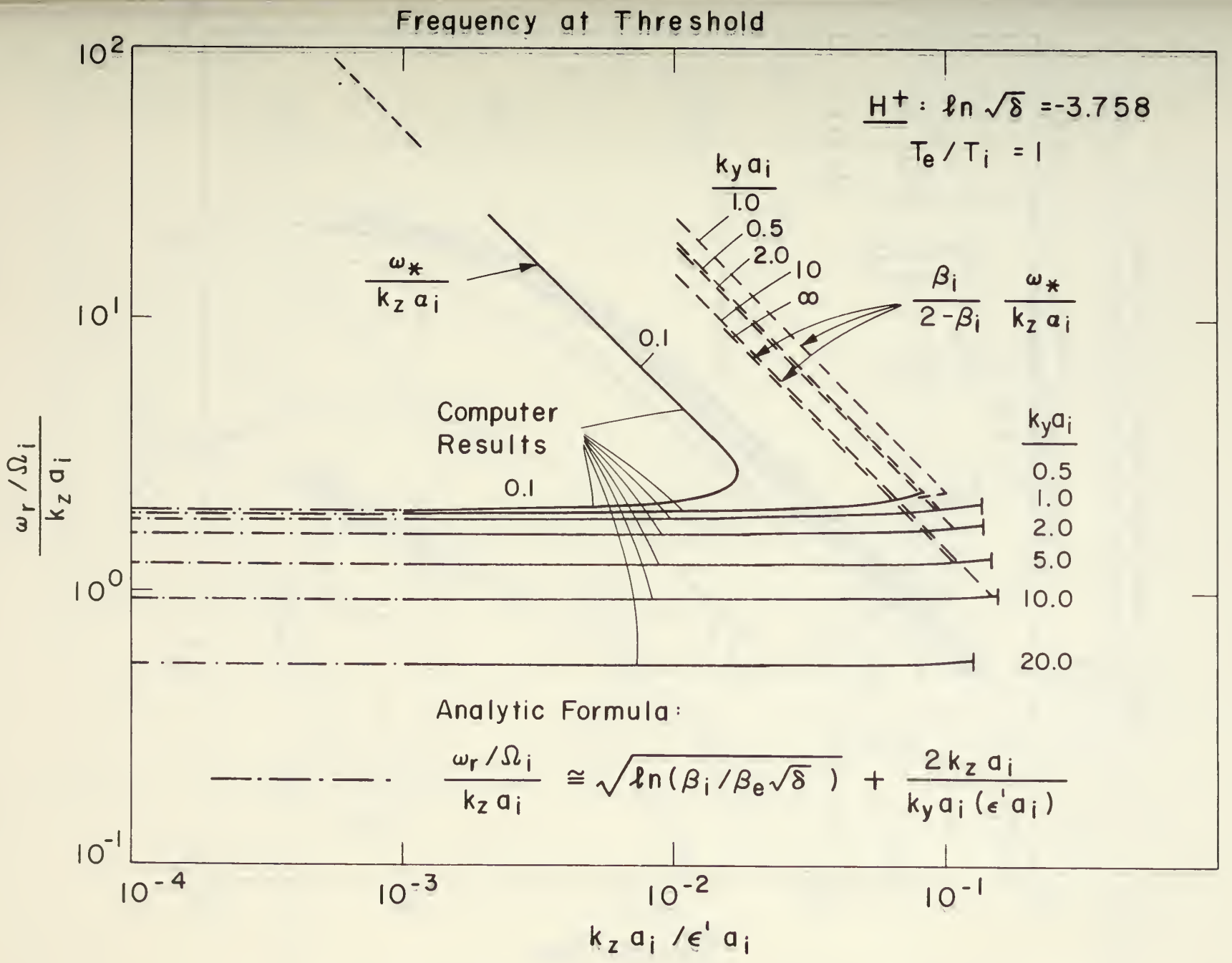
Frequency at Threshold
H^+ : $\ell n \sqrt{\delta}$ = -3.758
T_e / T_i = 1
$k_y a_i$
1.0
0.5
2.0
10
∞
$\frac{\omega_*}{k_z a_i}$
$\frac{\beta_i}{2-\beta_i} \frac{\omega_*}{k_z a_i}$
0.1
Computer Results
0.1
$k_y a_i$
0.5
1.0
2.0
5.0
10.0
20.0
Analytic Formula:
$\frac{\omega_r / \Omega_i}{k_z a_i} \cong \sqrt{\ell n (\beta_i / \beta_e \sqrt{\delta})} + \frac{2 k_z a_i}{k_y a_i (\epsilon' a_i)}$
$\frac{\omega_r / \Omega_i}{k_z a_i}$
10^2
10^1
10^0
10^{-1}
10^{-4}
10^{-3}
10^{-2}
10^{-1}
$k_z a_i / \epsilon' a_i$

Fig. 1

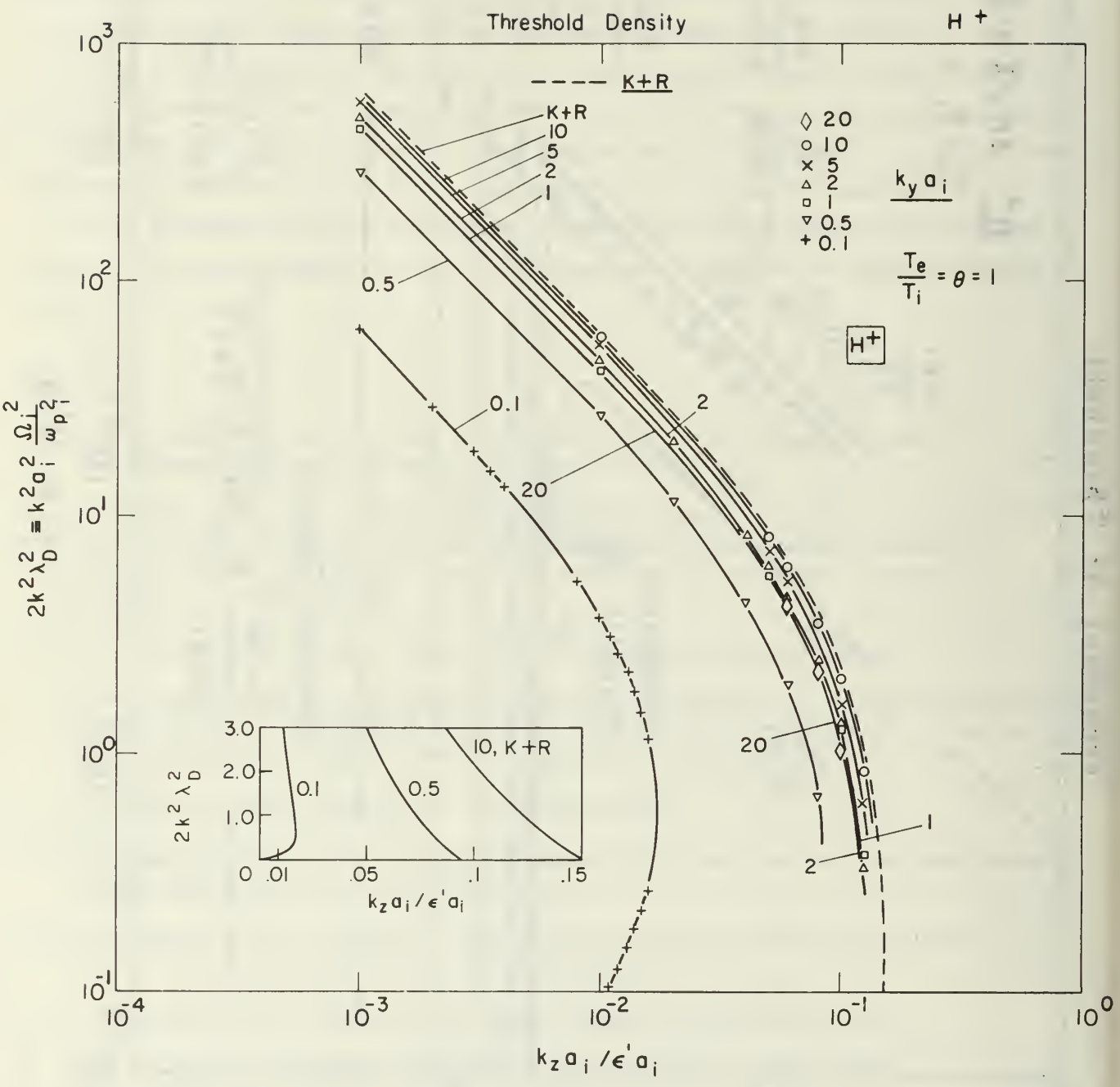
Threshold Density
H +
---- K+R
K+R
10
5
2
1
0.5
0.1
20
◇ 20
○ 10
× 5
△ 2
□ 1
▽ 0.5
+ 0.1
$k_y a_i$
$\frac{T_e}{T_i} = \theta = 1$
H+
$2k^2\lambda_D^2 \equiv k^2 a_i^2 \frac{\Omega_i^2}{\omega_{pi}^2}$
$k_z a_i / \epsilon' a_i$
$2k^2\lambda_D^2$
3.0
2.0
1.0
0
.01
.05
.1
.15
0.1
0.5
10, K+R

Fig. 2

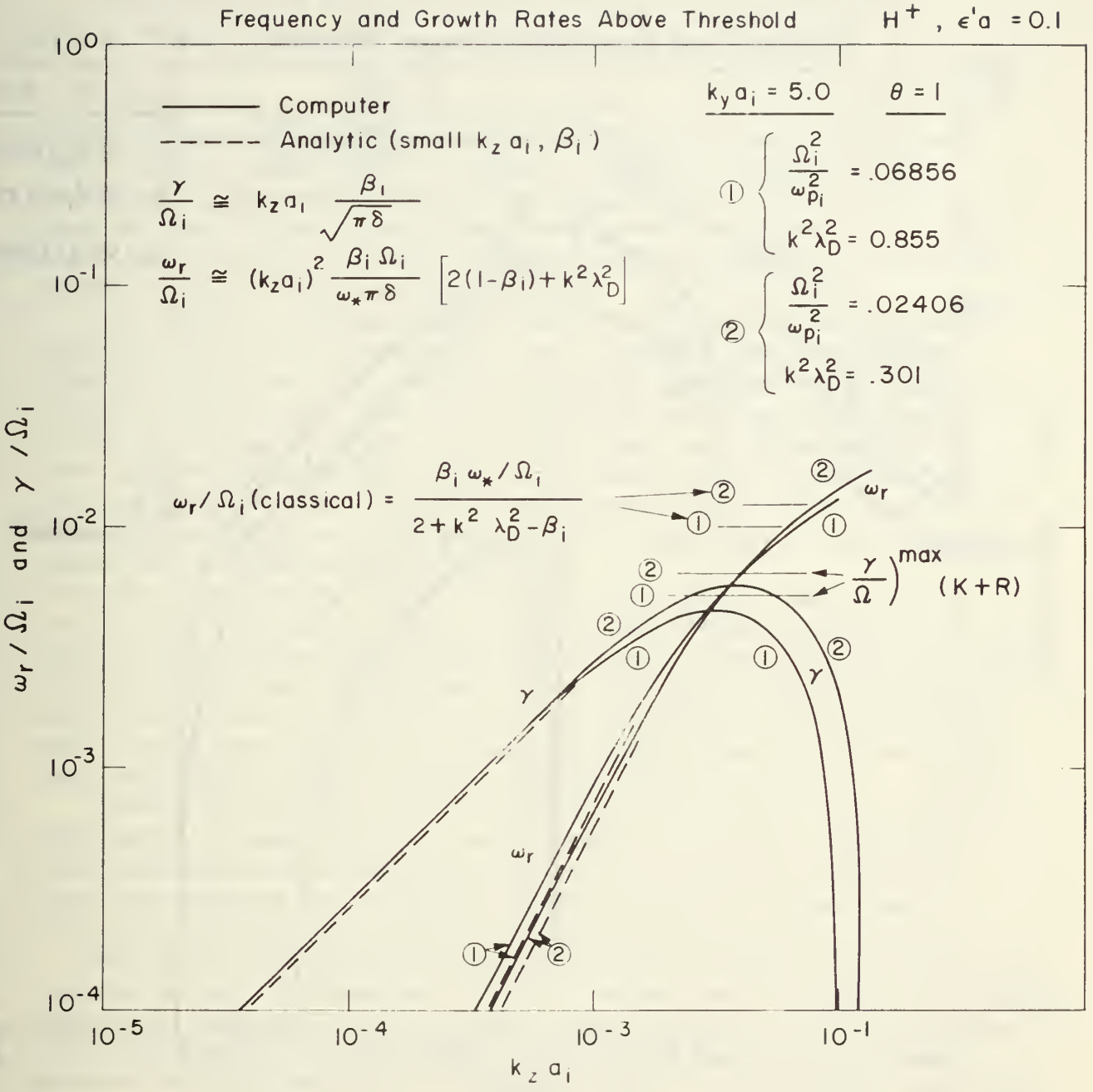
Frequency and Growth Rates Above Threshold
H+ , ϵ'a = 0.1
Computer
Analytic (small k_z a_i , β_i)
γ/Ω_i ≅ k_z a_i β_i / √(πδ)
ω_r/Ω_i ≅ (k_z a_i)^2 β_i Ω_i / (ω_* π δ) [2(1-β_i) + k^2 λ_D^2]
k_y a_i = 5.0
θ = 1
① Ω_i^2/ω_pi^2 = .06856
k^2 λ_D^2 = 0.855
② Ω_i^2/ω_pi^2 = .02406
k^2 λ_D^2 = .301
ω_r/Ω_i (classical) = β_i ω_*/Ω_i / (2 + k^2 λ_D^2 - β_i)
ω_r
γ
(γ/Ω)^max (K+R)
ω_r/Ω_i and γ/Ω_i
k_z a_i
10^0
10^-1
10^-2
10^-3
10^-4
10^-5
10^-4
10^-3
10^-1

Fig. 3

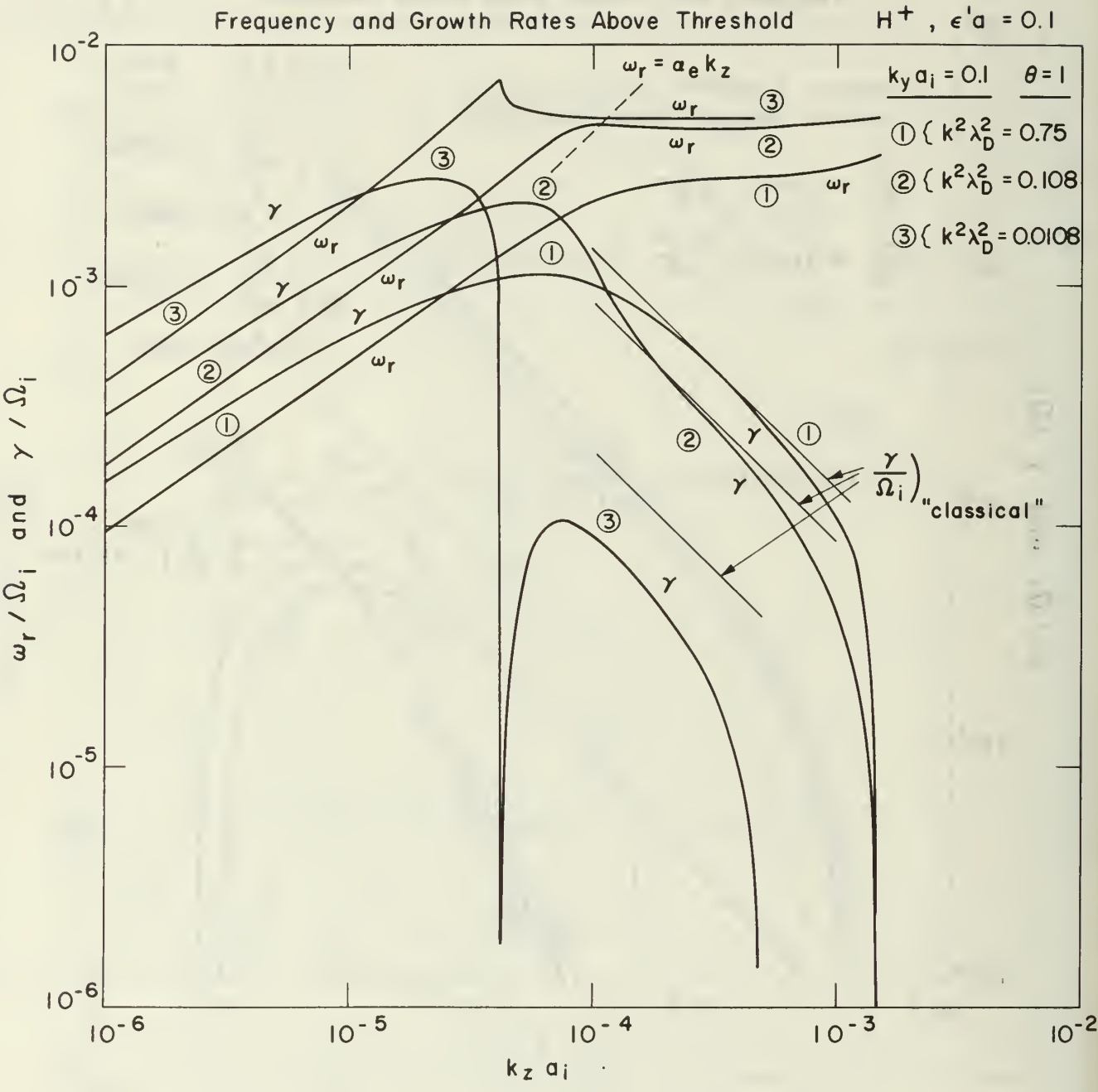
Frequency and Growth Rates Above Threshold
H+ , ε'a = 0.1
ω_r = a_e k_z
k_y a_i = 0.1
θ = 1
① { k²λ_D² = 0.75
② { k²λ_D² = 0.108
③ { k²λ_D² = 0.0108
ω_r / Ω_i and γ / Ω_i
k_z a_i
"classical"
10^-2
10^-3
10^-4
10^-5
10^-6

Fig. 4

Rotating R-Field Plasma for Thermonuclear Power Reactors

M. L. Pool - The Ohio State University

An inspiriting approach to a realistic thermonuclear reactor is now evinced through experimental results and through computer analyses. The former is secured by an auxiliary rotating electric field and a revolving magnetic field, both at the ion cyclotron frequency, impressed upon the main B_z magnetic field of the magnetic bottle employed. The latter is secured by submitting various pertinent boundary and operating conditions to a 360 IBM computer.

The auxiliary rotating electric field is normal to the direction of the central axis of the magnetic bottle and is obtained from neighboring electrical currents. The auxiliary revolving magnetic field is parallel to B_z. As an example, the electric field has a value of 10 volts cm^{-1} on the central axis and increases to twice that value 10 cm off the axis. The auxiliary magnetic field has zero strength on the central axis and increases with distance from the central axis. The radial variation of B_z is utilized to put an upper bound on the energy that an ion can achieve during its cyclotron excitation life time.

In the above fields a sample numerical calculation was made of the motion of a collisionless deuteron that started initially with 4 eV of energy and 4 cm from the central mirror axis. The rotating and revolving fields simultaneously heated the ion to a maximum energy of 57keV and moved the guiding center of the ion orbit to within 0.5 cm of the mirror axis. From then on the ion's energy oscillated between 7keV and 57 keV while the guiding center remained within 0.5 cm of the axis.

Motion in three dimensions has been also numerically analyzed. Although the magnetic mirrors tend to put the ion ahead in phase relative to the phase of the cyclotron frequency of the oscillator, the electric field impressed by the oscillator continually tends to rephase the ion in its orbit so that the gain in phase caused by the mirrors is nullified.

The effects of scattering on the motion of an ion have been numerically analyzed at each 0.15 degrees of arc of the ion's orbit. Many small angle scatterings contribute to give a single large R.M.S. scattering angle. The rephasing action of the electric field during the mean free time reduces the net large R.M.S. scattering angle. Consequently, nearly all the ions which initially have energies of even a few tenth of an electron volt, and therefore have many scattering experiences, reach energies in the keV range without being scattered out of the system. In most cases calculations were made where the small angles varied between 10 and 15 degrees of arc and where a scattering event occurred whenever the deflection probability reached or exceeded 40%.

Experimental results have been achieved with a gaseous ion source and with a disk plasma focus. Experience with an ion source initiated by a laser is currently very limited. However, data tend to point out many accrued advantages if a laser source were used in the present equipment.

In summary the salient characteristics of the current and / or projected ensemble are:

1. Rotating electric accelerating and revolving magnetic guiding fields are furnished by a two phase oscillator operating at the ion cyclotron frequency.
2. Ions are given arbitrarily chosen maximum energy limits above which no further energy is added.
3. The energetic ions are maintained in a parking orbit.
4. Scattering losses in energy, in phase, and in direction of motion are essentially nullified.
5. A laser initiated ion source would provide a copious supply of low energy ions for subsequent acceleration in an exceptionally clean system.

BROKEN SYMMETRIES AND CTR CONFINEMENT

Daniel R. Wells
University of Miami

In 1960 the author began investigations of plasma produced by a modified theta-pinch coil[1]. The coil was contoured into the shape of a cone with a 40° aperature angle. He observed that plasma blobs were formed which appeared to have a well-organized current and flow structure. These structures were fired down a long solenoidal drift tube and their properties were studied in some detail[2]. It was observed that they carried trapped azimuthal as well as longitudinal magnetic fields. Further investigation revealed that they were extremely stable and resisted efforts to disrupt their structure. The densities in these plasmoids were of the order of 10^{16} particles per cubic centimeter and the temperatures involved were of the order of 100 electron volts or less. The author put forth a heuristic theory describing these structures as plasma vortex rings or spheroids and began to make educated guesses about the details of their geometries. In the meantime, other investigators became enthused about the concept of plasma vorticity and began to look for similar structures in other plasma configurations and plasma guns. In particular, Dr. Winston Bostick reviewed his work on plasmoids which had been in progress since the early 1950's and came to the conclusion that the structures he had been studying were also plasma vortex structures, both of the type observed by the author and of other types never before observed or studied[3].

The author decided that since the structures were very stable that it might be interesting to attempt to build a thermonuclear reactor based on the principle of the interaction of plasma vortex structures. His studies indicated that the most useful arrangement might be the injection of a set of vortex rings produced in the throats of a set of mirror coils and allowed to interact at the center of the mirror geometry[4]. The idea was that since each ring carried a trapped magnetic field, in the same direction as its partner approaching from the other end of the machine, the resulting trapped fields would reverse the field of the main mirror coils and produce a minimum $\vec{B}$ geometry. The resulting minimum $\vec{B}$ confinement would last as long as the vortex rings continued to exist. Thus the rings would have the dual purpose of producing the confinement geometry and heating the plasma. The heating effect would be produced by the mutual annihilation of the vortex rings. This was the original application of the concept of "vortex burning".

A machine based on these principles was built at the Plasma Physics Laboratory of Princeton University in 1963. The machine performed exactly as predicted. The field was reversed, the plasma was heated at the center of the mirror and the resulting overall structure appeared to remain intact for several hundred microseconds. High density plasma remained in the mirror for times of the order of milliseconds, although this afterglow plasma appeared to be cold. The experiment was discontinued at Princeton in 1964 because no one except the author and Dr. Winston Bostick at that time believed that the concept of plasma vorticity could possibly play an important role in the CTR program. In 1969, many papers were published which attempt to show that "convective cells or plasmoids" are the basic cause of "pump out".

The machine was moved to the Plasma Physics Laboratory of the University of Miami where it has slowly been reconstructed and improved, as funding allowed, in an attempt to at least bring the experiment back to the densities and temperatures attained at Princeton in 1964. This has finally been achieved and the resulting structures are now under study utilizing the more sophisticated diagnostics made possible by a six year improvement in the state of the art.

In the meantime, other investigators at General Electric Corp.[5], Grumman Aircraft and Engineering Corp.[6], and lately at Sandia Corp.[7], have obtained similar results and the concept of plasma vorticity is now a respectable idea. The work of Cowan at Sandia is especially notable since he has used explosive generators to produce the plasma vortex rings. The generators are equivalent to a multi-megajoule capacitor bank and the rings carry trapped currents of three to four hundred thousand amperes. The same experiment will shortly be repeated utilizing the author's geometry of two rings meeting inside a magnetic mirror, only now one will have 2 megajoules of energy in each end of the machine. Cowan has also introduced the concept of using a planar shock wave passing through a theta-pinch coil, parallel to the axis of the coil to produce the vortex rings. This allows him to use explosive generators in producing both the planar shock and the theta-pinch field and augurs well for a more conventional machine at high energies because it eliminates the critical problem of the inherent coupling inefficiencies of a conical theta-pinch gun. It further eliminates the problem of impurities produced when the collapsing current sheet leaves the wall of the generator.

During the six years that have elapsed while attempts were being made to bring the machine up to high energies using surplus and outdated equipment, the author, along with Dr. Joseph Norwood, Jr., has been building a theory of plasma stability which not only describes the plasmoids generated in the conical theta-pinches, but also those generated by Dr. Bostick in his coaxial guns[8]. The theory is entirely new and unique in that it is a true global nonlinear theory and not just a small extension of the quasilinear or normal mode cascade theory now common in the CTR program. From rather heuristic beginnings, the theory has grown to one in which the concept of the space-time and various gauge symmetries of the magnetohydrodynamic flow field are utilized in order to find the constants of the motion involved[9]. For every symmetry there is a corresponding conserved integral (Noether's theorem). If that symmetry is broken, then that integral must not be applied to the problem. Once all of the symmetries and constraint integrals have been found, then one applies the principle of least constraint. This principle states that if the total energy of the plasmoid is varied, subject to a set of constraint integrals on the flow, then the fewer the number of constraint integrals applied, the more stable the resulting structure. Thus, the more symmetries that are broken, the more stable the corresponding structure. The minimum number of constraint integrals which apply to a linear (superposable) flow field results in a set of flow equations which describe a force-free collinear vortex ring. If linearity is sacrificed, then fewer constraints can be used and the resulting structure is a quasi-rigid rotator centered on the magnetic guide-field lines. Many other types of structures are possible depending on what symmetries are broken and thus what constraint integrals must be applied. It is possible to have several different types of stable vortex structures existing in the same plasma machine at the same time. The plasma will always try to form these structures if it can.

It is interesting to note that preliminary studies of Tokamak indicate that it consists of a force-free torroidal shell of plasma surrounding a torroidal quasi-rigid rotator.

Future plans are a projected study and correlation of the measured details of the structures and the spectrum of plasmoids predicted by the symmetry principles. If current experiments on the colliding vortex ring configuration further prove this geometry as a stable configuration, then a much more sophisticated version of the machine should be built.

REFERENCES

1 Wells, D.R. 1962, Phys. Fluids 5, 1016.

2 Wells, D.R. and Schmidt, G., 1963, Phys. Fluids 5, 418.

3 Bostick, W.H., Byfield, H., and Jermakian, A., 1966, Phys. Fluids 9, 2287.

4 Wells, D.R. 1966, Phys. Fluids 9, 1010.

5 Jones, W.B. and Miller, R.D. 1967, General Electric Research and Development Center, Report No. 67-C-178.

6 Small, R.L., Valsamakis, E.A. and Bostick, W.H. 1966, AIAA Plasmadynamics Conference, AIAA Paper No. 66-155, Monterey.

7 Cowan, M., Private Communication.

8 Wells, D.R. and Norwood, J., 1969, Jour. of Plasma Physics 3, 21.

9 Wells, D.R. MIAPH-PP-70.2, 1970, University of Miami Report.

PANEL 4. INSTRUMENTATION AND SIMULATION

Name	Topic
Dr. C. Barnes Institute for Plasma Research Stanford University Stanford, California 94305	Computer Experiments on Inertial Confinement
Dr. Robert L. Hickok Central Research Division Mobil Oil Corporation Princeton, New Jersey 08540	Beam Probe Measurements of Plasmas
Dr. R. M. Measures University of Toronto Institute for Aerospace Studies Toronto, Canada	Tuned Laser Diagnostics
Professor Joseph T. Verdeyen Department of Electrical Engineering University of Illinois Urbana, Illinois 61801	An Experimental Study of Electrostatic Plasma Confinement
J. L. Wyatt Bass Corporation Berkeley, California	Direct Nuclear Reactions During Slowing of Fast Ions

Computer Experiments on Inertial Confinement

by C. Barnes* and D. A. Dunn

The objective of this project is to understand the behavior of the electrostatic-inertial confinement device, a proposed method of fusion plasma generation in which no dc magnetic fields are applied. The device consists of a spherical chamber into which many high energy ion beams are injected radially inward. Electrons are created at the outer radius with essentially zero energy. It is then hoped that a sufficiently dense, energetic plasma will form in the spherical chamber for efficient fusion power generation. A report of theoretical and experimental work on this problem has been given by Hirsch.[1]

The work performed under this contract is based on the use of numerical simulation techniques such as those of Dunn and Ho[2] and of Burger.[3] The evolution of a simplified model of this device was simulated on a digital computer. A one-dimensional model was used, with only radial fields and motion allowed. The ions were injected at a single high velocity, radially inward. The electrons were injected at the same radius as the ions with a negligibly small energy.

There are two possible steady state solutions to the one dimensional spherical problem. If the computer run is started with the ion space charge dominating, an intermediate solution forms. Figure 1 illustrates the intermediate solution. Shown are velocity vs radius plots for electrons and ions as well as a potential vs radius plot. In all three plots the sphere center is on the right side and the injection radius is on the left side. The intermediate solution is characterized by a virtual anode at a non-zero radius and a virtual cathode within it at or near the center. As electrons are trapped, they tend to neutralize the ion beam and the virtual anode moves toward the center. At low ion beam currents, the virtual anode reaches the center and one of the two steady state solutions forms. At higher ion currents, the high energy ions streaming through the center cause a second virtual anode to form there and subsequently move outward until it merges with the first virtual anode. Figure 2 shows such a case with the second virtual anode having moved part way out to the first virtual

*Paper to be presented by C. Barnes

anode. The steady state solution thus formed (type-two solution) has a low energy ion plasma inside the virtual anode. The other steady-state solution (type-one solution) is one in which the ions stream through the center with no virtual anode forming (Figure 3).

The emphasis of the work performed this year has been to understand the above described behavior in terms of the static and small-signal theory of simpler systems of beams in finite regions. The basic model studied was a planar, one-dimensional diode into which a single velocity beam is injected. There is also a background of oppositely charged particles with little or no energy which may only partially neutralize the beam. A simple theory has been developed for a partially neutralized beam with an infinite mass background, and computer simulations of this configuration agree with the theory. An extension of the finite mass background theory of Faulkner and Ware[4] to backgrounds of smaller mass than that of the beam was made and computer simulations were made to check this theory. It was found that two types of instability were present. One was the beam instability of Birdsall and Bridges[5] with growth at zero frequency. The second instability was associated with the background species and predicted growth near the background species plasma frequency. The computer simulations confirmed the theory and demonstrated the behavior in the large amplitude, non-linear regime.

The results of these planar diode studies were then used to explain the behavior of the spherical inertial confinement device. The conditions for existence of the Type-One steady state solution were demonstrated and the formation of the second virtual anode was explained.

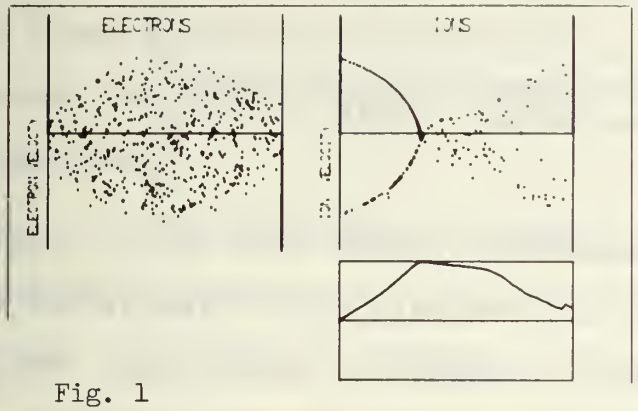

Fig. 1

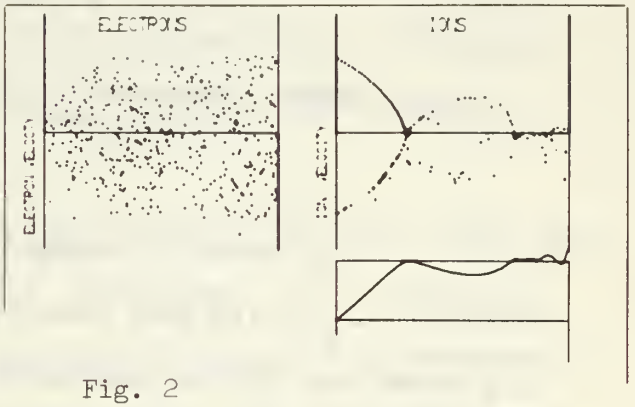

Fig. 2

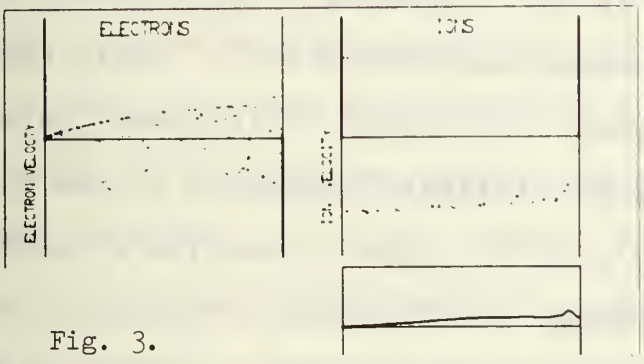

Fig. 3.

References:

1. R. L. Hirsch, JAP 38, 4522 (1967).

2. D. A. Dunn and I. Ho, AIAA J. 1, 2770 (December 1963).

3. P. Burger, J.A.P. 35, 3048, October (1964); Tech. Rept. No. 0254-1, Stanford Electronics Laboratories, April 1964.

4. J. E. Faulkner and A. A. Ware, JAP 40, 366 (1969).

5. C. K. Birdsall and W. B. Bridges, J.A.P. 32, 2611, December (1961); W. B. Bridges and C. K. Birdsall, J.A.P. 34, 2946, October (1963).

BEAM PROBE MEASUREMENTS OF PLASMAS

R. L. Hickok and F. C. Jobes

Mobil Research and Development Corporation
Princeton, New Jersey 08540

The density, space potential, change density (ρ), current density (J_z), and the electric and magnetic fields associated with a plasma can all be measured with a heavy-ion beam-probe. They are measured by measuring and mapping the number, energy, and momentum of doubly charged ions (such as Cs^{2+}) created by collisional ionization of a beam of singly ionized heavy ions (Cs^{+}). Well resolved beam-probe maps of an arc plasma show that n, ϕ, ρ, and J_z are all located in specific and somewhat different locations in the plasma.

The secondary (Cs^{2+}) ions are able to provide a localized measurement of the plasma because, at the point of creation, they undergo a step change in radius of curvature in the magnetic field, and so are separated from the main beam and also from ions created at other points along the beam path. A suitably placed detector thus can monitor the plasma at any arbitrary point, and the entire plasma can be mapped by sweeping the beam and by moving the detector; instead of moving the detector, however, an array of detectors can be used or the beam energy can be varied.

The basic measurements made on the secondary ions are: the number of 2+ ions relative to the number of 1+ ions; the difference in energy between the 2+ and 1+ ions; and the component of momentum parallel to the main magnetic field which is transferred to the 2+ ions. These three measurements give n (actually $n \cdot F(T)$), ϕ and an approximation to A_z, the component of the vector potential

parallel to the main magnetic field. The electric and magnetic fields, and the charge and current densities are obtained from maps of Φ and A_z by taking appropriate spatial derivatives: gradients to get the fields, and Laplacians to get the charge and current densities.

Our heavy-ion beam-probe system consists of a Cs^+ ion gun capable of emitting a 1 μa 5-30 KeV Cs^+ ion beam, and a combined energy and momentum analyzer. The ion gun consists of a thermionic Cs^+ emitter, an electrostatic lens system, and electrostatic sweep plates. The beam from this gun has a spot size 4 mm diameter at 1 meter, and an energy spread of less than 1 eV. The energy analyzer is a parallel plate electrostatic analyzer with the accelerator voltage on the positive plate, and a correction voltage on the negative plate. The ions enter the analyzer through a slit in the negative plate, are deflected by the field in the analyzer, and leave through a second slit to be collected on a split detector. The difference between the signals to the two halves of this detector is greatly amplified and applied as the correction voltage on the negative plate, thereby maintaining the beam of Cs^{2+} ions centered on the split detector: the required correction voltage is the space potential Φ at the point where the 2+ ion was created. The analyzer is mounted so that the ions are deflected in the x-y plane; ion motion along the z direction does not effect the energy measurement. The detector, however, is split in the z direction as well as in the x direction required for energy analysis, and a pair of sweep plates near the entrance slit of the analyzer serves to center the ions in the z direction. The voltage on these plates is proportional to the momentum P_z acquired by the 2+ ions from a

current flowing in the plasma. The sum of the signals to the four quadrants of the detector is proportional to the density at the creation point. The analyzer is thus able to simultaneously measure n, Φ, and A_z.

A set of four beam-probe maps (n, Φ, and ρ) of an arc plasma are shown in Figure 1. The space potential and density maps, although similar in appearance, are not the same: the peak of the space potential (~100 V) lies outside the density peak ($\sim 3 \times 10^{13}$ cm^{-3}). The grey scale in the left-hand charge density map was chosen so that an excess of electrons is white, an excess of ions black, and any shade of grey is neutral. In the right-hand map of ρ the contrast is chosen to show the variations in ρ: the positive and negative peaks correspond to excess ion (Z=2) and electron densities of 4×10^{8} cm^{-3}. The semicircle of electrons has the same radius as the arc cathode. A density and current density pair of maps is shown in Figure 2. Density contour lines at 30%, 50%, and 70% are also shown on the J_z map. The current is quite sharply peaked and is located in a region where $n \cdot F(T)$ is quite low.

At the request of the Princeton Plasma Physics Laboratory we are planning to install a heavy ion beam probe system on the Model T.S. Tokamak. This device, which is being constructed by converting the Model C stellerator to Tokamak geometry, will be the first Tokamak in the U. S. and is scheduled to go into operation in May, 1970. The heavy ion beam probe, which we hope to have operational by June, 1970, will be one of the major diagnostic systems on the T.S. Primary emphasis will be in measuring the plasma current distribution and the plasma space potential.

The T.S. Tokamak will have a major radius of 109 cm and a minor radius of 14 cm. The beam probe system is being designed to operate in the regime where the primary toroidal field on the axis of the donut is 20 kg and the total plasma current is 40 kAmp. Expected plasma density is of the order of 10^{13} cm^{-3} and electron temperature a few hundred eV. Anticipated energy confinment time is about 50 msec.

The heavy ion probe will consist of a 10 u amp, 200 kev beam of either Tl^+ or B_i^+. Measurements will be made right next to the plasma limiter, which is in the pumping port cross. The primary beam will enter through the top port of the cross and the secondary ions will exit through the side port and the pumping duct. The secondary ion detectors will be located approximately 200 cm from the center line of the plasma. Orbit calculations show that with the planned port facilities, it will be possible to map the current density, space potential, and particle density from the outer edge of the plasma to just inside the center line.

The anticipated spatial resolution for an individual measurement is about .03 cm^2. For the current density and particle density measurements the spacing between grid points can be made less than 1 cm if desired; but, at least initially, it is planned to use a somewhat coarser grid network--probably 2 or 3 cm. The grid spacing for the space potential measurements is a somewhat more difficult task because it appears that it will be necessary to use multiple electrostatic analyzers, and we have not yet worked out the geometric details of this installation. The temporal resolution for individual measurements will be of the order of 1 u sec, and it should be possible to make a 100 point map in 1 msec.

Fig 1

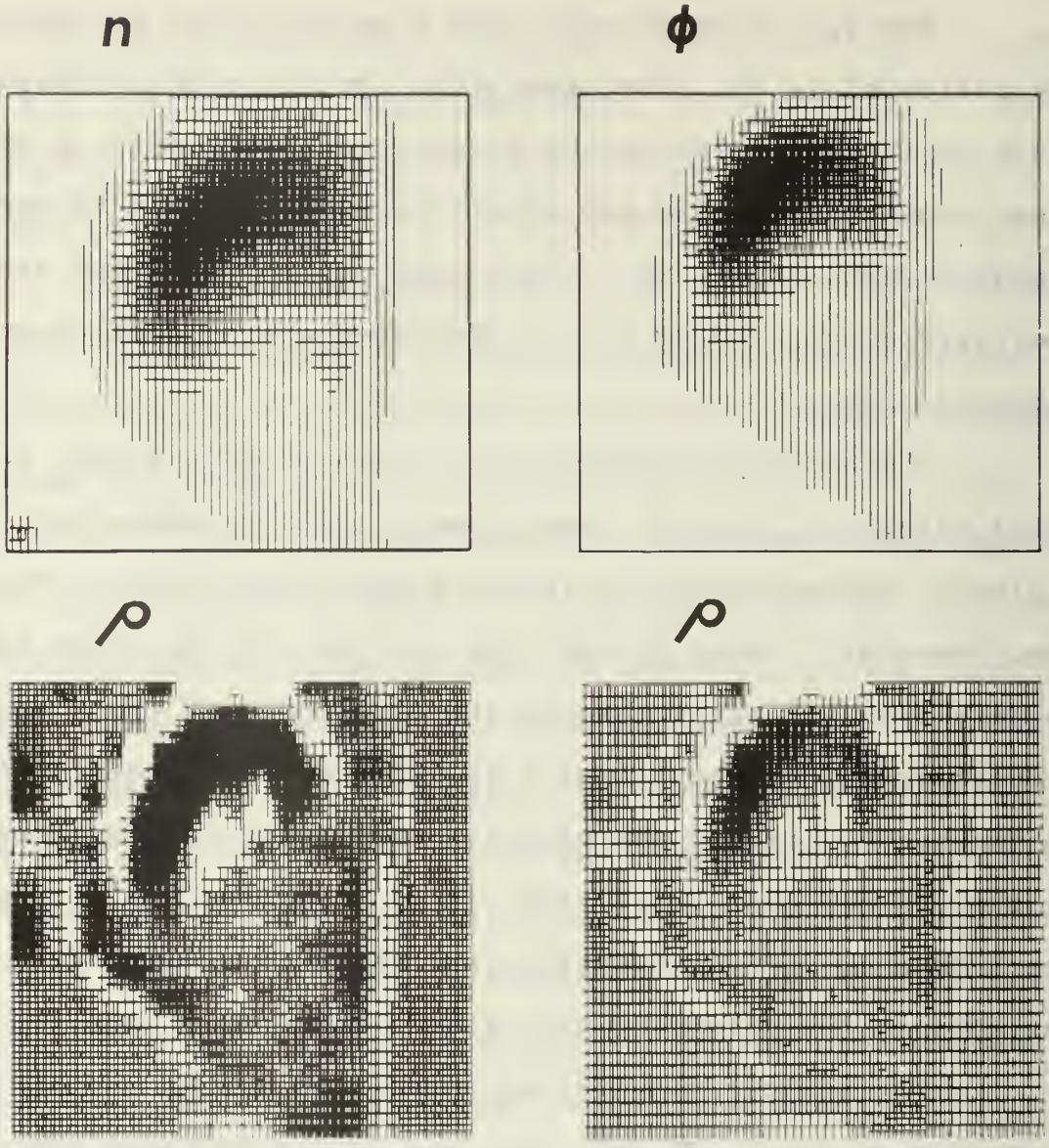

Fig 2

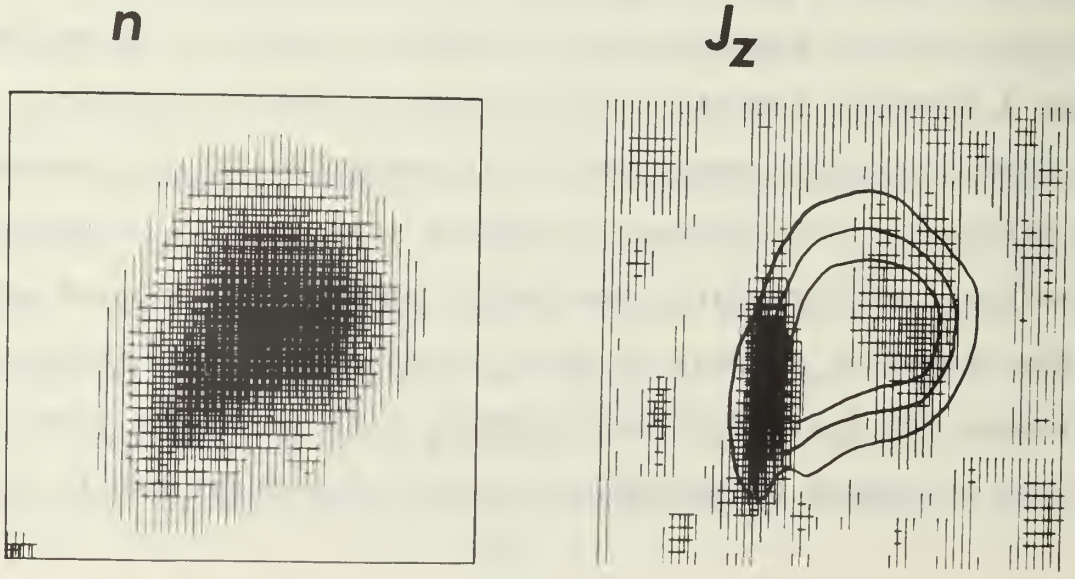

TUNED LASER DIAGNOSTICS

Dr. R. M. Measures
Institute for Aerospace Studies
University of Toronto
Toronto, Ontario
Canada

ABSTRACT

Preliminary experimental results have been attained from the experiment designed to test the concept of selective excitation spectroscopy. A low pressure potassium arc was used with a tunable ruby laser. The results obtained are encouraging for a signal has been observed which can only be accounted for on the basis of intensified spontaneous emission. Moreover the duration of this pulse is found to depend strongly on the electron density.

REVIEW AND OBJECTIVE

The concept of using the process referred to as selective excitation spectroscopy to diagnose a plasma was first suggested by the author[1]. This process relies upon the ability of a suitably tuned, powerful laser pulse to momentarily redistribute the population between the two states of the atoms or ions of interest. Under these circumstances the spontaneous emission emanating from the upper level of the pumped transition is considerably intensified and should be easy to identify against the background radiation. The duration and amplitude of this pulse of intensified emission are related to the local properties of the plasma. It was shown in reference 1 that for the limiting case of step excitation by a high power beam of radiation the peak intensification of the spontaneous emission depends only on the ratio of the populations in the two levels prior to irradiation. It was also shown that the decay of this pulse would depend strongly upon the electron density whilst being weakly dependent on the electron temperature. These results indicate that the local conditions within a plasma might be evaluated from relatively simple measurements of the intensified emission resulting from suitable excitation.

The objective of the current programme is to test this concept and ascertain the possible range of conditions over which it could be applied. A study is being made of the intensification of the spontaneous emission at 6911°A in potassium resulting from the excitation of the 6939°A line by a pulsed ruby laser. An important by product of this research has been the development of a new concept for preionization in the MHD power generation field. This involves enhancing both the electron temperature and number density of an alkali-seeded plasma by pumping the resonance lines of the alkali atoms with a suitably tuned powerful laser[2].

APPROACH AND RESULTS

A more realistic theoretical model has been developed to calculate

the intensification of the spontaneous emission resulting from the selective optical excitation of a specific transition within the atom of interest. The temporal variation of the exciting laser radiation was represented by an analytical expression which was found to agree quite closely with the shape of the experimental laser pulse. Both the close coupling between adjacent energy levels and the degree of overlap between the laser wavelength and the wavelength of the line being excited has been taken into account.

Figure 1 illustrates how the pulse of intensified spontaneous emission at 6911°A in potassium might be expected to vary as the laser is progressively detuned from the 6939°A line. The conditions assumed in this calculation are, a potassium plasma with an electron density of 10^{12} cm^{-3}, electron temperature of 2500°K and a laser beam of 10^5 watts cm^{-2}. It can be seen from this figure that provided the laser wavelength falls within three Dopple widths of the line centre the pulse of intensified emission becomes essentially independent of the degree of overlap. It is also possible to interpret these curves as indicating the variation in the intensified emission for different laser powers when the laser wavelength coincides exactly with the line centre. Under these circumstances it is found that for laser powers greater than about 500 watts cm^{-2} the pulse of intensified emission becomes practically independent of the laser power. In Fig. 2 the variation of the pulse of intensified emission at 6911°A is calculated assuming a laser power of 30 watts cm^{-2} at a wavelength coincident with the centre of the 6939°A line. The electron temperature was taken to be 3000°K.

The experimental programme uses a specially designed Q-switched ruby laser and a low pressure arc. The lasing wavelength of the ruby is varied by controlling its temperature. This is achieved by circulating cooled nitrogen within the laser cavity. Figure 3 presents the tuning curve and as indicated in the small insert a split Fabry-Perot ring system is used to determine the degree of overlap of the lasing wavelength with that of the 6939°A line in a potassium lamp. The discharge chamber had to be carefully designed and tested to ensure that laser scattered radiation was kept to a minimum.

The first results of this experiment have been attained. They clearly establish that the pulse of intensified emission can be identified against the background radiation of the arc and that scattered laser radiation is no problem. Several tests were conducted in order to ensure that the observed signal, an example of which is illustrated in Fig. 4(a), was due to intensified spontaneous emission. The radiation at wavelengths between the laser wavelength at 6939°A and 6911°A was monitored and found to have dropped effectively to zero by 6925°A. The laser was also detuned by about 0.2°A where upon the signal at 6911°A disappeared. To determine the degree of overlap between the laser and the 6939°A line, part of the lasers output was fed to a Fabry-Perot interferometer where its rings were compared to those created by the 6939°A emission from a potassium lamp. The Fabry-Perot ring system for the signal shown in Fig. 4(a) is illustrated in Fig. 4(b).

A comparison between the theoretical curves and this experimental signal is also shown in Fig. 2. The variation of the decay times for the 6911°A signal against the electron density as measured by a Langmuir probe is shown in Fig. 5. It is found that these results agree with those predicted theoretically if the cross-sections, used in the quenching of the

overpopulated $6^2S_{1/2}$ level, are taken to have a value of about (1/7) of that given by the Gryzinsky model. This could account for the extended duration of the experimental pulse compared to the theoretical profile since the curves shown in Fig. 2 were for the quenching rates given by the Gryzinsky cross sections. The large experimental error bars in the electron density, indicated in Fig. 5, are due to the uncertainties in the Langmuir probe measurements.

FUTURE PROGRAMME

The experimental results achieved to data are very encouraging although they are preliminary in nature. With suitable refinements more definitive measurements should be possible in the near future. It is clear that much work remains to be done in order that the range of applicability of this new diagnostic technique can be ascertained.

REFERENCES

1. R. M. Measures J. Appl. Phy. Vol.39, 11, pp 5232-5245 (Oct, 1968)

2. R. M. Measures J. Quant. Spect. Rad. Transf. (1970)

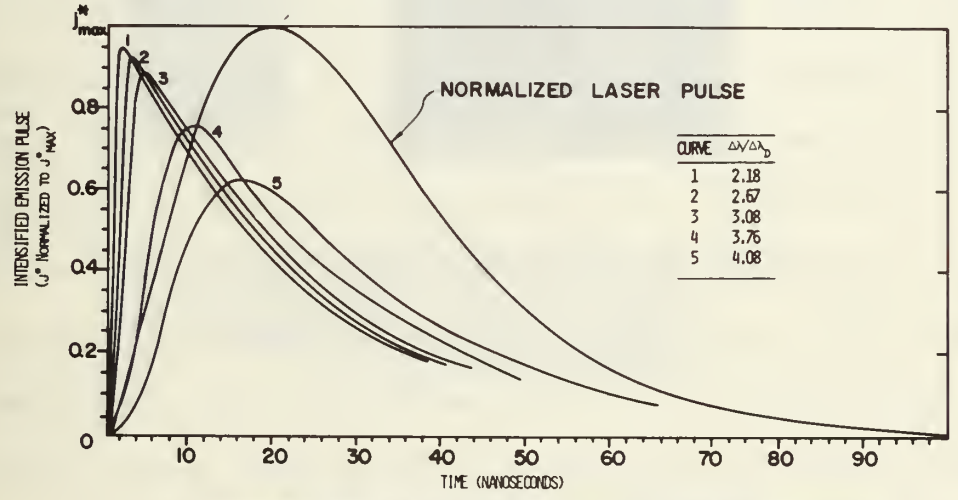

FIG. 1. VARIATION IN THE PULSE OF INTENSIFIED EMISSION WITH THE DEGREE OF OVERLAP BETWEEN LASER RADIATION AND ABSORPTION LINE CENTRE, $\Delta\lambda$ THE LINE IS ASSUMED TO BE DOPPLER BROADENED WITH HALF-INTENSITY HALF WIDTH, $\Delta\lambda_D$ AND THE LASER POWER, $Q^4(\lambda) = 10^5$ WATTS CM^{-2}.

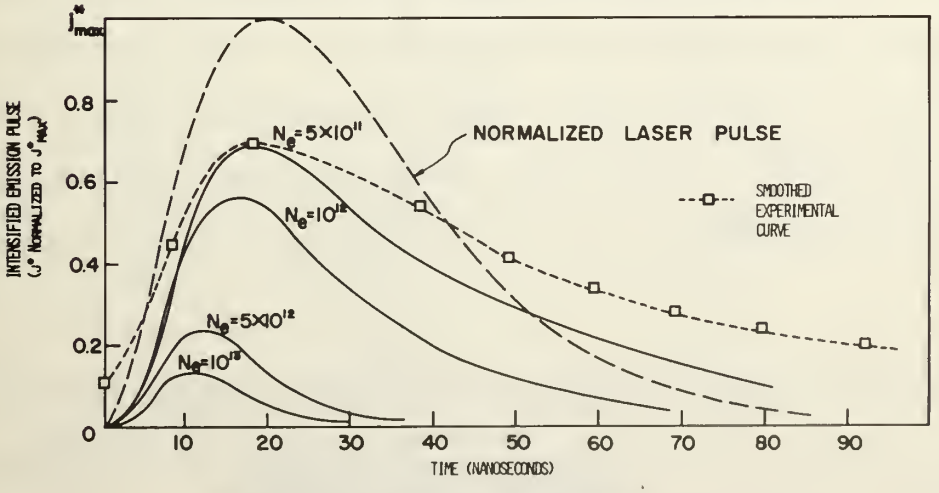

FIG. 2. VARIATION OF INTENSIFIED EMISSION PULSE AT 6911°A FOR DIFFERENT ELECTRON DENSITIES WHEN 6939°A LINE IN A POTASSIUM PLASMA SELECTIVELY EXCITED BY A PULSE OF LASER RADIATION (T_E - 3000°K).

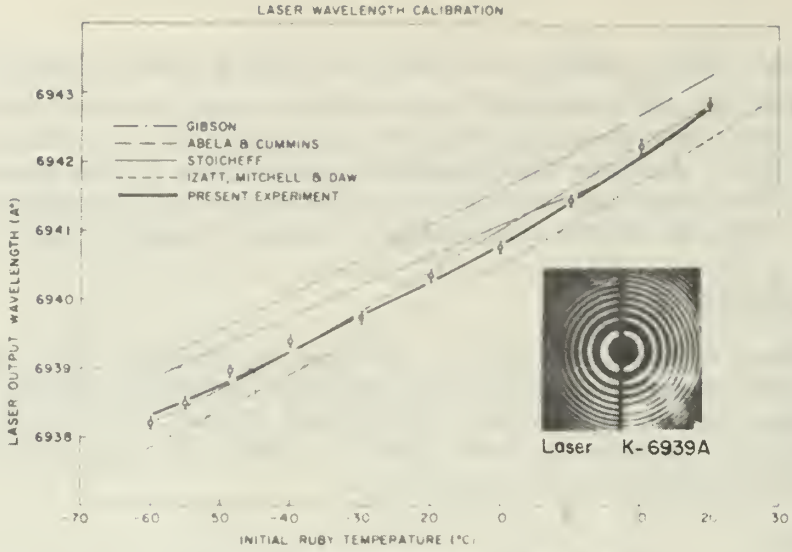

FIG. 3. LASER WAVELENGTH CALIBRATION CURVE WITH FABRY-PEROT INSERT.

FIG. 4. (a) INTENSIFIED EMISSION PULSE (20ns/cm) AT 6911°A WHEN POTASSIUM PLASMA SELECTIVELY EXCITED BY LASER RADIATION AT 6939°A. (b) SPLIT FABRY-PEROT RINGS ILLUSTRATING DEGREE OF OVERLAP BETWEEN LASER PULSE (RIGHT) AND 6939°A LINE FROM POTASSIUM LAMP (LEFT) FREE SPECTRAL RANGE 0.2°A.

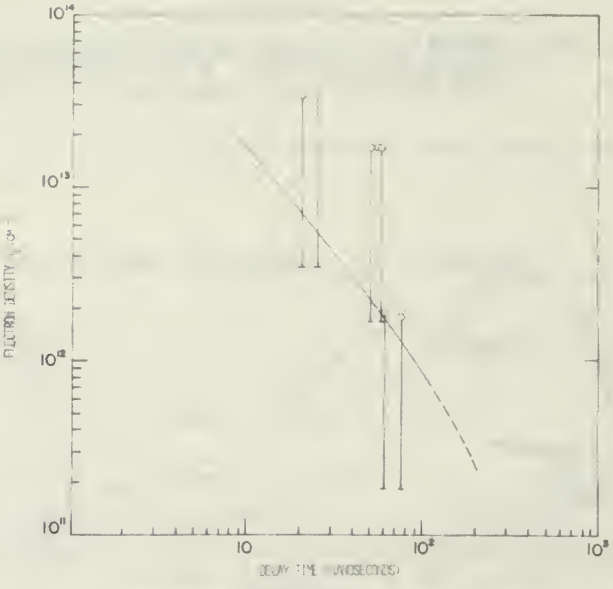

[illegible] OF DECAY TIME FOR POPULATION IN $6^2P_{1/2}$ LEVEL AGAINST [illegible] DENSITY. THEORETICAL CURVE USES 1/7 F DEGENERACY RATIO AND BRYZINSKY CROSS SECTIONS.

An Experimental Study of Electrostatic Plasma Confinement*

J. T. Verdeyen, B. E. Cherrington, T. Dolan, D. Meeker

University of Illinois, Urbana, Illinois 61801

The concept of inertially confining electrons and ions as originally proposed by P. T. Farnsworth and investigated by R. L. Hirsch is the subject of our experimental and theoretical investigations. Before launching into a detailed discussion of our experimental efforts, it is best to review the elementary theory of the device as enunciated by Hirsch.

One first considers a space charge limited emitter of ions of mass M which are attracted inward by a highly permeable grid structure. We will limit our discussion to the case of cylindrical geometry with injection inward towards r=o. If sufficient ion current is injected into the interior of the cylindrical grid, the potential is raised to a sufficiently high level to repel any additional charge. The virtual electrode thus formed on the interior has all of the characteristics (in theory) of the original emitter.

Now if we allow the permeable grid to also be an electron emitter, the charge structure of the interior becomes considerably more complicated. First, the electrons are attracted inwards by virtue of the excess positive space charge. Their inertia can carry them through the positive space charge and thus buildup a net negative charge. Such a picture is quite consistent with a simple solution to Poisson's

---

*Much of the work reported here is part of a Ph.D. thesis to be submitted by T. Dolan.

equation for two charge species with one dimensional radial motion and monenergetic particles. It could also be consistent with the experimental results obtained by Hirsch at ITT. If one integrated the equations inward from the grid, an infinite number of such charge layers or virtual electrodes would be formed. Obviously such a picture is much too elementary.

Last year at the AFOSR contractors meeting in Illinois, we heard the results of a computer study of such a problem by C. Barnes. Although one dimensional radial motion was still retained, no restriction was placed on the distribution function of the particles. More important, he was able to follow the time history of the development of the potentials. His results seem to indicate that one virtual electrode or a potential well could be formed, but that the interior of this would be filled with a quasi-neutral low energy plasma.

Our experimental efforts have been devoted to the diagnostics of a device which was built to approximate the theoretical model. The three diagnostic tools utilized have been:

1. laser heterodyne diagnostics using a He:Ne laser operating at 6401Å
2. Collimation studies of the excitation light emitted by the plasma.
3. Studies of electron beam deflection by the potentials.

Both (1) and (2) have been studied in detail in our cylindrical system involving two charge species, whereas we are using (3) to study electron injection in spherical geometry.

In our experimental apparatus, the ions are formed by a pulsed discharge between a grid and 6 thermionic cathodes placed symmetrically

around the periphery of the cylindrical structure. These ions (or electrons) are then accelerated inwards toward a highly open (73-92%) grid structure which is 4 cm in diameter. Impact ionization of the low pressure neutral background gas (1-10μ of neon) within the inner cylindrical structure provides the electron source required for the two charge specie model. We initially planned to measure the electron density within the device by using laser heterodyne techniques. Unfortunately, our densities were below the limit of detection by laser techniques ($2 \times 10^{11} cm^{-3}$) so we took advantage, instead, of the anomalous dispersion between the laser line in He-Ne at 6401Å and an absorption line at 6402Å from the metastable $1s_5$ state of neon. Since neon was the background gas for this experiment, a sufficient density of these states were produced by electron impact to allow us to measure them with a laser.

However since the metastable state can only be destroyed by collisions either with the wall or with another particle, the measurement of the radial distribution of metastables does not necessarily reflect the radial distribution of the excitation. Computer studies indicate that the initial metastable density accurately reflects the spatial profile of the source for early times in a pulse discharge, but rapidly smears out due to diffusion.

The spatial profile of the metastable density and the excitation light indicates a shallow potential well forming on the interior of the center grid. Most significant is the fact that the depth of the well appears to be critically dependent upon the mesh spacing of the grid wires. Consider two cases with the same circulating current and the same transmission factor of the grid structure, but with different spacings. The metastable density

will be considerably higher on the interior for the smaller mesh spacing. We attribute this to the shielding effect of the low energy plasma on field lines terminating on the grid wires.

The detailed theory of the measurements and the results will be discussed at the meeting.

The energy transfer between the various components of a typical plasma system of interest here is illustrated in the diagram:

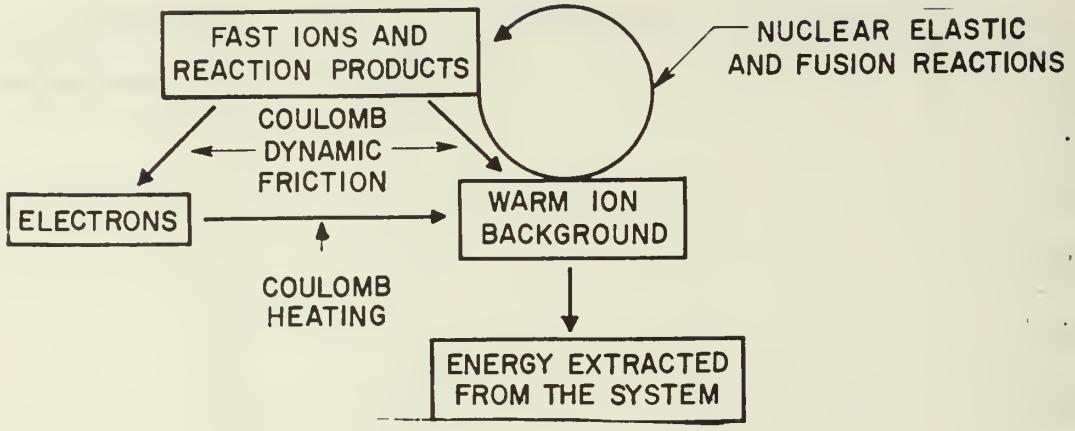

Eventually the entire chain of reactions set off by an initial fast ion either dies away, or it may combine with fusion reactions to create an even-larger population of highly-energetic ions. The possibility of such fusion and knock-on reactions linking sufficiently to form runaway chains was asserted by Gryzinski some years ago as a possible supernova mechanism.[3] His estimates of the slow down rates appear to be low, however, and the conditions quoted for supercritical chains to occur do not correspond to those obtained from our calculations (as discussed in the next section) even when neglecting, as did Gryzinski, the contribution to the stopping power from the ion-ion Coulomb interactions.

Even though the individual reaction chains may die away, the effects on the energy balance and energy transfer rate of secondary reactions and knock-ons of superthermal particles in a hot electron plasma can still be substantial.

---

[3] M. Gryzinski, Phys. Rev. 115, 1087 (1959).

For example, the alpha from a D-T or D-He^3 reaction (born at an energy of about 4 MeV) creates with significant probability fast deuterons of about 1 MeV energy, because of the large resonance in the alpha-deuterium scattering at 2.2 MeV alpha energy.

The most convenient formulation of the population kinetics problem from the point of view of numerical calculations combines a Fokker-Planck description of the Coulomb dynamics, as given by Rosenbluth, et al[4], with nuclear collision transport terms to describe the disruptive nuclear collisions and fusion events, for which a Fokker-Planck approximation is inappropriate.[5] The evolution in time of the distribution functions $N^i(E,t)$ in a uniform and isotropic slowing down medium is determined by the set of coupled F-P equations:

$$\frac{\partial N^i}{\partial t}(E,t) - \frac{\partial}{\partial E}\left(E\, N^i(E,t)/T_s^i(E)\right) - \frac{\partial^2}{\partial E^2}\left(D^i(E)N^i(E,t)\right)$$

$$= \Sigma_j \; C_j^i \; N^j(E,T) + I^i(E,t),$$

where the C_j^i are effective nuclear elastic energy transport and the I^i and T_s^i have their previous meanings as injection sources and Coulomb-process slowing down times for the ith species. The functions $D^i(E)$ represent the

---

[4] M. Rosenbluth, et al., Phys. Rev. 107, 1 (1957).

[5] J. Wyatt, et al., op. cit.

dispersive component of the slowing down by Coulomb processes, which is generally small for ion energies well above the mean electron energy. In the numerical calculations on the slowing down reactions reported here, the dispersive component of the Coulomb dynamics was neglected. In deuterium and especially in mixed D-T backgrounds at high electron temperatures, or in systems in which a major fraction of the background ion distribution has a mean energy comparable to the fast particle energies, the dispersive slowing terms can be important. Detailed numerical treament of both the ion an electron distribution dynamics and evaluations of conventional high energy injection energy balances in open geometries, which include these terms but ignore the nuclear scattering, have been published previously.[6,7]

The coupling of particle species by nuclear reactions requires that in a hot electron plasma with good fast ion containment, all of the five particle types: proton, deuteron, triton, He^3, and alpha be considered simultaneously. Calculations with the program OLFIN also have an option to include a sixth (neutron) species. This allows one to evaluate what the contributions of neutron-produced knock-ons to the population dynamics would be in a sufficiently large or sufficiently dense system.

RESULTS AND CONCLUSIONS

With no geometrical mirror losses and Coulomb slowing contributed by the electrons alone, not only substantial energy multiplication but divergent chain reactions were found to be possible, as shown in the Figure for a 50-50 D-T

---

[6] T. Fowler and M. Rankin, J. Nucl. Energy. Pt. C, 8, 121 (1966).

[7] D. Fisher, et al., Proceedings of Int. Conf. on Plasma Confined in Open-Ended Geometries, p. 280 (1967) .

mixture. With modest fast ion loss rates corresponding to a mirror ratio of 2, the divergent chains disappeared, although substantial energy gains remained at the higher electron temperatures.

Calculations including the contribution of the background ions to the Coulomb dynamic friction signficantly alter the results given in Fig. B-4 for electron temperatures above 30 keV. Divergent fusion chains are no longer achievable without including neutron knock-ons. With these knock-ons, the divergent chains reappear at an electron temperature of about 80 keV. Further study of the conditions for super-critical chains is being carried out using a more complete description of the Coulomb dynamics in the lower range of fast ion energies, where the dispersive components of the ion scattering may become important and the strong D-T fusion resonance occurs.

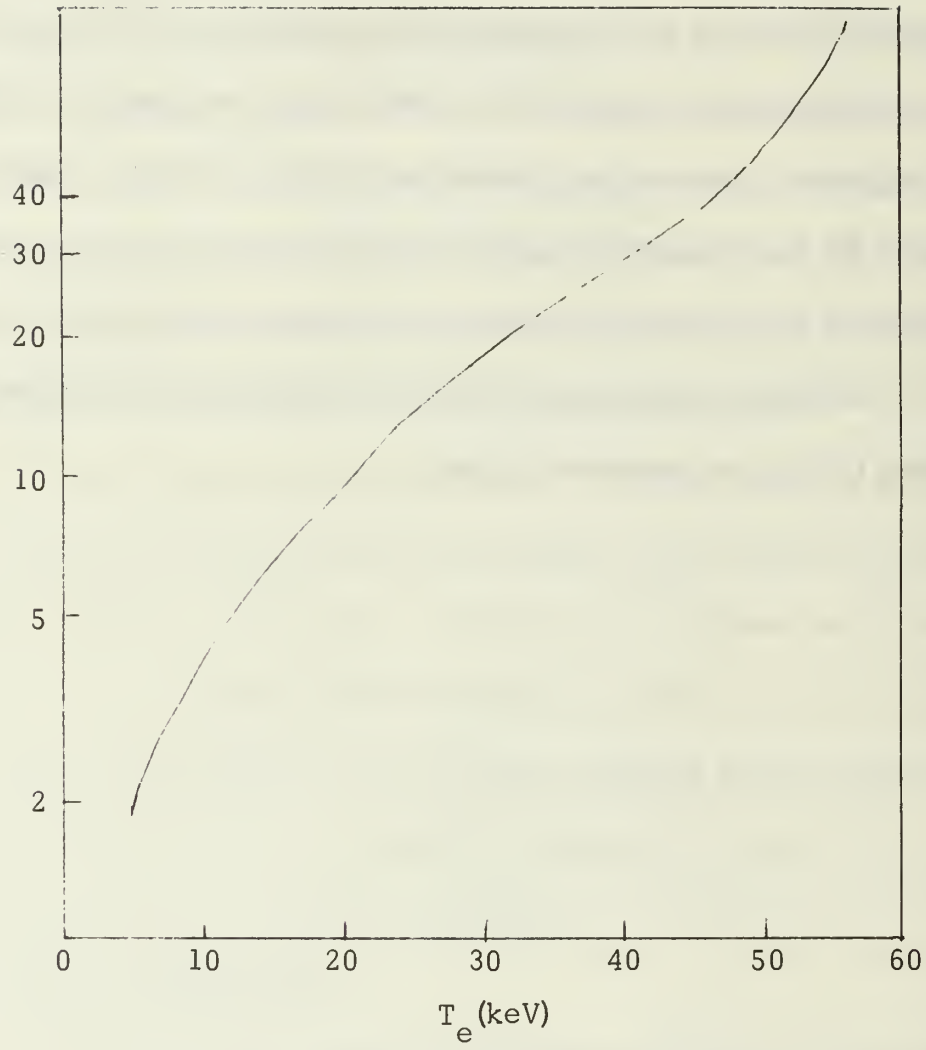

Relative Energy Release from Fast Triton Slowing from 400 keV in 50-50 DT Plasma vs. T_e.

PANEL 5. LOW TEMPERATURE PLASMAS

Name	Topic
Dr. C. L. Dailey Space Technologies Labs TRW Systems, Inc. One Space Park Redondo Beach, California 90278	Inductive Pulsed Plasma Current Sheets
Mr. S. T. Demetriades President, STD Research Corporation P. O. Box 4127, Catalina Station Pasadena, California 91106	Nonlinear Time-Dependent Phenomena in Real J x B Devices
Dr. John B. Dicks Physics Department University of Tennessee Space Institute Tullahoma, Tennessee 37388	
Mr. A. C. Ducati Plasmadyne Division Goetel Inc. Santa Ana, California 92702	Energy Transfer Mechanisms in a Plasma Jet
Professor Robert Eustis Mechanical Dengineering Department Stanford University Stanford, California 94301	Non-Equilibrium Phenomena in Flowing Plasmas
Dr. Nima Geffen Tel-Aviv University Tel-Aviv, Israel	
Dr. Richard M Patrick Avco Everett Research Laboratory AVCO Corporation Everett, Massachusetts 02149	Investigation of the Production of High Density Stable Plasmas
Dr. Jan Rosciszewski Air Vehicle Corporation 8873 Balboa Avenue San Diego, California 92123	Calculations of Flow in Magnetic Nozzles and Flows with Radiation Energy Exchange

INDUCTIVE PULSED PLASMA CURRENT SHEETS

C. L. Dailey, TRW Inc., Redondo Beach, California

Current Sheet Diagnostics

An impulsive current sheet is formed in argon by pulsing current through an 8" diameter flat, spiral coil. At the pressure of 500 millitorr (1.6×10^{16} atoms per cc.), used for these experiments, the current sheet is diamagnetic and less than a centimeter thick. It is formed during the first few tenths of a microsecond while the current in the coil is rising in the first quarter cycle of the discharge. No pre-ionization is required.

The accelerator circuit is shown schematically in Figure 1, and physically in Figure 2. The capacitor bank comprises 9 small capacitors having a total capacitance of 4 microfarads and storing 288 joules at 12 kv. The coil is placed in a glass cylinder having a uniform gas pressure of 500 millitorr of argon.

The physical processes occurring within the current sheet are investigated by means of miniature probes that measure electric fields, magnetic fields and plasma current density throughout the current sheet. In addition a laser light-scattering technique is used to measure the plasma mass distribution and electron temperature. With these measurements we intend to develop a physically plausible and consistent description of the current sheet.

At the time of writing, the probe measurements are complete. The laser measurements are underway, but have not yet produced definite results.

A representative summary of the probe results is shown in Figure 3. Shown here are the plasma current density, the tangential electric field that produces the current, the radial magnetic field that is supported by the current sheet and the space-charge electric field that accelerates the ions. The dashed line in the figure is the electron density inferred from the expression

$$n_e = \frac{-j_\theta B_r}{e E_z} \qquad (1)$$

where electrons are assumed to be the only current carriers and the force due to electron pressure gradient is ignored.

The curves shown in Figure 3 form a consistent picture of the current sheet in which a low density electron current front is followed by a thin sheet of high density plasma. However, since the electron density was inferred from the other data, this interpretation is not necessarily valid. In fact, earlier investigation with a 4" diameter inductive accelerator[1] and with electrode-type impulsive accelerators[2], have shown that when the plasma density is determined by some independent method, it is not in agreement with that obtained from Equation (1). This implies that ions must carry some of the current, a situation that seems impossible in the inductive geometry because the coil is presumably not able to supply the required torque.

Thus, the laser measurement of density is crucial in order to complete the description of the current sheet in the present accelerator and to understand the physics of plasma acceleration in an impulsive current sheet.

Thruster Performance Evaluation

A thruster employing an 8" diameter coil has been built and tested on a thrust balance. The primary difference between this device and the accelerator is the use of a fast-opening valve to discharge gas from a small high-pressure plenum to the region in front of the coil. Gas density distributions, measured by means of a fast ionization gauge, showed that only one-third of the gas initially in the plenum was close enough to the coil to be accelerated. The efficiency, based on the mass accelerated, was higher than that for an MPD ammonia thruster for xenon and krypton propellants and was about the same for argon and ammonia.[3]

For many reasons, e.g., pulsed-mode of operation for spinning satellites, possibility of accelerated life testing, system fully operational at atmospheric pressure for systems integration and launch pad testing, the pulsed inductive thruster appears attractive. This initial evaluation of its performance shows the device to be feasible although development of a better propellant injection valve is essential.

The thruster is shown on the balance in Figure 4 and is seen during firing in Figure 5.

Advanced Thruster Investigations

The pulsed inductive thruster employs the magnetic pressure between the coil and the current sheet to accelerate the propellant mass. In effect this field "contains" the plasma away from the spacecraft.

A different method of accelerating plasma is the "field-annihilation" effect. This is illustrated in Figure 6 for a pair of oppositely directed, flat, spiral coils. When the axially accelerated current sheets collide midway between the coils, the oppositely directed radial magnetic fields behind these sheets diffuse into each other and are annihilated, transferring their energy to radial plasma motion. For the geometry shown, some plasma is driven radially outward and the rest is compressed toward the axis. This is convenient for experimental reasons. However, in a thruster, concentric coils would be used with plasma in the annular space between the coils being ejected axially as the radially moving current sheets diffuse together.

---

1. Dailey, C. L., "Investigation of Plasma Rotation in a Pulsed Inductive Accelerator," AIAA J. Vol. 7, No. 1, p 13 (1969).

2. Lovberg, R. H., "Acceleration of Plasma by Displacement Currents Resulting from Ionization," Proc. 6th Int. Conf. on the Ionization Phenomena in Gases (1963). Also General Atomic Rept. GA-4363.

3. Dailey, C. L., "Thrust Measurement for a Pulsed Inductive Thruster," Special AFOSR Rept. Contract No. F44620-68-C-0042 (1970).

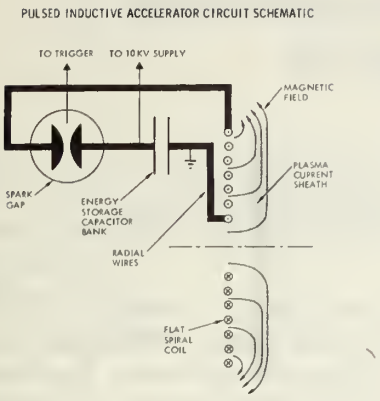

Figure 1.

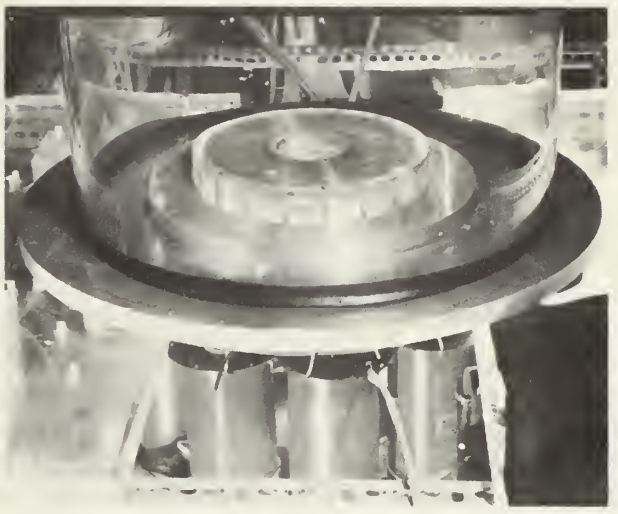

Figure 2. Accelerator Assembly

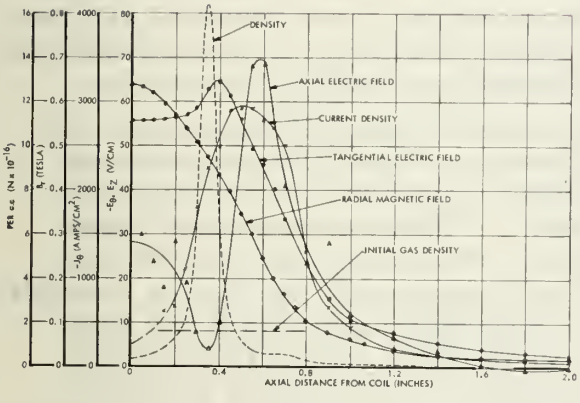

Figure 3. Current Sheet Properties

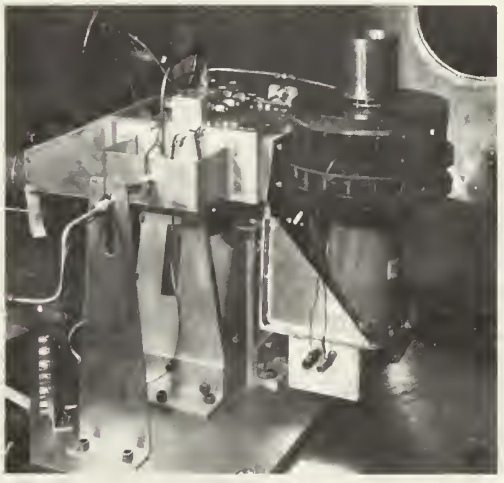

Figure 4. Thruster on Test Stand

Figure 5. Thruster Firing

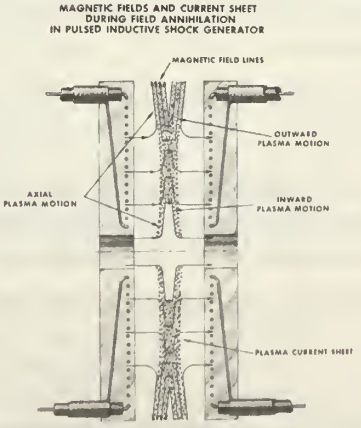

Figure 6.

NONLINEAR TIME-DEPENDENT PHENOMENA IN REAL J × B DEVICES

by

S. T. Demetriades and G. S. Argyropoulos
STD Research Corporation, Pasadena, California

Even today – after 10 years of intensive effort – there is little agreement between theory and experiment in J × B devices. Previous theories do not provide a realistic description of the basic phenomena, because they make highly unrealistic oversimplifications and ignore physical mechanisms that have controlling influence on the performance and stability of these devices.

Many interdependent physical mechanisms act simultaneously upon the flowing plasma and thus affect the local behavior (both in time and space) as well as the overall characteristics of a J × B device. These mechanisms and the resulting non-linear phenomena have become the object of realistic study at STD Research Corporation. This study has up to now analyzed the influence of thermal diffusion, thermal and velocity boundary layers, finite reaction rates, and electron energy convection on the local behavior and the overall characteristics in the stable mode of operation; the present research extends this analysis to the unstable (time-dependent) mode of operation.

In MHD channels operating at high values of the Hall parameter $\omega\tau$, the fields and plasma properties undergo time-dependent fluctuations that are characterized by five different time scales. (By time scales we mean the characteristic period of such fluctuations.) These time scales differ from each other by many orders of magnitude, depending on the geometry and the operating conditions. The overall performance of the device depends critically on which time scale is larger. If a physical process has a time scale that is orders of magnitude larger than the time scale of all others, temporal variations will be controlled exclusively by the slower process, while the faster processes can safely be assumed to proceed instantaneously. On the other hand, when such scales, arising from different physical mechanisms, are comparably large, then the performance depends on the interaction of all corresponding mechanisms.

The five important time scales in MHD channels with segmented electrodes are:

(1) The "time of flight" of the gas past an electrode period,

$$t_f = L/U \,, \tag{1}$$

where L is the electrode period and U is the gas velocity in the core of the flow; it reflects the influence of the geometry and of the boundaries on the time-development of the current and plasma property distributions.

(2) The ionization-recombination time[1]

$$t_R = 0.433 \Big/ \left[r(T_{e,o})\, n_{e,o}^2 \right] \tag{2}$$

where $r(T_{e,o})$ is the recombination rate for the three-body collisional recombination of the main ionizing species, evaluated at the reference temperature $T_{e,o}$, and $n_{e,o}$ is the electron number density corresponding to Saha equilibrium at $T_{e,o}$.

(3) The electron energy relaxation time[1]

$$t_E = \frac{4}{3}\left[\ln\left(1 + \frac{\gamma T_{e,o}}{T_{e,o} - T_g}\right) - \gamma\right] / (\nu_t \delta_{eff} \gamma^2) \qquad (3)$$

where T_g is the gas temperature, ν_t is the total collision frequency for electrons, δ_{eff} is the effective energy loss factor[2] for collisional energy transfer between electrons and heavy particles and $\gamma = 2kT_g/\epsilon_i$ where k is Boltzmann's constant and ϵ_i is the ionization potential of the main ionizing species.

(4) The electron momentum transfer time[3]

$$t_e = \nu_t^{-1} \qquad (4)$$

It is determined by the electron inertia term and describes the time necessary for acceleration of the electrons by the electric field to a given value of the drift velocity $\vec{W}_e$ in the presence of collisions.

(5) The time constant for electromagnetic propagation

$$t_{em} = L/c \qquad (5)$$

where c is the velocity of light; it is defined from Maxwell's equations.

It is clear that t_{em} will be very short, and the same is true for t_e, compared to the slower time scales t_f, t_R and t_E. Among the last three, it is not possible to distinguish one that will be the slowest under all operating conditions (see Table). All three, and the corresponding physical processes, must be considered simultaneously. This is done in our study, in contrast to previous investigations which considered only t_E.

This work has immediate application in evaluating the results of pulsed experiments which are used as models for continuous devices. Pulsed experiments are not subject to time scales that are bigger than the duration of the pulse, whereas continuous experiments are subject to all five time scales. Since each time scale is a function of the geometry and a very strong function of the operating conditions, their relative magnitude can be manipulated by the designer. Consequently, when the mechanisms that account for the difference between pulsed and continuous experiments have been identified, it is possible to define regimes by which continuous devices are governed by the same time scales as pulsed models.

This work is based on a realistic numerical solution for the time-dependent current distribution. Such realistic solution is indispendable in a non-linear problem of this complexity, and it has shown that, under the influence of the aforementioned effects, the current distribution in J × B channels can indeed be very different from the predictions of previous theories.

This work is complemented by experimental measurement of the time scale associated with the electron temperature rise in plasmas. Laboratory experiments consist of observation, by spectroscopic means, of the relaxation of electron-temperature dependent properties of plasmas after a sudden change of electron temperature is produced by an externally applied microwave field, which heats the electrons but not (directly) the heavy particles, and therefore can selectively simulate some of the processes in J × B channels. This technique has also been used successfully to obtain laser output modulation through control of the electron temperature.

References

1. K. Lackner, G. S. Argyropoulos, and S. T. Demetriades, "Relaxation Effects in J × B Devices," AIAA J. 6, 949-951 (1968).
2. S. T. Demetriades, "Determination of Energy Loss Factors for Slow Electrons in Hot Gases," Phys. Review 158, 215-217 (1967).
3. S. T. Demetriades and G. S. Argyropoulos, "Ohm's Law in Multicomponent Nonisothermal Plasmas with Temperature and Pressure Gradients," Phys. Fluids 9, 2136-2149 (1966).

TABLE

TIME SCALES IN TWO EXPERIMENTAL DEVICES

	Device 1	Device 2
Gas:	Nitrogen + 1% Potassium	Air + 0.2% Potassium
L =	15.0 mm	42.8 mm
B =	2.0 Wb/m^2	2.85 Wb/m^2
p =	0.5 atm	4.2 atm
T_g =	3000 ^oK	3054 ^oK
U =	3000 m/s	2925 m/s
t_{em} =	1.5×10^{-10} sec	4.3×10^{-10} sec
t_f =	5.0×10^{-6} sec	1.5×10^{-5} sec

T_e (^oK)	t_e (sec)	t_R (sec)	t_E (sec)	t_e (sec)	t_R (sec)	t_E (sec)
3200	9.9×10^{-12}	6.3×10^{-6}	1.7×10^{-6}	1.6×10^{-12}	1.6×10^{-6}	4.7×10^{-8}
3400	8.3	4.1	1.0	1.4	9.9×10^{-7}	2.5
3600	7.1	3.0	6.9×10^{-7}	1.3	6.8	1.7
3800	6.2	2.3	5.2	1.2	4.9	1.3
4000	5.5	2.0	4.1	1.1	3.8	1.0
4200	5.0	1.9	3.3	1.0	3.2	8.4×10^{-9}
4400	4.7	1.9	2.8	9.4×10^{-13}	2.8	7.1
4600	4.6	2.0	2.4	8.9	2.6	6.1

ENERGY TRANSFER MECHANISMS IN A PLASMA JET

Adriano C. Ducati

Plasmadyne, a division of Geotel, Inc.
Santa Ana, California

This activity has been primarily concerned with the study of interactions between MPD thrusters and their environment. Strong evidence has recently been obtained that a substantial fraction of the arc energy in an MPD thruster is expended outside of the thruster, with a significant portion imparted to the ambient gas. Resulting interaction effects must be understood and evaluated so that the potential of this type of thruster operating in space can be determined. It is difficult to make measurements that distinguish between thrust produced by acceleration of the propellant and by acceleration of the ambient gas by direct action of the arc and associated magnetic fields. Two approaches that are intended to complement each other are being used. First, the flow pattern in the vicinity of the thruster is being studied to see how much ambient gas is drawn into the active region near the nozzle exit. Patterns are determined by making a large number of surveys with calibrated orifice probes connected to sensitive gauges in a temperature-controlled enclosure. An earlier program using cold flow showed the entrained rate near the nozzle to be high. Measurements have now been extended to the hot gas case which, as would be predicted by theory, shows more rapid entrainment rates. Second, the behavior of the arc in the external region is being investigated to establish mechanisms by which directed energy can be imparted to the ambient gas and to determine the importance of these effects. To accomplish this, a thruster has been constructed for which the arc path is essentially all external. The complete arc region is accessible to probes and to photographic observation. Any thrust produced in this case is clearly a result of externally produced interaction forces. The unit can be operated with and without energizing a field coil, which permits results to be compared for cases with a magnetic nozzle effect as well as for cases for which self-field forces predominate. During the first tests, difficulties in starting and maintaining the stability of this unconventional geometry were encountered. A strong influence of the electrodes condition, especially of the cathode, was found. Another problem is concerned with the need for uniform erosion of electrodes and insulating parts so that a suitable geometry can be maintained

while these parts are continuously renewed by feeding. Techniques have recently been developed for taking motion pictures of the electrodes while the arc is in operation and with erosion taking place. These are very helpful in understanding the erosion process. They show molten material forming in drops that tend to concentrate the arc action and increase the local melting until the drop grows larger and is carried away by the flow. They also show the formation of cracks that tend to concentrate the arc, thereby increasing the thermal stress and the crack growth rate. Two newer areas of study are beginning to receive attention. First, the eventual interference of the operation of a plasma jet with radio communication. A plume of ionized gas can refract or attenuate radio signals, and the operation of the arc can generate radio frequency noise that could mask weak incoming signals. Since the maintenance of communication is of serious concern, it is necessary to assess the importance of factors that may interfere with communication. The large fiberglass reinforced vacuum chamber in use at Plasmadyne is well-suited for a study of this type. Measurements that have already been reported suggest a correlation between the frequency of arc oscillations and the dominant frequency of noise produced. Work is now being initiated for determining the noise spectrum with different arc geometries and for evaluating possible ways of reducing the noise or of avoiding interference between the communication frequency and the noise frequency. The second area of study is based upon the assumption that forces due to interactions with the ambient gas can be put to use to produce thrust in the upper atmosphere. Assuming the availability of a sustained electrical power supply, a propulsion device using ambient gas could produce a usable reaction force. A preliminary examination indicates that sufficient electrical power might be made available to overcome vehicle drag at altitudes above 200 kilometers. It is necessary to explore the feasibility of influencing a large volume of rarefied gas in the free molecular flow regime, and to evaluate the possibility of sustaining an electrical discharge under these conditions. Although it seems difficult to simulate the correct velocity and density conditions in the laboratory, useful information is expected to be obtained by testing MPD thrusters designed to produce large interactions with the ambient gas. Some of the tests made to determine laboratory measurement errors due to interaction effects can help to study the feasibility of the before-mentioned application.

(Contract F44620-70-C-0002)

NON-EQUILIBRIUM PHENOMENA IN FLOWING PLASMAS

M. Mitchner, C.H. Kruger, and R.H. Eustis

In what follows, we describe two investigations currently in progress under this research program. References to recent publications of the results of other studies are listed at the end of this report.

Non-equilibrium in Rapid Expansions

Over the past decade, a considerable amount of study has been devoted to the phenomenon of vibrational relaxation of a single species of diatomic molecule. Characteristic times for the response of the vibrational temperature to either a sudden increase (e.g., a shock wave) or a sudden decrease (e.g., a rapid expansion) in translational temperature have been measured and calculated. These processes are governed by the exchange of energy upon collisions, between the vibrational and the translational modes, referred to as V-T exchanges. One of the outstanding problems in this area is that for some species the measured relaxation times for expansions are an order of magnitude smaller than for shock waves.

In comparison with the preceeding situation, very little work has been done on the relaxation of mixtures of different molecular species. In a non-equilibrium gas mixture containing more than one diatomic species, the vibrational temperature of each species can be different and the vibrational energies of the individual species can change through collisions involving primarily an interchange in vibrational states, referred to as a V-V process. For polyatomic species, different vibrational temperatures need to be considered for each normal mode.

A theory of vibration-vibration energy exchange between different species was first developed in 1952 by Schwartz, Slawsky, and Herzfeld [1]. However, no experimental data were reported until 1966. Taylor, Camac, and Feinberg [2] measured the V-V exchange between various molecular species behind a normal shock wave. Measurements of V-V coupling for temperatures up to 1000°K have also been made using a laser-fluorescence technique [3,4,5]. For most mixtures, the Schwartz, Slawsky, and Herzfeld theory is in qualitative agreement with the experimental

data, but does not yield the correct magnitude nor the exact temperature dependence. Thus, the theory cannot be used to give quantitative results and experimental measurements are needed to obtain V-V coupling rates over a wide range of conditions.

The purpose of this study is to investigate the vibrational interactions of molecular mixtures using rapid expansions. In particular, the objective of the present effort is directed at investigating the V-V coupling between nitrogen and carbon dioxide. Data for this interaction will contribute to a quantitative understanding of the operation of CO_2 - N_2 lasers.

Preliminary measurements have been made of the nitrogen vibrational temperature in expansions of dilute N_2 in argon and mixtures of N_2 and CO_2 in argon. These measurements were made using sodium D-line reversal and spectroscopic line emission methods. The measurements were made in a free jet. The use of the free jet enables measurements to be made as a function of distance in the flow direction without the necessity of constructing separate viewing windows for each axial location.

The results without CO_2 are in agreement with those of Hurle, Russo, and Hall [6,7] in that they can be correlated using a relaxation time 1/15th of that measured behind a shock wave. Measurements for N_2-CO_2-A mixtures show that a small amount of CO_2 has a large effect in decreasing the relaxation time of the nitrogen vibrational temperature. These data have been interpreted using a set of simplified rate equations, and indicate that the N_2-CO_2 V-V coupling is considerably stronger in an expansion flow than behind a normal shock wave. This preliminary result is the first indication that V-V relaxations may be faster in expansions than in shocks, in analogy with the situation for V-T exchanges.

Present work is directed at refining and supplementing our preliminary measurements. We plan to measure directly the relaxation of the assymetric stretching mode of the CO_2 using an infrared band reversal technique. This measurement, in conjunction with measurements of the N_2 vibrational temperature, will enable us to determine directly the N_2-CO_2 V-V interaction coefficient. The measurements will be compared with calculations based on a more general set of coupled rate equations.

Ionization Instabilities

The performance of non-equilibrium noble gas MHD generators has been found to be seriously affected by the presence of the ionization, or electrothermal, instability. The instability is observed as a fluctuation in the electron number density and all associated plasma properties. It has been found that there is a

critical value (β_{crit}) of the Hall parameter $\omega\tau$ at which the instability arises. Further increases in $\omega\tau$ result in a decrease in the effective conductivity and a saturation value β_{eff} for the effective Hall parameter, i.e. the arctan of the angle between the average current vector and the average electric field vector in the gas frame of reference.

It was suggested by Brederlow and Hodgson [8] that β_{eff} and β_{crit} may be influenced by the size of the testing channel. Furthermore, Belousov [9] has indicated a dependence of wavelength on channel size. Gilpin [10], on the other hand, predicted a wavelength independently of the channel boundaries. Experiments to more precisely determine the nature of channel-size effects are currently in progress. The material presented here describes the initial stages of this investigation.

This portion of our program consists of an experimental study of the ionization instability in a continuous-electrode simulated MHD generator. The initial effort centered mainly on whether the behavior of the instability in a continuous-electrode experiment is consistent with the predictions of the present theories and with the existing experimental data taken in axial-discharge and Faraday-generator experiments. Our more general objective is to understand the effect of boundary conditions and channel size on the wavelength and amplitude of the instability and on the critical Hall parameter, the effective Hall angle, and the effective conductivity. Such information is expected to have an important bearing on the extrapolation of results from present small-scale experiments to future MHD applications.

Experiments have been conducted in atmospheric-pressure argon at 2300°K seeded with 0.11 % potassium. The channel had an electrode length of 15cm and an electrode separation of 2cm. The gas velocity was 130 m/sec, the magnetic field varied up to 1 Tesla, and the applied electric fields varied up to 500 v/m discounting the electrode losses. Measurements of the fluctuations in electric field were taken from a 1cm x 1cm region near the center of the electrodes by platinum probes projecting into the gas flow and separated by 5mm. The current distribution along each electrode was measured by segmenting the electrodes.

It was found that the instability followed closely the behavior noted by previous experimenters and the predictions of the theories. At current densities less than 0.1 amp/cm^2 and for Hall parameters $\omega\tau$ up to 10 the instability was not apparent to any significant degree. At larger current densities the amplitude and RMS value of the electric field fluctuations increased with current density and magnetic field. The critical Hall parameter was found to be near 2. As $\omega\tau$ was increased above 2 the effective Hall angle remained near arctan 2 and the fluctuating

component of the electric field increased to 200 v/m (RMS). The regular fluctuations in electric field observed for $\omega\tau = 4$ became increasingly irregular at larger $\omega\tau$, suggesting breakup of plane wave structure.

Voltage-probe data taken near the entrance region of the test section was much more irregular than that described above taken near the center of the section. Motion pictures taken in the entrance region show a very definite ionization front inclined to the electrodes at an angle very near the effective Hall angle.

In an attempt to short the fluctuating electric fields on a length scale much smaller than the electrode separation, three grids formed of 16 per inch tungsten wires were equally spaced between the electrodes. These grids were parallel to the electrodes and extended over the entire length of the electrodes. It was found that with the grids the instability was still present but the amplitude of the electric field fluctuations decreased.

More detailed experiments concerning the influence of channel size on the wavelength of the instability and shorting effects in Faraday generators are currently in progress.

References

1. Schwartz, R.N., Slawsky, Z.I., and Herzfeld, K.F., "Calculation of Vibrational Relaxation Times in Gases," J. Chem. Phys. 20, 1591 (1952).

2. Taylor, R.L., Camac, M., and Feinberg, R.M., "Measurements of Vibration-Vibration Coupling in Gas Mixtures," Eleventh Symposium (International) on Combustion (1966), p. 49.

3. Moore, C.B., Wood, R.E., Hu, Bei-Lok, and Yardley, J.R., "Vibrational Energy Transfer in CO_2 Lasers," J. Chem. Phys. 46, 4222 (1967).

4. Hocker, L.O., Kovacs, M.A., and Rhodes, C.K., "Vibrational Relaxation Measurements in CO_2 Using an Induced Fluorescence Technique," Phys. Rev. Letters 17, 233 (1966).

5. Rosser, W.A. Jr., Wood, A.D., and Gerry, G.T., "The Deactivation of Vibrationally Excited Carbon Dioxide (V_3) by Collision with Carbon Dioxide or with Nitrogen," Avco Everett Research Report 306, January 1969.

6. Hurle, I.R., Russo, A.L., and Hall, J.G., "Spectroscopic Studies of Vibrational Nonequilibrium in Supersonic Nozzle Flows," J. Chem. Phys. 40, 2076 (1964).

7. Hurle, I.R. and Russo, A.L., "Spectrum-Line Reversal Measurements of Free-Electron and Coupled N_2 Vibrational Temperature in Expansion Flows," J. Chem. Phys. 43, 4433 (1965).

8. Brederlow, G., and Hodgson, R.T., "Electrical Conductivity in Seeded Noble Gas Plasmas in Crossed Electric and Magnetic Fields," AIAA Journal 6, 7, July 1968.

9. Belousov, V.N., Yeliseyev, V.V., and Shipuk, I. Ya., "Ionization Instability and Turbulent Conductivity of a Nonequilibrium Plasma," International Symposium on MHD Electrical Power Generation, Salzburg, 1966, paper 74/88.

10. Gilpin, R.W., "Experimental and Theoretical Studies of the Electrothermal Instability in a Nonequilibrium Plasma," Ph.D. Thesis, California Institute of Technology, 1968.

Recent Publications

(1) "Effects of Non-elastic Collisions in Partially Ionized Gases," J.F. Shaw, Stanford University, Institute for Plasma Research, Report No. 254, August 1968.

(2) "Two-Temperature Boundary Layer Measurements," R.T. Brown and M. Mitchner, Tenth Symposium on Engineering Aspects of MHD, 1969.

(3) "Measurements in a Two-Temperature Plasma Boundary Layer," R.T. Brown and M. Mitchner, AIAA Fluid and Plasma Dynamcis Conference, San Francisco, June 1969; AIAA Paper No. 69-693.

(4) "Effects of Nonelastic Collisions in Partially Ionized Gases, Part I - Analytical Solutions and Results," J.F. Shaw, M. Mitchner, and C.H. Kruger. Accepted for publication by Physics of Fluids.

(5) "Effects of Nonelastic Collisions in Partially Ionized Gases, Part II - Numerical Solutions and Results," J.F. Shaw, M. Mitchner, and C.H. Kruger. Accepted for publication by Physics of Fluids.

(6) "Ionization Rate Calculations for Pre-Ionizers, D.D. McGregor, J.F. Shaw, and M. Mitchner, Tenth Symposium of Engineering Aspects of MHD, 1969. Also accepted for publication by AIAA Journal.

(7) "Electron Temperature and Number Density Measurements in a Nonequilibrium Plasma Boundary Layer," R. T. Brown, Ph.D Thesis, Stanford University (SU-IPR Report No. 350, January 1970, Institute for Plasma Research, Stanford University).

(8) "Experiments on Hartmann Flow in Plasmas," O.K. Sonju and C.H. Kruger, Physics of Fluids, 12, 2548, December 1969.

(9) "Ionization Instabilities in a Continuous Electrode Generator," R.M. Evans, J.F. Louis, M. Mitchner, and C.H. Kruger, Eleventh Symposium on Engineering Aspects of MHD, Pasadena, Calif. 1970.

INVESTIGATION OF THE PRODUCTION OF HIGH DENSITY STABLE PLASMAS

by

R. M. Patrick, E. R. Pugh and D. H. Douglas-Hamilton
Avco Everett Research Laboratory, Everett, Massachusetts

I. INTRODUCTION

A stable ionized plasma is required for many of the most interesting applications of plasma physics.

Classically, stable plasma discharges are produced by working in the region where diffusion of the charged species to the walls stabilizes the discharge. The electron temperature in the discharge is raised (by adjusting the electric field E/P) until the ionization rate due to these electrons equals the rate at which ionized molecules are lost at the walls. However, the diffusion time becomes large compared to other instability times in the plasma, and the discharge spokes or arcs. Many of these instabilities are associated with the ionization process and its coupling with the electron temperature. AERL has constructed a facility under a company-sponsored program which produces uniform discharges in which the electron density, n_e, can be varied independent of the electron temperature T_e. Separation of the ionization process from the electron temperature is achieved in this facility by having a separate control on each, resulting in a stable discharge over a wide range of pressure and scale size.

We achieve the separation of plasma ionization from the electron temperature by using a beam of high energy electrons to create a uniform ionization throughout the volume of the plasma. Using the high energy electrons to provide the ionization, the electron temperature is varied independently by adjusting the electric field. It is found that if the electron temperature is kept low so that the ionization due to the discharge electrons is small compared to the ionization due to the high energy electrons, the discharge remains uniform over the range of pressures investigated, up to one atmosphere. As

the electric field is raised, the two ionization processes became equal and the discharge becomes nonuniform and eventually arcs.

In the present program, we are using this facility to investigate the stability limits of such a discharge. These limits, of course, reflect upon the volumetric stability of other discharges important to practical applications, such as those occurring in an extrathermal MHD generator. Volumetric instabilities depend upon the recombination processes. This report describes some initial measurements at high pressure (300 Torr). Subsequent work will involve investigation of various discharge stability limits, relating these limits to specific applications.

II. DESCRIPTION OF AERL E-BEAM PLASMA FACILITY

Theory

Electron beam current is limited by the heating effect on the foil. The foil is not permitted to rise in temperature to a level where its structural strength is significantly reduced, which would lead to pinholes and tears. The condition is that the total energy deposited in the foil during the pulse must produce a temperature rise less than 200°K.

The fraction of the electron beam lost in the foil has been investigated by Borries and Knoll,[1] and the rate of energy loss going through the foil by Bethe and tabulated by Berger and Seltzer.[2] For the aluminum foil, thickness 10^{-3} cm, and incident electron energy, 50 kV, used in the present experiments, the fraction of the incident beam energy lost in the foil is 80%.

Assuming all the energy is deposited in the foil, a lower limit on the incident current density I (amp/cm^2) in terms of the incident beam energy E (volts) and the pulse length (t) can be obtained.

$$EIt < 0.5 \text{ joule}$$

If E = 50 kV and t = 20 μsec, I < 0.5 amp/cm^2. Approximately 20% of the incident electrons are transmitted, and the mean energy is reduced by 10 kV. These electrons are available for ionization of the gas.

The production rate of ions in a gas per cm^3 is

$$p = \frac{I\rho \left\langle \frac{\partial E}{\partial m} \right\rangle}{e E_i} \text{ cm}^{-3} \text{ sec}^{-1},$$

where

ρ = gas density, gm cm^{-3},

I = emergent electron beam current density, amp cm^{-2},

$\left\langle \frac{\partial E}{\partial m} \right\rangle$ = mean energy loss rate, volt cm^2 gm^{-1},

---

[1] Borries and Knoll, Phys. Z. 35, 279 (1934).

[2] Berger and Seltzer, Tables of Energy Losses and Ranges of Electrons and Positrons, National Bureau of Standards.

E_i = mean energy loss per ionization, volt,

e = charge on electron, coulomb.

The electron density n_e is given by

$$\frac{dn_e}{dt} = -\alpha n_e^2 + p \qquad (1)$$

where α is effective recombination rate and p is production rate. Hence, in equilibrium, (times greater than the characteristic time $\tau = 1/\alpha n_e$), $(dn_e/dt = 0)$, and

$$n_e = \left[\frac{IP \left\langle \frac{\partial E}{\partial m} \right\rangle}{\alpha T} \cdot \frac{M m_p}{k e E_i} \right]^{\frac{1}{2}} \qquad (2)$$

where

P = gas pressure, dynes cm^{-2},

T = gas temperature, ^oK,

α = effective recombination coefficient, $cm^3\ sec^{-1}$,

M = molecular weight of gas,

m_p = proton mass, gm,

k = Boltzmann's constant, $erg/^oK$.

Approximate maximum values of n_e for a typical electron beam, current density 1 mA/cm^2, in N_2 and He are given below, with characteristic decay time τ and range R at E = 50 kV, using E_i = 50 volts.

P_{Torr}	N_2			He		
	n_e cm^{-3}	R cm	τ μsec	n_e cm^{-3}	R cm	τ msec
30	4×10^{11}	122	12	7×10^{12}	659	1.4
300	1.2×10^{12}	12	4	2.1×10^{13}	66	0.5
760	2×10^{12}	4.8	2.4	4×10^{13}	26	0.3

When the electron beam is turned off, p = 0, and Eq. (1) may be integrated, giving

$$n_e = \frac{n_0}{1 + \alpha n_0 t}, \qquad (3)$$

where n_0 is the electron density at $t = 0$.

For values of time $t \gg 1/\alpha n_0$, we have

$$n_e = 1/\alpha t. \tag{4}$$

Thus, a value of α can be determined by measuring the value of n_e at times $t \gg 1/\alpha n_0$.

Apparatus

A broad, fairly uniform beam of high energy electrons is generated by the apparatus shown in Fig. 1 and schematically in Fig. 2. Thermionic electrons from a tungsten filament are modulated by a grid whose potential can be varied with respect to the filament, and accelerated through a potential V_0 (~ 50 kV) to a thin foil, in our experiments of aluminum. The foil divides the electron gun, maintained at a vacuum (< 0.1 μ), from the discharge chamber which may be at any pressure from below 1 μ up to one atmosphere.

After passing through the foil, the beam penetrates the discharge chamber through a wide mesh grid of stainless steel. This is used as the cathode, and a gold-plated disk opposite acts as the anode. Between these the plasma discharge voltage V_s (< 10 kV) is maintained. The grid is required to prevent damage to the foil, and the gold plate on the anode serves to reflect a proportion of the incident primary electrons, thus increasing the ionization in the gas. The grid structure containing the filaments is maintained at -50 kV with respect to the foil (which is near ground) by a 5 μF capacitor which supplies the electron beam current. The filaments are pulsed negative 500 V with respect to the grid. It is estimated theoretically that approximately 1% of the electron beam current incident on the foil support structure penetrates the foil and the cathode grid and is thus available for ionizing the gas. The foil support structure is a perforated plate to take the pressure of the gas in the discharge region. The effects of secondary electrons from these structures and ionization of the residual gas make this a difficult measurement, and it has not been done in a convincing manner as yet.

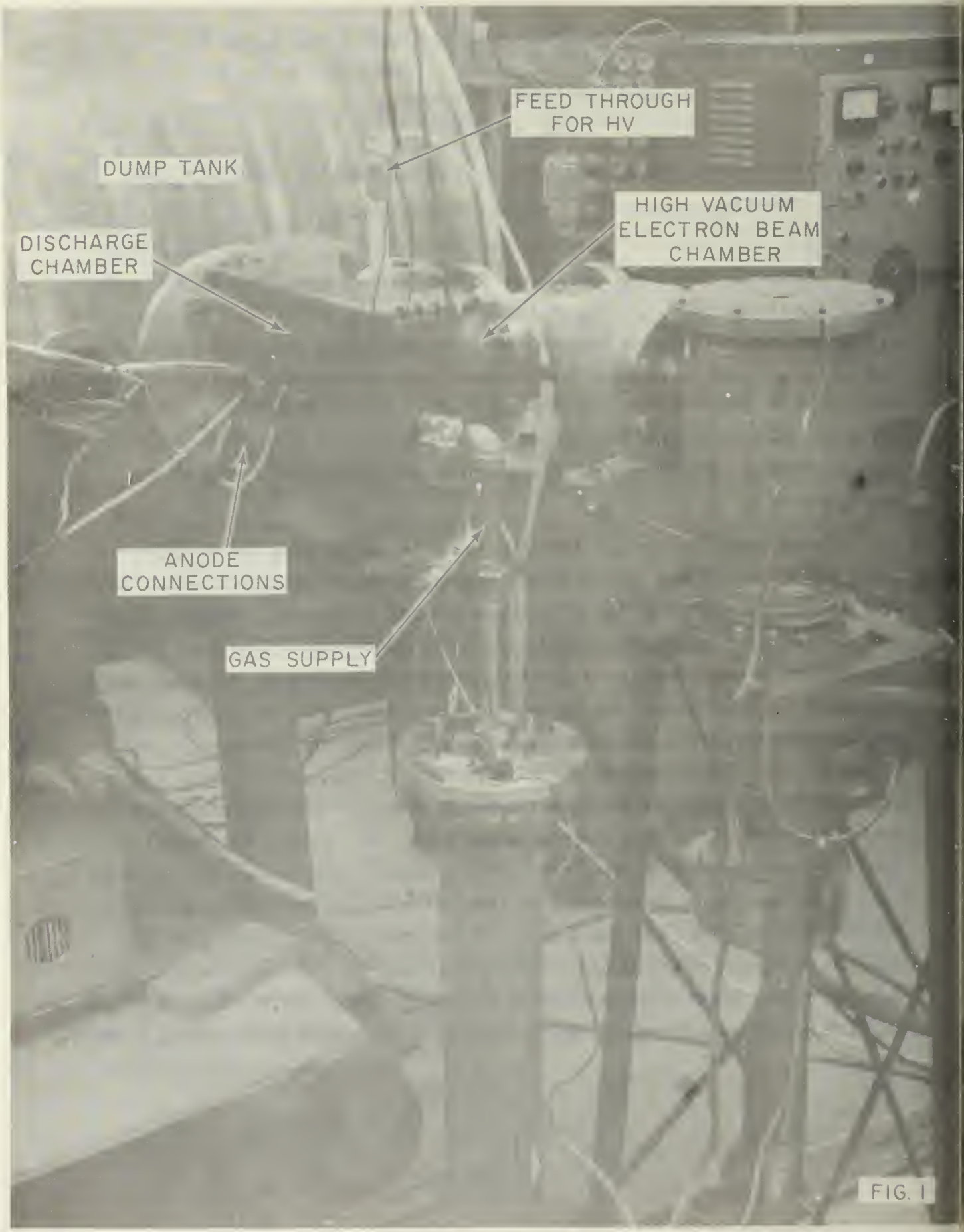
FEED THROUGH FOR HV
DUMP TANK
HIGH VACUUM ELECTRON BEAM CHAMBER
DISCHARGE CHAMBER
ANODE CONNECTIONS
GAS SUPPLY

FIG. 1

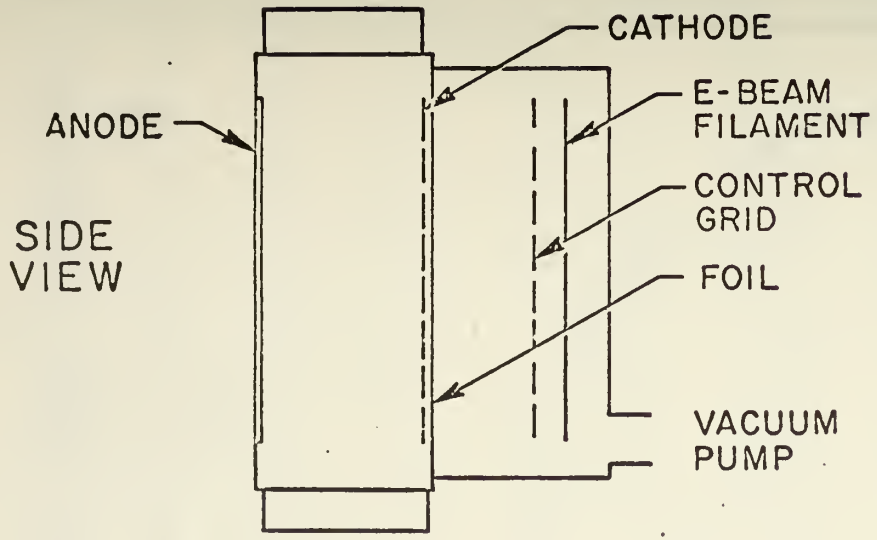

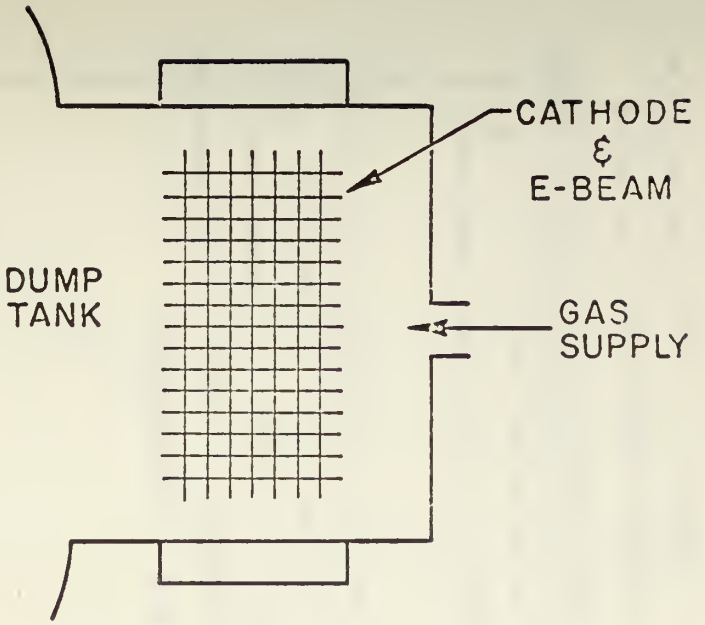

END VIEW CROSS SECTION
ANODE WALL REMOVED

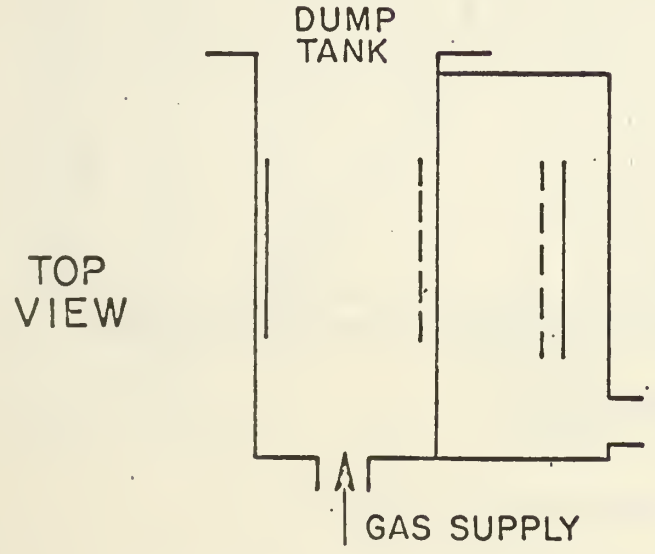

FIG. 2. SCHEMATIC DRAWING OF E-BEAM IONIZATION EXPERIMENT

The plasma discharge current is supplied by a 250 μF capacitor at voltages up to 10 kV. Either the anode or the cathode can be grounded.

The gas being studied flows through the discharge chamber normal to the electron beam. Its velocity can be varied up to Mach 1, but up to the present time only quasistatic velocities (~ 1 M/s) have been used, and only nitrogen has been examined.

The uniformity of the electron beam in the discharge region and its approximate intensity variation was determined by replacing the anode wall with a lucite wall coated with sodium salicylate, a substance that is fluorescent when excited by high energy electrons. This was photographed and the intensity distribution shown in Fig. 3 was obtained.

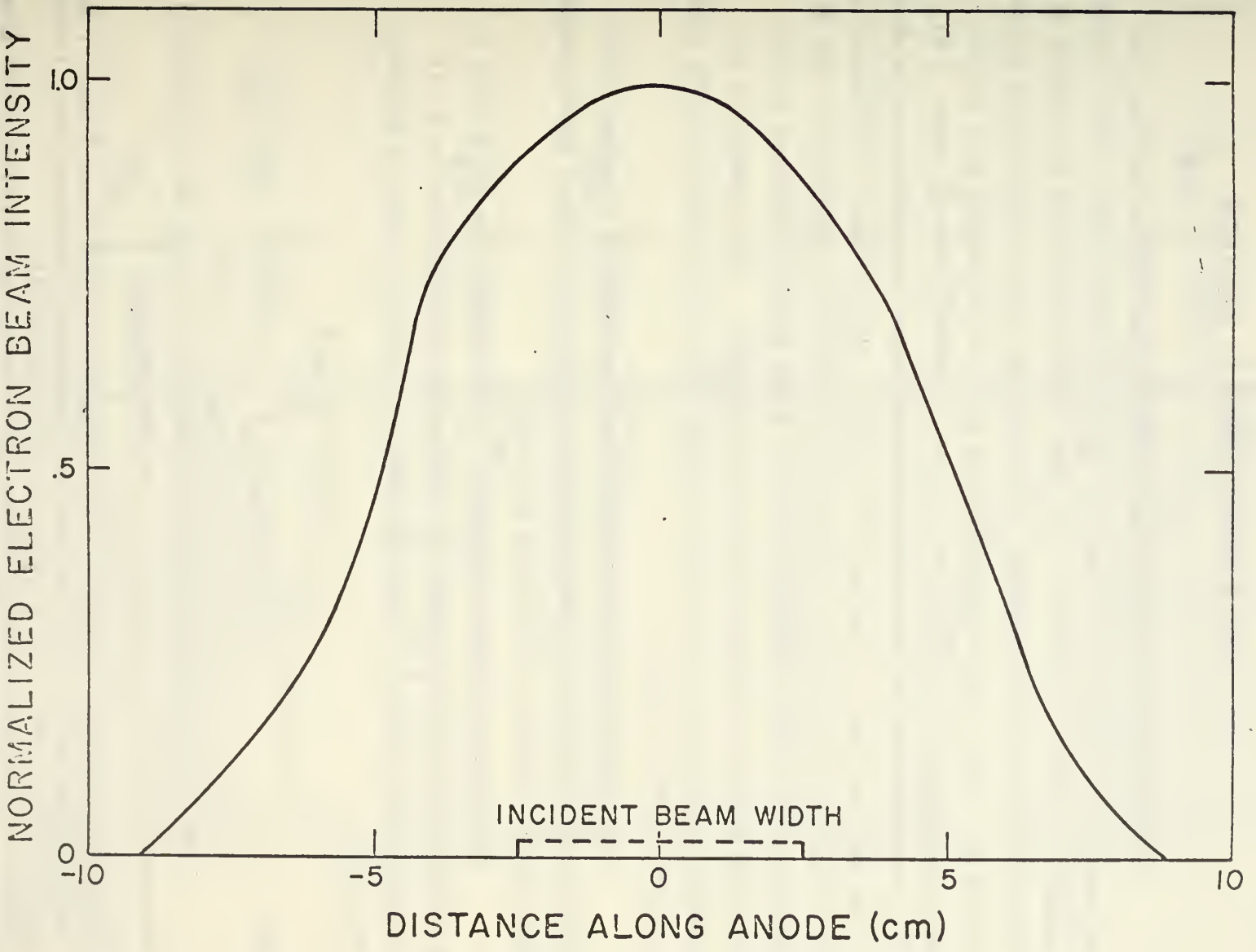

FIG. 3. Electron beam intensity distribution.

III. INITIAL EXPERIMENTAL RESULTS

Figure 4 shows a typical set of oscillogram traces showing the current and voltage measurements in the plasma discharge. The measurements were made at 300 Torr in N_2 with 5000 volts across the plasma discharge with the anode grounded. The electron beam energy hitting the foil was 50 kV. The electron beam current between the pulsed grid and the foil is measured by an induction coil and is shown in the top trace of Fig. 4. The current in the discharge was measured across a resistor and is shown at two different gains in the next two traces. The potential distribution was determined by two probes 1.5 mm in dia and 40 mm long placed in the discharge with a 10 MΩ impedance anode. Each probe was placed two cm from the anode or cathode and thus one cm apart. The voltages on the cathode and probes as well as the voltage difference between the two probes are also shown in Fig. 4.

The current density was determined by isolating a region of the anode 2.5 cm in dia and measuring the current to it. These measurements indicated an effective anode area of 80 cm^2.

The time variation of E/P in a typical experiment (V_s = 5000 V, P = 300 Torr) is shown in Fig. 5. The corresponding value of V_D is obtained from Phelps[3,4]; over the range of interest, it can be approximated by:

$$V_D = 7.5 \times 10^5 \ (E/P)^{\frac{1}{2}}$$

and

$$T_e = f(E/P).$$

The electron number density is determined from the current measurements and the drift velocity V_D by the equation

---

[3]Engelhardt, Phelps and Risk, "Determination of Momentum Transfer and Inelastic Collision Cross Sections for Electrons in Nitrogen using Transport Coefficients," Phys. -Rev. 135, No. 6A, 1566(1964).

[4]Phelps, "Rotational and Vibrational Excitation of Molecules by Low Energy Electrons," Westinghouse Research Laboratories, Scientific Paper 67-1E2-GASES-P2, 1967.

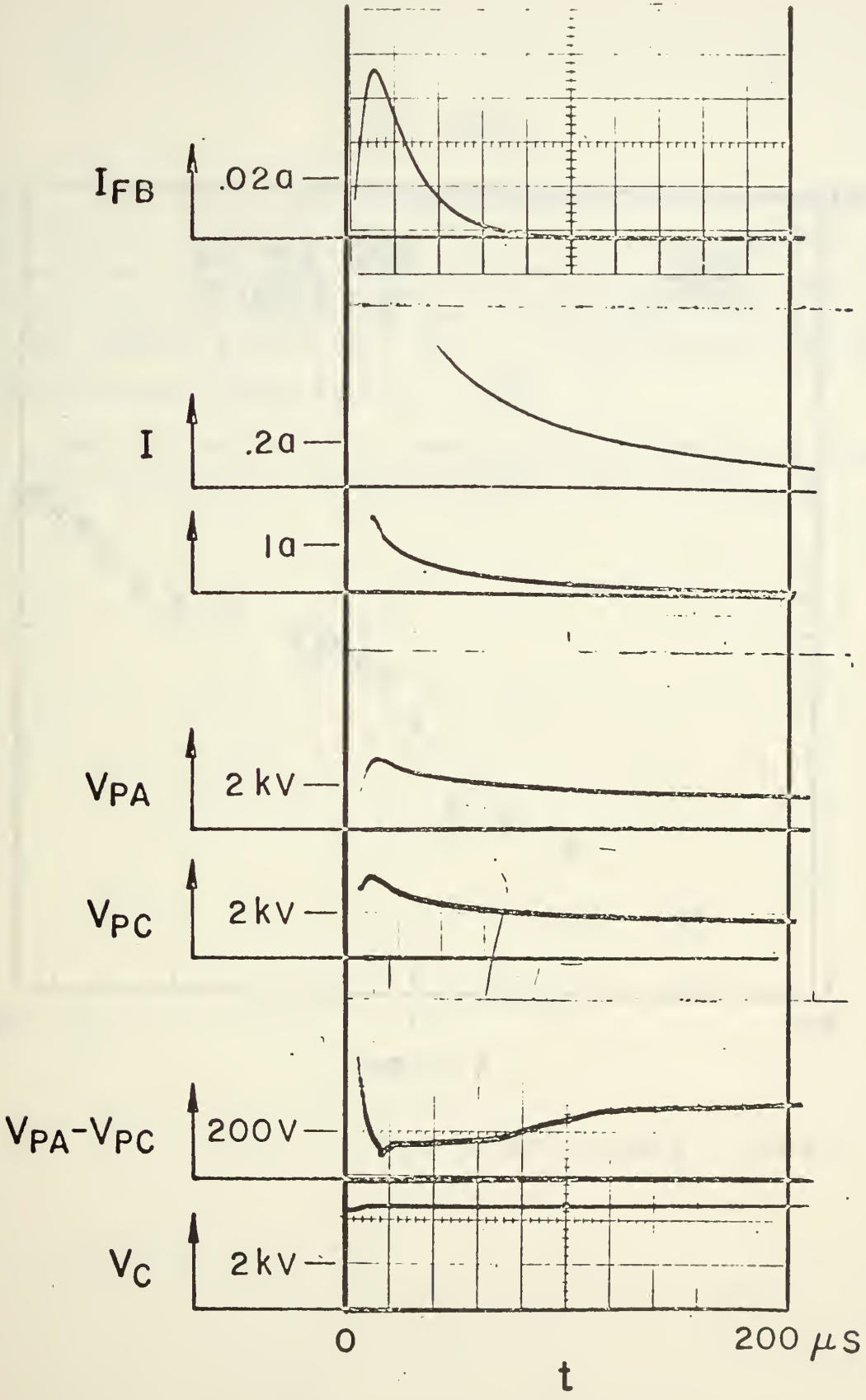

FIG. 4 Oscilloscope traces. 300 torr nitrogen.

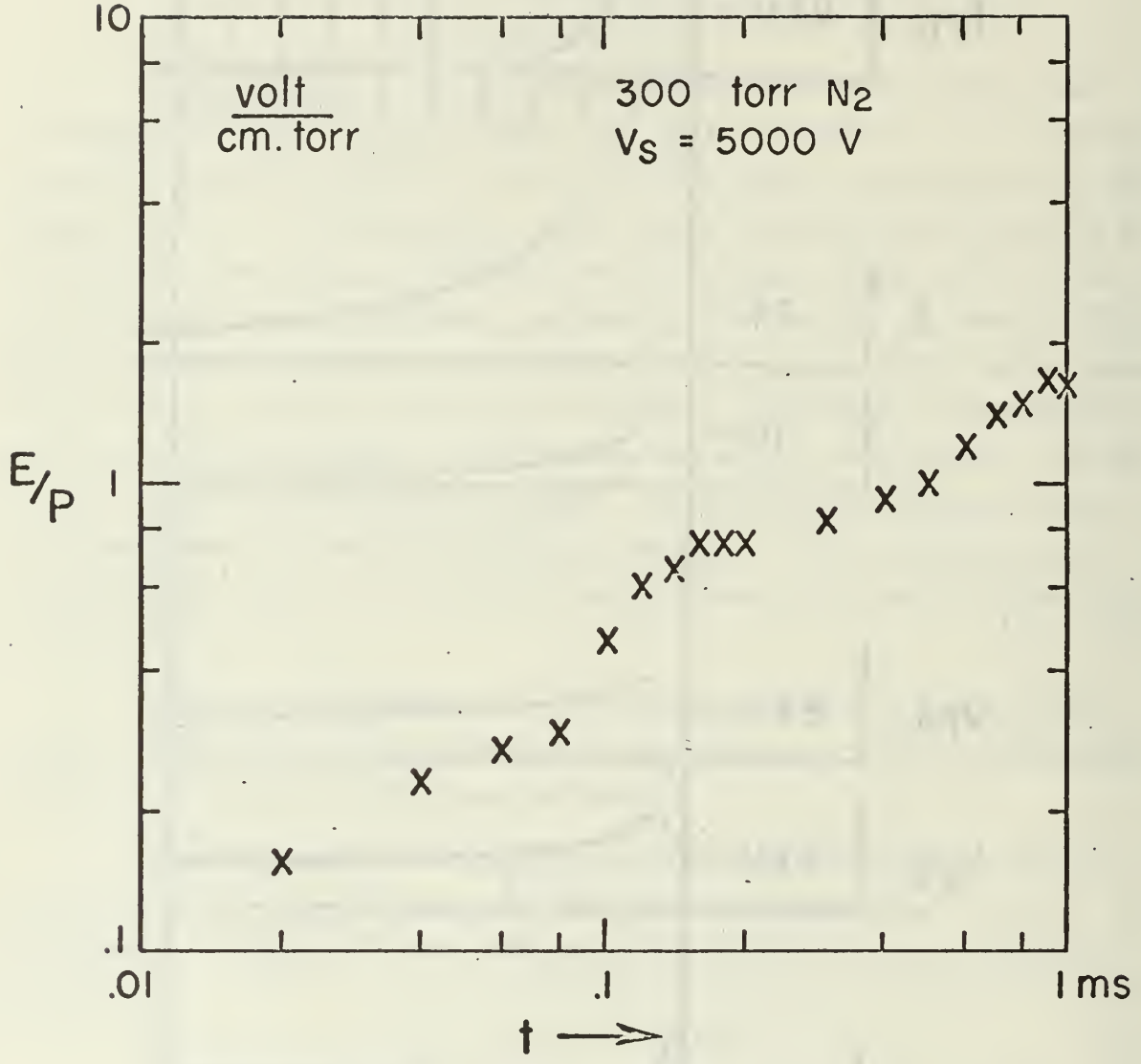

FIG. 5. Electric field vs. time.

$$n_e = \frac{I}{Ae\ V_D}$$

where I is the discharge current shown in Fig. 4, A is the effective area of the discharge (80 cm^2) and e is the electron charge. Values of n_e for different times are shown in Fig. 6. The straight line has a slope -1 indicating a 1/t time dependence. The recombination coefficient given by $\alpha = 1/n_e t$ is thus 0.8×10^{-7} cm^{-3} sec^{-1}, in rough agreement with the results of previous workers for $T_e \approx 0.5^{\circ}K$.

The maximum value of n_e obtained, ~ 8×10^{11} cm^{-3}, is in agreement with estimates made from the beam intensity and range in N_2.

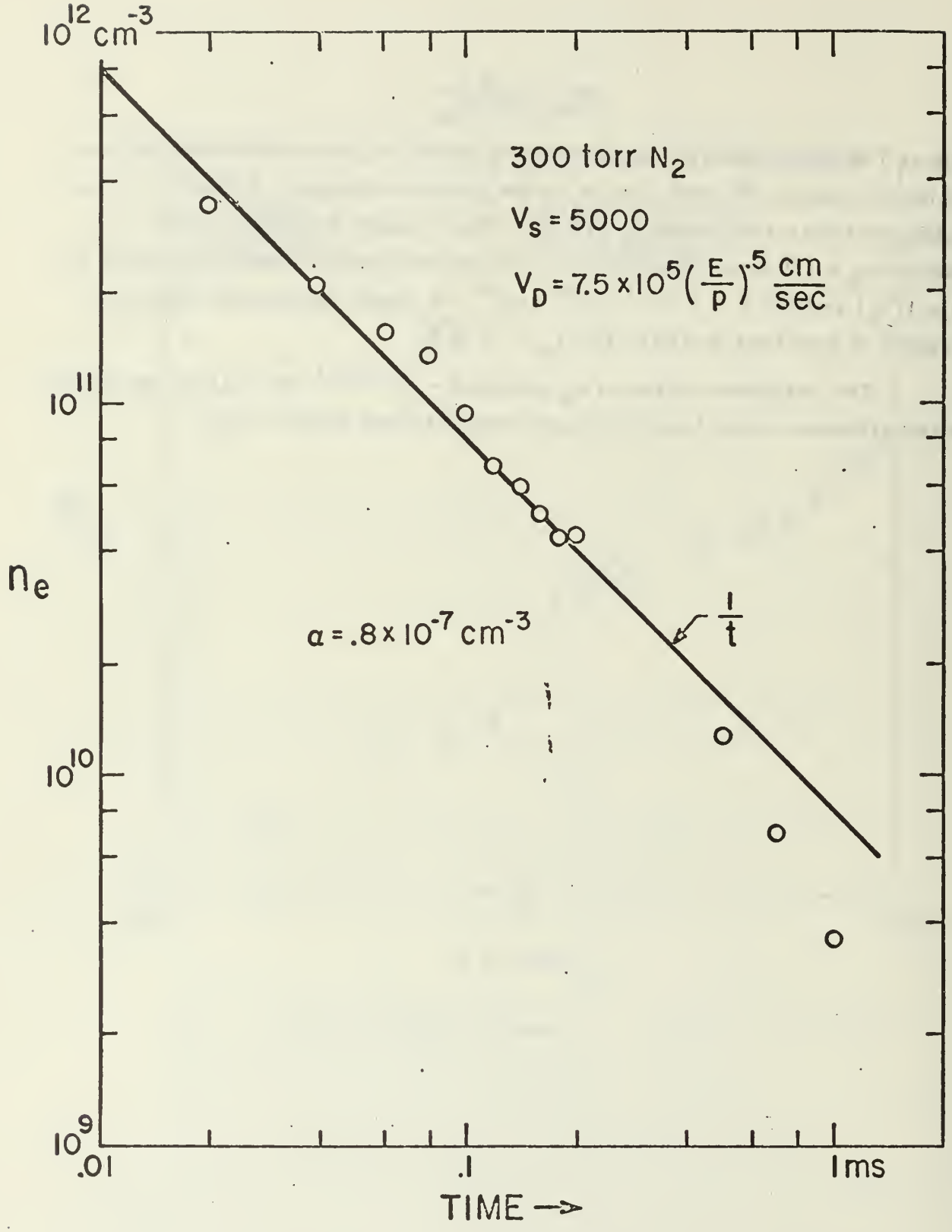

FIG. 6. Electron number density vs. time.

IV. SUMMARY AND FUTURE PLANS

AERL has a facility for making uniform discharges with variable T_e at high pressures and large volumes. Presently, in this facility the discharge is uniform at pressures as high as one atmosphere with discharge current densities up to 0.1 amp/cm^2.

Using this facility, some preliminary measurements were made concerning recombination rates at high gas pressure and variable T_e. Initial measurements of the discharge voltage and current indicate that the effective recombination rate in N_2 is approximately 10^{-7} cm^{-3} sec^{-1} in agreement with previous work.

Future work will validate these preliminary results and expand them to wider ranges of pressure, electron currents, discharge currents, and different gases. The limits on electron temperature for maintaining a uniform discharge and the basic instabilities involved will be studied.

SUMMARY OF RESEARCH

Supported by AFOSR Contract No. F44620-69-C-0109

J. Rosciszewski

CALCULATIONS OF FLOW IN MAGNETIC NOZZLES AND FLOWS WITH RADIATION ENERGY EXCHANGE

Continuation of research was conducted in three major groups:

1. Problems associated with operation of an MPD arc-jet with pure magnetic nozzle.
2. Transient flows with strong interaction with electromagnetic field or with intense radiation energy absorption.
3. Explosion with radiation cooling wave.

1. MPD arc-jet with "pure" magnetic nozzle.

The first group pf problems is a continuation of research aimed toward understanding the acceleration process in an MPD arc-jet. This research was designed as a joint effort with A. Ducati's experimental group at Plasmadyne Corp. In order to cut down the anode potential drop a device with a very short electrode was selected where the magnetic field is perpendicular to the anode and forms a "virtual electrode" (Fig. 1). Because electrons can move easily along magnetic field lines, the anode drop should be reduced to zero and the device will operate as a pure magnetic nozzle.

Experiments by A. Ducati indicated trouble by starting an arc in such a wall-less device. This is due to a fact that neutral gas exposed to a vacuum is streaming radially. The motion of neutral gas across an arc sheet, taking into account finite rate of ionization, was calculated on the computer and it was found that for $1 eV$, the current sheet thickness of this sheet should be at least $1 cm$ to prevent escape of neutrals. In order to cut down the escape of neutrals one could provide outside walls parallel to the magnetic nozzle (Fig. 1).

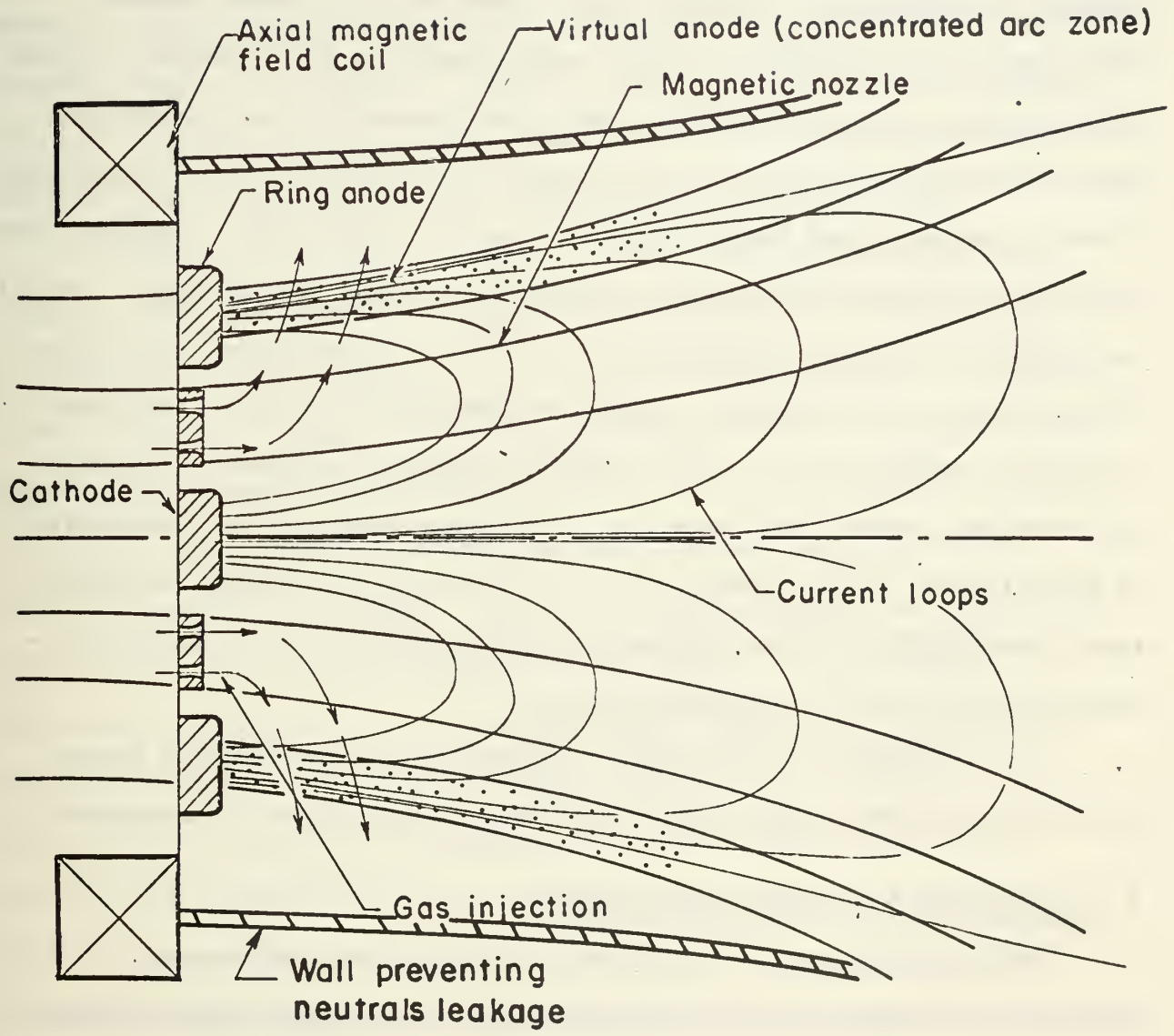

Figure 1. Pure magnetic nozzle MPD arc-jet.

2. Transient flows with strong interaction with electromagnetic field or with intense radiation energy absorption.

Last year's effort of simulation of non-steady shock-induced MHD flow is continued with alternation of a basic mathematical tool and different applications. A modified Lax-Wendroff method was applied to shock-induced MHD flow in order to simulate experimental conditions of B. Zauderer. The resulting paper was presented last year at the Seventh International Shock Tube Symposium in Toronto, and will appear in transactions of the Symposium. General agreement with experiment turns out to be fairly good. However, there are some details which the present mathematical model cannot handle. One of the problems is difficulty in introduction of the relaxation time. This is due to the smeared shock thickness over a few mesh points. The present effort is aimed to application of the Lax-Wendroff method to equations in a system of coordinates moving with the shock. In this way shock will be represented by discontinuity. At the same time one could obtain a secondary "smeared" shock resulting from strong interaction. This will make it possible to introduce relaxation time in the MHD problem.

As an example of application of the method the flow behind a strong shock wave with absorption of a parallel beam of laser light is considered.

3. Explosion with radiation cooling wave.

The latest analytical effort is devoted to analytical treatment of transient flows with radiation energy exchange. The author's interest was induced by many still unsolved basic problems of high temperature flow important in the defense field. A classical problem is that of point explosion. Solution of this problem neglecting ambient pressure and assuming atmosphere with a uniform density was first given by Sedov (ref. 1) and by Taylor (ref. 2). This solution was obtained by introduction of a similarity parameter $\eta = r/R(t)$ as an only independent variable. Here, small r denotes radius

and $R(t)$ shock wave radius. In this way the system of partial differential equations reduces to ordinary differential equations which could be solved in a closed form.

Since the time of the classical Sedov-Taylor solution, many works have appeared including ambient pressure, atmospheric density variation, etc. An entire book by Korobeinikov has been devoted to the explosion problem (ref. 3). In this book most of the problems are solved by assuming small deviation from a similarity solution leading to linearized equation.

Another very simplified solution assuming that all the mass is concentrated at the shock wave was given by Chernyi (ref. 4). A recent paper by Laumbach and Probstein (ref. 5) also gives a similar simplified approach to the solution of a problem assuming concentrated mass at the shock. More general methods are based on finite difference treatment. However, such methods are extremely time-consuming and are always associated with numerical instability problems. Moreover, such methods do not take advantage of the known solution of a simplified case where similarity solution is applicable. It seems that any numerical method which does not include such a "skeleton solution," which chould be easily obtained in the simplified case, could not be too successful. Recognizing these facts, the author of this proposal spent considerable time in obtaining a solution of an explosion problem using a very general method of integral relations. Such a solution is not restricted by an assumption of concentrated mass at the shock, etc. The method was checked in the simplified case where a similarity solution is applicable. A simple solution was obtained using asymptotic methods, and agreement with exact theory is excellent.

As the next step, the author applied a multi-strip integral method to an explosion problem, including propagation of a cooling wave. Analysis

of singularity gives the initial condition for a cooling wave propagation. It was shown that the initial velocity of a cooling wave is exactly equal to relative gas velocity with respect to a shock wave. This is a kind of Chapmann-Jouget condition. A cooling wave must be therefore initially tangential to a shock wave (Fig. 2).

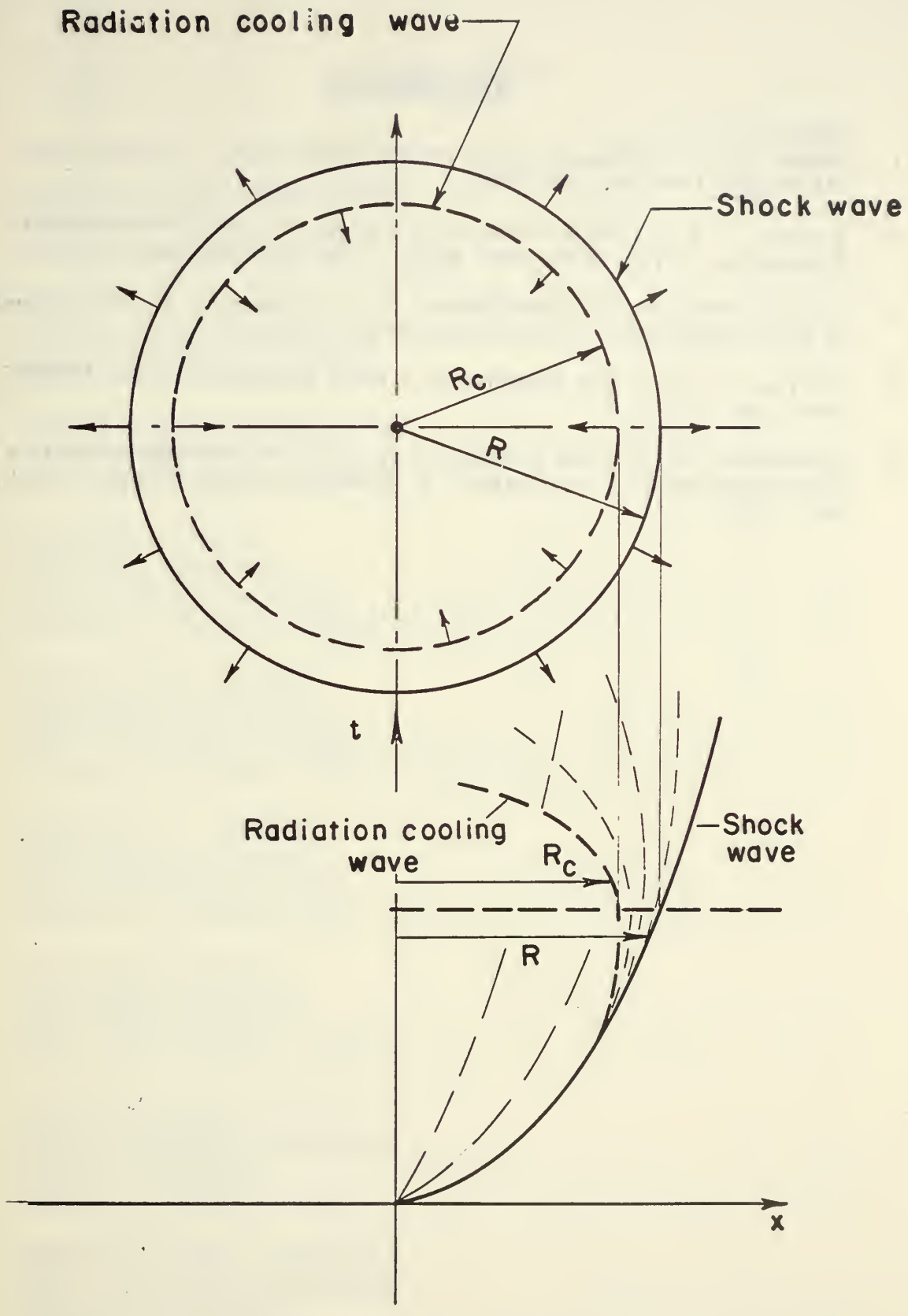

Figure 2. Explosion with radiation cooling.

REFERENCES

1. Sedov, L. I.: "Propagation of Strong Blast Waves," Prikt. Mat. MRKH 10, 1946, pp. 241-250.

2. Taylor, G. I.: "The Formation of a Blast Wave by a Very Intense Explosion," Proc. Roy. Soc. A201, 1950, pp. 159-186.

3. Korobeinikov, W. P.; Mielnikova, N. S.; Rjazanov, E. V.: "Theory of Point Explosion," (in Russian) Moskva 1961.

4. Chernyi, C. G.: The Problem of a Point Explosion, Dohl ANSSSR 112, 1957, pp. 213, 216.

5. Laumbach, D. D., and Probstein, R. F.: "A Point Explosion in a Cold Exponential Atmosphere," J. Fluid Mech. 35,, Part 1, 1969, pp. 53-57.

DISTRIBUTION

	No. of Copies
Defense Documentation Center Cameron Station Alexandria, Virginia 22314	20
Library Naval Postgraduate School Monterey, California 93940	1
Dean of Research Administration Naval Postgraduate School Monterey, California 93940	2
Professor O. Heinz Department of Physics Naval Postgraduate School Monterey, California 93940	1
Professor Fred Schwirzke Department of Physics Naval Postgraduate School Monterey, California 93940	25
Professor J. N. Cooper Department of Physics Naval Postgraduate School Monterey, California 93940	1
Dr. Jan Rosciszewski Air Vehicle Corporation 8873 Balboa Avenue San Diego, California 92123	1
Professor Donald A. Dunn Dept. of Electrical Engineering Stanford University Stanford, California 94305	1
Professor Joseph T. Verdeyen Dept. of Electrical Engineering University of Illinois Urbana, Illinois 61801	1

	No. of Copies
Dr. C B. Cherrington Department of Electrical Engineering University of Illinois Urbana, Illinois 61801	1
Professor T. Dolan Department of Electrical Engineering University of Illinois Urbana, Illinois 61801	1
Professor D. Meeker Department of Electrical Engineering University of Illinois Urbana, Illinois 61801	1
Professor James E. McCune Dept. of Aeronautics and Astronautics Massachusetts Institute of Technology Cambridge, Massachusetts 02139	1
Professor J. D. Callen Dept. of Aeronautics and Astronautics Massachusetts Institute of Technology Cambridge , Massachusetts 02139	1
Dr. John G. Siambis Department of Electrical Engineering Carnegie-Mellon University Pittsburgh, Pennsylvania 15213	1
Professor A J. Lichtenberg Dept. of Electrical Engineering & Computer Science University of California Berkeley, California 94720	1
Professor M. Lieberman Department of Electrical Engineering University of California Berkeley, California 94710	1
Dr. Willard H. Bennett Department of Physics North Carolina State University Raleigh, North Carolina 27607	1

	No. of Copies
Professor M. Kristiansen Department of Electrical Engineering Texas Technological University Lubbock, Texas 79409	1
Professor M. O. Hagler Department of Electrical Engineering Texas Technological University Lubbock, Texas 79409	1
Dr. John B. Dicks Department of Physics University of Tennessee Space Institute Tullahoma, Tennessee 37388	1
Dr. Winston Bostick Department of Physics Stevens Institute of Technology Hoboken, New Jersey 07030	1
Professor L. Grunberger Department of Physics Stevens Institute of Technology Hoboken, New Jersey 07030	1
Professor V. Nardi Department of Physics Stevens Institute of Technology Hoboken, New Jersey 07030	1
Professor W. Prior Department of Physics Stevens Institute of Technology Hoboken, New Jersey 07030	1
Dr. A. Anastassaides Nuclear Research Center Greek Atomic Energy Commission Aghia Paraskevi, Attikis Athens, Greece	1
Dr. C. N. Dailey Space Technologies Labs TRW Systems, Inc. One Space Park Redondo Beach, California 90278	1

No. of Copies

Mr. A. C. Ducati 1
Plasmadyne Division
Geotel Inc.
Santa Ana, California 92702

Dr. Robert A. Gross 1
Department of Applied Science & Engineering
Columbia University
New York, N. Y. 10027

Professor C. D. Hendricks 1
Department of Electrical Engineering
University of Illinois
Urbana, Illinois 61801

Professor A. W. Dipert 1
Department of Electrical Engineering
University of Illinois
Urbana, Illinois 61801

Professor S. Grodzinsky 1
Department of Electrical Engineering
University of Illinois
Urbana, Illinois 61801

Dr. G. S. Janes 1
Avco Everett Research Laboratory
AVCO Corp.
Everett, Massachusetts 02149

Dr. Richard M. Patrick 1
Avco Everett Research Laboratory
AVCO Corporation
Everett, Massachusetts 02149

J. D. Daugherty 1
Avco Everett Research Laboratory
AVCO Corporation
Everett, Massachusetts 02149

J. E. Eninger 1
Avco Everett Research Laboratory
AVCO Corporation
Everett, Massachusetts 02149

	No. of Copies
R. H. Levy Avco Everett Research Laboratory AVCO Corporation Everett, Massachusetts 02149	1
Dr. M. L. Pool Ohio State University Research Foundation Department of Physics Columbus, Ohio 43212	1
Professor Robert Eustis Department of Mechanical Engineering Stanford University Stanford, California 94301	1
M. Mitchner Department of Mechanical Engineering Stanford University Stanford, California 94301	1
C. H. Kruger Department of Mechanical Engineering Stanford University Stanford, California 94301	1
Dr. Norman C. Jen City College Research Foundation City University of New York New York, N. Y. 10031	1
Dr. A. Haught United Aircraft Research Labs United Aircraft Corporation East Hartford, Connecticut 06108	1
D. H. Polk United Aircraft Research Labs United Aircraft Corporation East Hartford, Connecticut 06108	1
W. J. Fader United Aircraft Research Labs United Aircraft Corporation East Hartford, Connecticut 06108	1

	No. of Copies
J. C. Woo United Aircraft Research Labs United Aircraft Corporation East Hartford, Connecticut 06108	1
Professor D. R. Wells Department of Physics Miami University Coral Gables, Florida 33124	1
Dr. Robert L. Hickok Central Research Division Mobil Oil Corporation Princeton, New Jersey 08540	1
F. C. Jobes Central Research Division Mobile Oil Corporation Princeton, New Jersey 08540	1
Mr. S. T. Demetriades President, STD Research Corporation P. O. Box 4127, Catalina Station Pasadena, California 91106	1
G. S. Argyropoulos STD Research Corporation P. O. Box 4127, Catalina Station Pasadena, California 91106	1
Dr. R. M. Measures University of Toronto Institute for Aerospace Studies Toronto, Canada	1
Dr. M. Lubin Dept. of Mechanics & Aerospace Science University of Rochester Rochester, New York 14627	1
Dr. H. S. Dunn Dept. of Mechanics & Aerospace Science University of Rochester Rochester, New York 14627	1

No. of Copies

Professor F. Cap 1
University of Innsbruck
Institute for Theoretical Physics
Innsbruck, Austria

D. Floriani 1
University of Innsbruck
Institute for Theoretical Physics
Innsbruck, Austria

N. Ortner 1
University of Innsbruck
Institute for Theoretical Physics
Innsbruck, Austria

G. Auer 1
University of Innsbruck
Institute for Theoretical Physics
Innsbruck, Austria

E. H. Jager 1
University of Innsbruck
Institute for Theoretical Physics
Innsbruck, Austria

P. Unteregger 1
University of Innsbruck
Institute for Theoretical Physics
Innsbruck, Austria

S. Kuhn 1
University of Innsbruck
Institute for Theoretical Physics
Innsbruck, Austria

Dr. Nima Geffen 1
Tel-Aviv University
Tel-Aviv, Israel

J. L. Wyatt 1
Bass Corporation
Berkeley, California 94701

	No. of Copies
E. R. Pugh Avco Everett Research Laboratory AVCO Corporation Everett, Massachusetts 02149	1
D. H. Douglas-Hamilton Avco Everett Research Laboratory AVCO Corporation Everett, Massachusetts 02149	1
Professor S. Gruber Department of Engineering Case Western Reserve University Cleveland, Ohio 44106	1
Professor O. K. Mawardi Department of Engineering Case Western Reserve University Cleveland, Ohio 44106	1
Dr. T. K. Fowler Lawrence Radiation Laboratory Livermore, California 94550	1
Dr. W. Price AFOSR (SRG) 1400 Wilson Blvd Arlington, Virginia 22209	1
Mr. R. A. Gessow (RRP NASA Headquarters 6th and Independence Ave., S. W. Washington, D. C. 20546	1
Mr. H. G. Kosmahl NASA-Lewis Research Center Flight Propulsion Laboratory Cleveland, Ohio 44135	1
Colonel Ivan C. Atkinson AFSC (DoL)/SCTT Andrews AFB, D. C. 20331	1
Colonel O. A. Berthold AFSC (DoL)/SCTSP Andrews AFB, D. C. 20331	1

	No. of Copies
Major Ben George AFSC (DoL)/SCTSP Andrews AFB, D. C. 20331	1
LCOL C. R. Flint SAMSO AF Unit Post Office Los Angeles, California 90045	1
Capt. Howard MacEwen SAMSO AF Unit Post Office Los Angeles, California 90045	1
LCOL F. F. Tolle AFIT, Dept. of Mechanical Engineering Wright Patterson AFB, Ohio 45433	1
Dr. Morton A. Levine AFCRL L. G. Hanscom Field Bedford, Massachusetts 01731	1
LCOL Richard T. Boverie EOAR (ERTE) APO, New York 09667	1
Mr. J. J. Murray U. S. Army Research Office Box CM, Duke Station Durham, North Carolina 27706	1
Mr. James Patton Office of Naval Research, USN Washington, D. C. 20360	1
Mr. John Satkowski Office of Naval Research U. S. Dept. of the Navy Washington, D.C. 20360	1
Dr.Ralph Roberts Office of Naval Research U. S. Dept. of the Navy Washington, D. C. 20360	1

	No. of Copies
Mr. C. W. Schnare (RPP) Advanced Plans and Analysis HQS AF Flight Test Center Edwards AFB, California 93523	1
Mr. G. Seikel NASA-Lewis Research Center 21000 Brookpark Road Cleveland, Ohio 44135	1
Mr. Jerry Mullin NASA/OART Washington, D. C. 20546	1
LCOL William Jackomis ARL (ARE) Wright Paterson AFB, Ohio 45433	1
Dr. Roy Gould U. S. Atomic Energy Commission Washington, D. C. 20545	1
Dr. Robert Hirsch U. S. Atomic Energy Commission Washington, D. C. 20545	1
Mr. R. D. Shelton Electrical Propulsion Branch NASA/MSFC Huntsville, Alabama 35812	1
Dr. A. Shine Chairman, Dept. of Mechanical Engineering (AFIT) Wright-Patterson AFB, Ohio 45433	1
Mr. Robert Supp AFAPL (APP) Wright-Patterson AFB, Ohio 45433	1
Mr. Frank Patella AFAPL (APP-1) Wright-Patterson AFB, Ohio 45433	1

	No. of Copies
Mr. C. Michaels AFAPL (APG) Wright-Patterson AFB, Ohio 45433	1
HQ OAR (Major E. T. Scambos/PGSG) 1400 Wilson Blvd. Arlington, Virginia 22209	1
Major G. Starkey HQS USAF (AFRDC) Washington, D. C. 20330	1
Colonel D. Cheatham ARL (ARH) Wright Patterson AFB, Ohio 45433	1
Dr. Milton M. Slawsky AFOSR (SRE) 1400 Wilson Blvd. Arlington, Virginia 22209	1
Dr. Joseph F. Masi AFOSR (SREP) 1400 Wilson Blvd. Arlington, Virginia 22209	1
Dr. Langdon Crane Director, Inst. of Fluid Dynamics and Applied Mathematics University of Maryland College Park, Maryland 20740	1
Dr. Arthur Guenther AFWL Kirtland AFB Albuquerque, New Mexico 87117	1
Mr. K. Cramer ARL (ARN) Wright Patterson AFB, Ohio 45433	1
Mr. Robert Cooper AFAPL (APIE-2) Wright Patterson AFB, Ohio 45433	1

	No. of Copies
Dr. Hans Von Ohain ARL (ARD-1) Wright Patterson AFB, Ohio 45433	1
Mr. Christopher Kurrle HQS USAF (AFRDC) Washington, D. C. 20330	1
Mr. William Downs HQS USAF (AFRDC) Washington, D. C. 20330	1
AFSC/STLO NASA-Lewis Research Center 21000 Brookpark Road Cleveland, Ohio 45433	1
Major James T. Carpenter AFOSR (SRPP) 1400 Wilson Blvd. Arlington, Virginia 22209	1
Dr. Sinclair National Science Foundation 1800 G Street, N. W. Washington, D. C. 20550	1
Mr. J. Jones SAFRD Washington, D. C. 20330	1
Commander Mischke Office of Naval Research U. S. Dept of the Navy Washington, D.C. 20360	1
LCOL William Metscher ODDR&E The Pentagon Washington, D. C. 20330	1
Dr. C. Branson Smith ODDR&E The Pentagon Washington, D. C. 20330	1

	No. of Copies
Colonel E. A. Kawkens HQ USAF (AFRDD) The Pentagon Washington, D. C. 20330	1
Dr. Louis A. Tamburino ARL (ARP) Wright Patterson AFB, Ohio 45433	1
Mr. Clifford Hurd AF Rocket Propulsion Laboratory Edwards AFB, California 93523	1
LT Richard Gullickson AF Weapons Laboratory (WLREX) Kirtland AFB, New Mexico 87117	1
Dr. Wesley O. Doggett North Carolina State University Box 5367 Raleigh, North Carolina 27607	1
Dr. D. G. Samaras AFOSR (SREP) 1400 Wilson Blvd. Arlington, Virginia 22209	50
LCOL Howard W. Jackson AFOSR (SREE) 1400 Wilson Blvd. Arlington, Virginia 22209	1
Dr. Charles S. Cook General Electric Company Valley Forge, Pennsylvania 19101	1
Commander Gayland J. Mischke Department of the Navy Office of Naval Research Power Branch (Code 429) Washington, D. C. 20360	1
Commanding Officer Office of Naval Research, Branch Office Box 39, FPO, New York, N. Y. 09510	1

	No. of Copies
Director, Technical Information Division Naval Research Laboratory Attn: 2027 Washington, D. C. 20390	1
Mr. Frank J. Mollura Rome Air Development Center Attn: EMEAM Griffiss AFB, New York 13440	1
Frank Shields U. S. Army Mobility Equipment Research & Development Center Fort Belvoir, Virginia 22060 Attn: SMEFB-EA	1
Dr. B. Lubarsky Chief, Space Power Systems Division NASA, Lewis Research Center 21000 Brookpark Road Cleveland, Ohio 44135	1
Mr. Philip Stover (APIE) AF Aero Propulsion Laboratory Wright Patterson AFB, Ohio 45433	1
Colonel William K. Moran, Jr. Aerospace Research Laboratories Wright Patterson AFB, Ohio 45433	1
Major B. W. George HQ AFSC (SCTSP) Andrews AFB, D. C. 20311	1
Wolfgang E. Moeckel NASA-Lewis Research Center Propulsion Division 21000 Brookpark Road Cleveland, Ohio 44135	1

DOCUMENT CONTROL DATA - R & D

(Security classification of title, body of abstract and indexing annotation must be entered when the overall report is classified)

1. ORIGINATING ACTIVITY *(Corporate author)*
Naval Postgraduate School
Monterey, California 93940

2a. REPORT SECURITY CLASSIFICATION
UNCLASSIFIED

2b. GROUP

3. REPORT TITLE
COMPILATION OF RESEARCH SUMMARIES - THIRTEENTH AFOSR CONTRACTORS' MEETING ON PHYSICAL ENERGETICS

4. DESCRIPTIVE NOTES *(Type of report and inclusive dates)*

5. AUTHOR(S) *(First name, middle initial, last name)*
Fred Schwirzke
Alfred W. Cooper

6. REPORT DATE
15 April 1970

7a. TOTAL NO. OF PAGES
198

7b. NO. OF REFS

8a. CONTRACT OR GRANT NO.
MIPR 70-0001

b. PROJECT NO.
9725-01

c. 61102F

d. 681308

9a. ORIGINATOR'S REPORT NUMBER(S)
NPS-61SW0031A

9b. OTHER REPORT NO(S) *(Any other numbers that may be assigned this report)*

10. DISTRIBUTION STATEMENT
This document has been approved for public release and sale; its distribution is unlimited.

11. SUPPLEMENTARY NOTES
AF Office of Scientific Research (SREP)
1400 Wilson Boulevard
Arlington, Virginia 22209

12. SPONSORING MILITARY ACTIVITY
Naval Postgraduate School
Monterey, California 93940

13. ABSTRACT

This report contains the material presented in the form of panel discussions at the Thirteenth Annual Air Force Office of Scientific Research Contractors' Conference on Physical Energetics held at the Naval Postgraduate School, Monterey, California, from the 5th to the 7th of May 1970

It was the purpose of this conference to facilitate the exchange of latest information on research in non-chemical energy sources, release mechanisms and conversion processes. The conference was attended by the AFOSR contractors and grantees performing research in these areas together with representatives of the Army, Navy, Air Force, DOD, NASA and AEC.

14 KEY WORDS	LINK A		LINK B		LINK C	
	ROLE	WT	ROLE	WT	ROLE	WT
Research Summaries 13th AFOSR Conference Physical Energetics						